

UNIVERSITÉ DU QUÉBEC

**THÈSE PRÉSENTÉE À
L'UNIVERSITÉ DU QUÉBEC À TROIS-RIVIÈRES**

**COMME EXIGENCE PARTIELLE
DU DOCTORAT EN GÉNIE ÉLECTRIQUE**

**PAR
SGHAIER M. GUIZANI**

**OPTICAL POST CHROMATIC DISPERSION
COMPENSATION IN AN OPTICAL
FIBER COMMUNICATION SYSTEM**

MAI 2008

Université du Québec à Trois-Rivières

Service de la bibliothèque

Avertissement

L'auteur de ce mémoire ou de cette thèse a autorisé l'Université du Québec à Trois-Rivières à diffuser, à des fins non lucratives, une copie de son mémoire ou de sa thèse.

Cette diffusion n'entraîne pas une renonciation de la part de l'auteur à ses droits de propriété intellectuelle, incluant le droit d'auteur, sur ce mémoire ou cette thèse. Notamment, la reproduction ou la publication de la totalité ou d'une partie importante de ce mémoire ou de cette thèse requiert son autorisation.

Dedication

In loving memory of

My parents:

∞ **Mokhtar Guizani** ∞
(1923 - 1999)
&
∞ **Mbarka Ounais** ∞
(1924 - 2004)

...❧ May Allah SWT bless them ❧...

... Their voices are still echoing ...

Résumé

Comme toutes les voies de transmission, les fibres optiques ne sont pas des moyens parfaits. Elles sont dotées de caractéristiques qui fixent une limite à la vitesse maximum de communication qu'elles peuvent manipuler. Pour répondre au besoin mondial croissant d'une plus grande vitesse de transmission, le progrès technique est dirigé vers la construction de nouvelles fibres capables de manipuler l'augmentation rapide du trafic. Cependant, construire une liaison de fibres optiques est un important investissement qu'on n'est pas prêt à changer aussi facilement. Par exemple, les câbles à fibres optiques installés pendant les années 80 se composent de plus de 50 millions de kilomètres de fibre monomode "standard". Puisque les anciennes fibres optiques ne peuvent pas être facilement remplacées avec des nouvelles, la mise au point de techniques innovatrices afin d'exploiter la largeur de bande disponible est donc cruciale.

Parmi les inconvénients importants qui limitent la transmission à haut débit binaire avec la fibre monomode standard est la dispersion chromatique (DC). C'est particulièrement problématique pour des systèmes fonctionnant dans la bande de 1550 nanomètres, où la limite chromatique de dispersion diminue rapidement de façon inversement proportionnelle au carré de débit binaire. Nous avons choisi effectivement de compenser la dispersion chromatique en utilisant des techniques optiques, ce qui est tout à fait justifié car la DC relève du domaine optique. Néanmoins, l'égalisation électrique existe

et peut offrir les avantages d'un coût inférieur et d'une plus petite taille par l'intégration d'un émetteur-récepteur électronique.

Abstract

Like all communication channels, optical fibers are not ideal media. They have impairments that limit the maximum communication speed they can handle. Driven by the world's growing need for communication bandwidth, progress is constantly being reported in the building of newer fibers capable of handling the rapid increase in traffic. However, building an optical fiber link is a major investment that is very expensive to replace. For example, the optical fiber cables installed during the 1980s consist of more than 50 million kilometers of "standard" single-mode fiber. Since old optical fibers cannot be easily replaced with newer ones, innovative methods of exploiting the available bandwidth are crucial.

A major impairment that restricts the achievement of higher bit rates with standard single mode fiber is chromatic dispersion (CD). This is particularly problematic for systems operating in the 1550 nm band, where the chromatic dispersion limit decreases rapidly in inverse proportion to the square of the bit rate. We opted in effect to compensate the chromatic dispersion using optical techniques, which is only natural to expect, given that CD originates in the optical domain. Nevertheless, electrical equalization exists and can offer the advantages of a lower cost and smaller size through integration within the electronics transceiver. Taking advantage of the Talbot effect (a self-imaging phenomenon that occurs when a periodic signal propagates through a dispersive medium at a given distance named Talbot distance) in the regeneration of a periodic signal where one period is

similar to the initial transmitted signal, we propose a new technique that mitigates the signal at the receiver. Our solution is extended to the combination of second and third order chromatic dispersion. These can be handled either separately or simultaneously by our TEChDC technique. Then, we assess the performance of the TEChDC scheme under realistic transmission impairments. To prove the feasibility of the TEChDC architecture, an applet was created to simulate all possible conditions including second and third order dispersion. The simulation results show that the TEChDC method is capable of carrying enormous data through long distance.

Acknowledgment

I want to express my deepest thanks to my supervisors, Professor Ahmed Cheriti and Professor Habib Hamam, for their endless support, encouragement and guidance, and most of all, for providing me with every possible opportunity for success. They have my profound appreciation and respect. I also wish to thank the members of the jury (Professor Adel Omar Dahmane, Dr. Khalifa Hettak, and Professor Habib FathAllah) for accepting to serve on my committee. I extend my gratitude to all members of the Electrical Engineering Department of the UQTR as well as to those in the Engineering Department at Moncton University, NB. Special thanks go to Professors Jamel Ghouili, Yassine Bouslimani and Mustapha Razzak for their invaluable advice, expertise, insight and support in the lab at Moncton University. Many thanks as well to Dr. Naim Ben Hmida and to my old and best friends Lanour Hajji and Hamda Timoumi for their encouragement and support during my early days in Ottawa. Special thanks go to Mohamed Amin for the French translation.

Last, but definitely not least, I would like to thank all members of my family for their love, encouragement, patience and constant assistance. I am grateful to my brother, Dr. Mohsen Guizani, my leader, inspirer and teacher always. Thanks to my wife Basma Saadallah for her support and patience all during the study period, and to my children, Khobaib, Khalil and Al-Mokhtar.

Table of contents

Résumé.....	iii
Abstract	v
Acknowledgment	vii
Table of contents	viii
List of tables	xvi
List of figures	xvii
List of symbols	xx
Chapter 1 - Résumé en français	1
1.1 Résumé	1
1.2 Introduction	1
1.3 Chaîne de transmission sur fibre optique	2
1.3.1 Introduction.....	2
1.3.2 Émetteurs optiques.....	3
1.3.2.1 <i>Diodes</i>	3
1.3.2.2 <i>Laser</i>	4
1.3.2.3 <i>Modulateurs interférométriques</i>	4

1.3.3	Systèmes de traitement et régénération du signal optique	4
1.3.3.1	<i>Média de transmission optique</i>	4
1.3.3.2	<i>Amplificateurs optiques</i>	5
1.3.3.3	<i>Régénérateur et répéteur</i>	5
1.3.3.4	<i>Jonctions optiques</i>	5
1.3.3.5	<i>Séparateurs optiques et coupleurs</i>	6
1.3.4	Récepteurs optiques	6
1.3.4.1	<i>Filtres optiques</i>	6
1.3.4.2	<i>Photodétecteurs</i>	6
1.3.5	Conclusion	6
1.4	Filtres optiques et propagation	7
1.4.1	Types de fibres optiques	7
1.4.1.1	<i>Fibre multimodes à saut d'indice</i>	7
1.4.1.2	<i>Fibre monomode</i>	8
1.4.1.3	<i>Fibres à cristaux photoniques</i>	9
1.4.1.4	<i>Fibres à cristaux liquides</i>	9
1.4.1.5	<i>Fibres en Plastic</i>	10
1.4.2	Fabrication des fibres optiques	10
1.4.3	Propagation de la lumière dans la fibre optique.....	10

1.4.4	Problèmes liés à la propagation	11
1.4.4.1	<i>Dispersion chromatique</i>	13
1.4.4.2	<i>Dispersion de mode de polarisation</i>	17
1.4.4.3	<i>Effets non linéaires</i>	18
i.	Modulation non linéaire de phase	19
ii.	Auto Modulation de Phase	19
iii.	Modulation Croisée de phase	19
iv.	Mélange à quatre ondes	20
v.	Diffusion Stimulée de Raman	20
1.5	Méthodes de compensation de la dispersion chromatique	21
1.6	Effet Talbot.....	22
1.6.1	Reproduction intégrale spatiale.....	22
1.6.2	Effet Talbot	25
1.6.3	Effet Talbot fractionnaire spatial	25
1.6.4	Effet Talbot temporel.....	26
1.7	Solution proposée	29
1.7.1	Architecture.....	29
1.7.2	Implémentation de la périodisation.....	30
1.7.3	Simulations	31

1.8 Conclusion.....	36
Chapter 2 - Introduction.....	37
2.1 Context and main objective.....	38
2.2 Literature findings.....	39
2.3 Originality.....	44
2.4 Thesis contribution.....	45
2.5 Problematic issues.....	47
2.6 Attenuations.....	48
2.7 Chromatic dispersion (CD).....	48
2.8 Polarization-mode dispersion (PMD).....	49
2.9 Nonlinear optical effect.....	50
2.9.1 Nonlinear phase modulation.....	50
2.9.2 Self- phase modulation (SPM).....	51
2.9.3 Cross-phase modulation (XPM).....	51
2.9.4 Four-Wave Mixing (FWM).....	51
2.10 Conclusion.....	52
Chapter 3 - Optical Fiber Transmission Systems.....	53
3.1 Introduction.....	53
3.2 Overview.....	54

3.3	System concepts	56
3.4	Optical transmitters	58
3.4.1	Light-emitting diode	59
3.4.2	Lasers	59
3.4.3	Mach-Zehender interferometer modulators	60
3.5	Optical transmission medium	61
3.5.1	Optical amplifiers.....	62
3.5.2	Repeaters and regenerators	62
3.5.3	Optical splices.....	62
3.5.4	Optical splitters and couplers.....	62
3.5.5	Optical receivers	63
3.5.6	Optical filters	63
3.5.7	Photo-detectors	63
3.6	Conclusion.....	64
Chapter 4 - Optical fiber and light propagation		65
4.1	Conventional fibers	65
4.1.1	Multi-mode step-index fiber	66
4.1.2	Single-mode fiber.....	68
4.2	Non-conventional fiber.....	70

4.2.1	Photonic crystal fiber	70
4.2.2	Liquid crystal fiber.....	72
4.2.3	Plastic optical fiber	72
4.3	Fiber fabrication	73
4.4	Propagation of light in optical fibers.....	74
4.4.1	Nature of light and its propagation characteristics	74
4.4.2	Light as an electromagnetic wave.....	75
4.4.3	Light propagation in multi-mode fiber	77
4.4.4	Geometrical optics laws and parameters.....	78
4.4.4.1	Snell's law.....	78
4.4.4.2	Critical angle	79
4.4.4.3	Numerical aperture	80
4.4.4.4	Refractive index.....	82
4.5	Fiber impairments.....	83
4.5.1	Signal distortion.....	85
4.5.1.1	Chromatic dispersion.....	85
4.5.1.2	Polarization-mode dispersion (PMD).....	90
4.5.2	Nonlinear optical effects	92
4.5.2.1	Nonlinear phase modulation.....	93

4.5.2.2	Self-phase modulation (SPM)	93
4.5.2.3	Cross-phase modulation (XPM)	95
4.5.2.4	Four-wave mixing (FWM)	96
4.5.2.5	Stimulated light scattering	97
4.5.2.6	Stimulated raman scattering (SRS)	97
4.5.2.7	Stimulated brillouin scattering (SBS)	98
4.6	Conclusion	99
Chapter 5 - Proposed optical solution & theoretical analysis		100
5.1	Pulse propagation in an optical fiber	100
5.2	Chromatic dispersion compensation	102
5.3	Temporal Talbot effect	103
5.4	Fractional third order Talbot distances	105
5.5	Proposed optical solution	107
5.5.1	Optical nature	107
5.5.2	Principle	108
5.5.3	Periodization process	109
5.5.3.1	Mach-Zehnder interferometer (MZI)	110
5.5.3.2	Long period fiber grating (LPFG)	112
5.5.4	Advantages	113

5.6 Conclusion.....	114
Chapter 6 - Simulation results.....	115
6.1 Introduction	115
6.2 Setup description	115
6.3 Simulation of 40 Gb/s results	118
6.4 Bit Error Rate (BER).....	121
6.5 Robustness of the TEChDC method with respect to fiber length	124
6.6 Algorithm to easily find the matching integers: a and b	127
6.7 Comparison with another recently developed method	135
6.8 Conclusion.....	136
Chapter 7 - Conclusion	138
7.1 Summary.....	138
7.2 Future Work.....	141
References	142
Appendix: Publications	148

List of tables

Table 5-1:	Parameters used in the simulation	117
Table 5-2:	Comparison table	136

List of figures

Figure 1.1	Le calcul de l'ouverture numérique.....	11
Figure 1.2	L'atténuation dans les fibres monomodes	12
Figure 1.3	Effet de la dispersion pour les fibres monomodes.....	14
Figure 1.4	Effet de la dispersion chromatique en fonction du débit.....	16
Figure 1.5	Variation de la phase du noyau de Fresnel (la partie réelle est en pointillés).....	23
Figure 1.6	Distribution en ensemble d'impulsions de Dirac a amplitude différente, et invariante par produit de convolution par le noyau de Fresnel.....	24
Figure 1.7	Cas général des Distribution en ensemble d'impulsions de Dirac périodiques et invariants par produit de convolution par le noyau de Fresnel.....	25
Figure 1.8	Architecture du système proposé.....	30
Figure 1.9	Vue générale de la solution proposée.....	31
Figure 1.10	Diagramme de l'œil du signal de sortie pré dispersé	33
Figure 1.11	Mesure du TEB pour différents niveaux de puissance du laser avant et après l'utilisation de la méthode proposée.....	33
Figure 1.12	Influence de l'erreur de la distance d'observation (longueur totale de la fibre) sur le signal de sortie.....	34
Figure 3.1	General optical fiber system transmission system layout.....	55
Figure 3.2	General view of an optical fiber link.....	57
Figure 3.3	Modulator using Mach-Zehender Interferometer (L: length, g: width and V: voltage).....	61
Figure 4.1	Multi-mode step-index fiber.....	66

Figure 4.2	Multi-mode graded index fiber.....	67
Figure 4.3	Single-mode fiber. The core diameter is typically between 8 and 9 microns while the cladding diameter is 125 microns.	68
Figure 4.4	Photonic crystal fiber cut-view.....	71
Figure 4.5	Electro-magnetic wave spectrum	75
Figure 4.6	Electric and magnetic fields are orthogonal to each other and to the direction of propagation.....	76
Figure 4.7	Light propagation in a multi-mode fiber	77
Figure 4.8	The Goos-Haenchen shift causes a phase shift of the reflected ray as if reflected from a reflecting surface very slightly deeper in the cladding layer	77
Figure 4.9	Refraction	78
Figure 4.10	Critical angle	79
Figure 4.11	Calculating the Numerical Aperture.....	81
Figure 4.12	Attenuation for single-mode fiber	84
Figure 4.13	CD Effect - spreading the signal pulses [56].....	86
Figure 4.14	Total dispersion, D, and relative contributions of material dispersion, DM, and wave guide dispersion, DW, for a SSMF	87
Figure 4.15	Chromatic dispersion effect with respect to bit rate and distances	89
Figure 4.16	Dispersion types: a) PMD and b) CD.....	91
Figure 4.17	Phenomenological description of the spectral broadening of a pulse due to self-phase modulation.	94
Figure 6.1	General view of the TEChDC	116
Figure 6.2	Simulated receiver eye diagrams of noise-free pre-distorted 40-Gb/s.....	120
Figure 6.3	Receiver performance when transmitting a 40 Gb/s through.....	122
Figure 6.4	Comparing receiver sensitivity before and after applying the TEChDC method through 5000 km	122

Figure 6.5	a, b, c)Receiver performance for different fiber lengths in terms of BER with respect to laser power	124
Figure 6.6	Effect of the inaccuracy (5%) of the observation distance on the received signal	127
Figure 6.7	Tolerance and coefficients (a & b) relation.....	132
Figure 6.8	Duplication of the signal when we observe the replay field at $4Z_{T2} + Z_{T2}/4$ (x-axis is time and y-axis is amplitude)	134
Figure 6.9	Using the half Talbot distance $Z_T/2$ instead of Z_T itself (x-axis is time and y-axis is amplitude)	135

List of symbols

APD	Avalanche Photodiode
BER	Bit-Error-Rate
CWDM	Coarse Wavelength Division Multiplexing
DCF	Dispersion-Compensating Fiber
DCM	Dispersion-Compensating Module
DSF	Dispersion Shifted Fiber
DWDM	Dense Wavelength Division Multiplexing
EAM	Electro Absorption Modulator
EDFA	Erbium-Doped Fiber Amplifier
EO	Electro-Optical
ER	Extinction Ratio
FBG	Fiber Bragg Grating
FWM	Four Wave Mixing
GVD	Group Velocity Dispersion
IF	Intermediate Frequency
MUX	Multiplexer

MZM	Mach-Zhender Modulator
NZ-DSF	Non-Zero Dispersion-Shifted Fiber
NRZ	Non-return to Zero
OE	Opto-Electronic
OFC	Optical Fiber Communication
OOK	On-Off Keying
PM	Phase Modulation
PMD	Polarization Mode Dispersion
RZ	Return to Zero
SOA	Semiconductor Optical Amplifier
SPM	Self Phase Modulation
SRS	Stimulated Raman Scattering
SSB	Single Sideband
SMF	Single-Mode Fiber
SSMF	Standard Single-Mode Fiber
TEChDC	Talbot Effect Chromatic Dispersion Compensation
WDM	Wavelength Division Multiplexing
XPM	Cross Phase Modulation

Chapter 1 - Résumé en Français

1.1 Résumé

La fibre optique présente un milieu de transmission dont les performances sont assez prometteuses pour répondre à la demande sans cesse croissante en bande passante. La solution consiste à monter en fréquence, ce qui revient à réduire la taille de l'impulsion et par conséquent augmenter le débit. Cependant, de nombreuses limitations physiques se manifestent ainsi. On se propose de remédier à ces limitations en utilisant une méthode basée sur un phénomène physique, l'effet Talbot, tout en restant compatible avec les technologies émergentes en optique, et en particulier les techniques de multiplexage en longueurs d'onde WDM.

1.2 Introduction

La fibre optique, bien qu'elle soit le meilleur support en termes de performances, reste toujours, comme tout autre média de transmission, limitée par des effets physiques perturbateurs.

Pour répondre au besoin mondial croissant en bande passante, les nouvelles technologies ont permis de concevoir des nouvelles fibres qui évitent ces limitations. Cependant, ceci n'a jamais été une solution pratique, surtout que l'installation des liaisons fibrées est déjà en place et le remplacement de ces fibres enterrées semble être une opération aussi délicate que coûteuse.

Parmi les limitations physiques que rencontrent les transmissions optiques sur fibre, la dispersion chromatique présente la cause principale de la dégradation des performances des systèmes fonctionnant dans la bande de 1550 nanomètres.

Ce travail cherche à compenser la dispersion chromatique en utilisant une technique tout optique qui offre de nombreux avantages par rapport aux techniques d'égalisation électrique existantes.

1.3 Chaîne de transmission sur fibre optique

1.3.1 Introduction

Par rapport aux autres supports filaires classiques, les avantages qu'offre la fibre optique en termes de débit découlent essentiellement des propriétés physiques parfaitement adaptées aux transmissions à très haut débit. En effet, le rapport signal sur bruit élevé a permis de réaliser des transmissions longues distances avec des débits qui ont atteint aujourd'hui 111 Gb/s/canal, soit un total de 14 Tb/s.

Les techniques de modulation utilisées au niveau des émetteurs optiques sont essentiellement le NRZ « non return to zero » et le RZ « return to zero », vu la facilité d'implémentation avec les très hauts débits offerts par la fibre.

Des techniques de multiplexage sont aussi utilisées pour rehausser le débit en exploitant au maximum la bande passante offerte par le support optique. En effet, la dimension temporelle est divisée en slots temporels considérés dans l'ensemble comme des canaux pour le multiplexage temporel. D'autre part, par analogie avec les techniques de modulation fréquentielle, on emploie le multiplexage en longueur d'onde connu sous l'acronyme WDM « Wavelength Division Multiplex ». Ceci consiste à envoyer de l'information sur

différentes longueurs d'onde suffisamment écartées pour éviter toute interférence entre signaux.

L'architecture de la chaîne de transmission optique sur fibre comporte trois principaux blocs : un bloc émetteur qui englobe les différents équipements de génération du signal optique, un second bloc de traitement de signal qui sert essentiellement à régénérer le signal affaibli (atténué) en cours de transmission et un dernier bloc de réception représentant les équipements de détection du signal optique à l'autre bout de la fibre optique.

1.3.2 Émetteurs optiques

Les émetteurs optiques fonctionnent comme modulateurs de signaux optiques. Il existe deux façons de les implémenter : soit directement à partir de la source (diodes, lasers), ce qui offre la rapidité, mais à coût élevé, ou au moyen de composants optiques intermédiaires qui servent à moduler l'intensité.

Moduler l'intensité de la lumière directement à partir de la source peut engendrer des effets non linéaires indésirables, car les propriétés de l'onde émise dépendent de la tension appliquée au semi-conducteur. Ceci nécessite dans le cas des transmissions hauts débits, un étage modulateur externe pour palier à ce problème.

1.3.2.1 Diodes

Une diode électroluminescente se présente comme une jonction PN à semi-conducteur, qui émet de la lumière une fois parcourue par un courant électrique. La partie active d'une diode est une cavité à semi-conducteur constituée par deux régions dites P et N séparées par une jonction. La région P est chargée positivement, alors que N est chargée négativement. La jonction intermédiaire sert comme obstacle contre l'échange d'électrons.

Une différence de potentiel (ddp), appliquée entre les deux régions P et N, pousse les électrons de la région N à combler les trous de la région P en émettant un photon d'énergie $h\nu = E_i - E_f$

1.3.2.2 Laser

Le fonctionnement des lasers est similaire à celui des diodes électroluminescentes. Comme expliqué dans le paragraphe précédent, la longueur d'onde de l'onde émise est proportionnelle à l'énergie de gap $E_g = E_i - E_f$ entre les deux jonctions P et N. Dans le cas des lasers, la lumière émise est cohérente et peut être concentrée à l'aide des collimateurs optiques.

1.3.2.3 Modulateurs interférométriques

L'interféromètre de Mach Zehnder est utilisé pour diviser un signal optique en deux signaux pour parcourir deux branches différentes et les recombiner de façon à favoriser l'interférence entre les deux. Cette interférence peut être totalement ou partiellement constructive ou destructive. De cette façon, si on fait changer la phase de l'un des deux signaux, on fait varier l'amplitude du signal de sortie. D'où un basculement en phase entre les deux valeurs 0 et π , donne à la sortie un signal optique d'amplitude variant de 0 à 1 (interférence totalement destructive à totalement constructive).

1.3.3 Systèmes de traitement et régénération du signal optique

1.3.3.1 Média de transmission optique

La fibre optique est le média de transmission des signaux optiques. Mais bien que considérées comme le support de transmission le plus fiable en télécommunications, les

propriétés physiques et les imperfections de fabrication des fibres imposent des problèmes d'atténuation et de déformation (dispersion, ...) du signal transmis à travers ce support.

Les atténuations causent la chute de l'intensité du signal, alors que l'étalement des pulses, dû à la dispersion, cause l'augmentation de l'erreur binaire (BER) et par conséquent la réduction du rapport signal sur bruit (SNR).

La réponse spectrale de la fibre affiche des valeurs faibles de l'atténuation et de la dispersion entre 1250 et 1650 nanomètres.

1.3.3.2 Amplificateurs optiques

Les amplificateurs tout optiques amplifient le signal sans le convertir en électrique, lui permettant ainsi de parcourir des distances plus importantes. L'amplificateur à fibre dopé à l'erbium (erbium-doped fibre amplifier - EDFA) a l'avantage d'amplifier plusieurs longueurs d'onde en même temps, ce qui le rend très adapté à la technique WDM.

1.3.3.3 Régénérateur et répéteur

Ces systèmes fonctionnent en deux phases : convertissent le signal optique en électrique puis régénèrent un second signal optique. Ils permettent de sauver la forme du signal (information) avant qu'elle soit irrécupérable du fait des déformations (dispersion, ...).

1.3.3.4 Jonctions optiques

Ces composants servent à connecter les fibres entre elles, ou aux différents équipements optiques. Le soudage optique à l'arc est la méthode la plus utilisée pour relier deux tronçons de fibres ensemble.

1.3.3.5 Séparateurs optiques et coupleurs

Les séparateurs optiques sont des composants qui servent à diviser un signal optique en deux parties, voire plus. Dans la fibre cette même fonction est réalisée avec les coupleurs optiques qui sont des composants fibrés reliant trois bouts de fibre, voire plus.

1.3.4 Récepteurs optiques

Les récepteurs optiques sont les composants de terminaison de la chaîne de transmission optique. Généralement, ces composants font transformer la forme optique du signal en une autre forme (électrique, ondulatoire millimétrique)

1.3.4.1 Filtres optiques

Ces composants laissent passer une portion du signal optique selon certaines propriétés en bloquant l'autre partie (les réseaux de Bragg par exemple sont des filtres sélectifs en longueurs d'onde).

1.3.4.2 Photodétecteurs

Le rôle de ces composants est de moduler un signal électrique avec l'enveloppe du signal optique à la réception : C'est le principe de conversion optique électrique.

Les critères de performance de ces composants sont le temps de réponse, le faible bruit, la haute sensibilité, le faible coût et le haut rendement.

1.3.5 Conclusion

Dans cette partie on a présenté la chaîne de transmission optique tout en décrivant très brièvement le rôle de chaque bloc et composant de cette chaîne optique.

1.4 Filtres optiques et propagation

Une fibre optique est un support de transmission de forme cylindrique de dimension proche de celle du cheveu humain. Il se compose de deux parties : gaine et cœur.

La gaine (extérieure) et le cœur (intérieur) sont deux cylindres coaxiaux. L'indice de réfraction du cœur est conçu légèrement plus élevé que celui de la gaine pour permettre la réflexion totale (sous des angles axiaux faibles) du signal optique et le confinent du faisceau à l'intérieur du cœur.

1.4.1 Types de fibres optiques

On distingue essentiellement deux grandes catégories de fibres optiques : conventionnelles et spéciales (fibres capteurs, de nouvelles générations : cristaux photoniques, ...).

Les fibres conventionnelles sont les plus utilisées. On y trouve trois catégories : les fibres monomodes (à saut d'indice), les fibres multimodes à saut d'indice et les fibres multimodes à gradient d'indice.

La différence entre les fibres monomodes et multimodes est le mode de propagation de la lumière dans la fibre.

1.4.1.1 Fibre multimodes à saut d'indice

Ce type de fibre a un diamètre de cœur relativement élevé (25 micromètres) pour permettre la propagation de plusieurs faisceaux en même temps en mode multi trajet.

Les modes se propageant donc dans la fibre par réflexion totale sur l'interface cœur gaine.

Le problème majeur avec ce mode de propagation est la différence entre les longueurs de chemins optiques pour les faisceaux en question. Ces derniers arrivent au bout de la fibre (en fin de parcours) à des instants différents et subissent l'effet de dispersion ce qui favorise l'interférence entre symboles.

Une correction de ce problème était les fibres à gradient d'indice. Il s'agit en effet de changer l'indice de réfraction de la fibre graduellement du centre au bord du cœur. Ainsi, un faisceau parcourant la fibre au centre du cœur de la fibre parcourt un indice de réfraction plus élevé qu'un faisceau parcourant la partie supérieure du cœur.

Les faisceaux ayant un chemin physique plus grand parcourent la fibre plus rapidement que ceux dont le chemin est physiquement plus court et arrivent par conséquent au même instant au bout de la fibre.

1.4.1.2 Fibre monomode

Ces fibres sont caractérisées par un diamètre de cœur plus faible et conçues pour la propagation d'un seul mode par direction de polarisation pour une longueur d'onde donnée.

L'onde électromagnétique est amenée à se propager le long de l'axe de la fibre. La majeure partie de l'énergie est concentrée autour du centre du cœur de la fibre alors que 20% de celle-ci est répartie sur la gaine. Les fibres monomodes sont les plus efficaces pour la propagation des signaux sur des longues distances. Dans les systèmes de transmissions à fibres monomodes le multiplexage temporel est souvent utilisé pour augmenter leurs capacités de transmission.

1.4.1.3 *Fibres à cristaux photoniques*

Ce sont des fibres en silice ayant une forme particulière. Ils sont aussi appelés les fibres à trous à cause des trous cylindriques et symétriques, conçus le long de l'axe principal, et contenant de l'air.

La forme la plus utilisée dans la pratique est celle qui présente un cœur plein en silice et une gaine sous forme de trous d'air espacés, sous différentes formes géométriques, par de la silice.

L'indice de réfraction de la gaine varie en fonction de la longueur d'onde. Il existe donc une certaine plage de longueurs d'onde qui vérifie une différence en indice de réfraction permettant de réaliser la réflexion totale dans la fibre.

La forme, les diamètres et l'emplacement des trous dans ces fibres peuvent affecter la courbe de dispersion de celle-ci. Cette conception fut le sujet de plusieurs travaux de recherche qui ont avancé la conception de ces fibres pour avoir des fibres à dispersion nulle pour une longueur d'onde de $1.55 \mu\text{m}$.

1.4.1.4 *Fibres à cristaux liquides*

Les cristaux liquides nématiques sont des matériaux anisotropes qui constituent des molécules de forme cylindrique et dont la direction peut être changée sous l'effet d'un champ électrique externe.

Cette direction peut aussi dépendre du volume de l'ensemble des cristaux liquides et peut être bien déterminée si on confine ce volume dans une cavité cylindrique en absence d'un effet extérieur (champ électromagnétique, chaleur).

1.4.1.5 *Fibres en Plastic*

Ces fibres construites à partir du plastic sont moins cher que celles fabriquées à partir de la silice. Elles sont utilisées pour les transmissions à courtes distances à cause de la forte atténuation.

1.4.2 *Fabrication des fibres optiques*

Le processus de fabrication des fibres optiques se fait en deux phases :

- fabriquer un modèle en grandes dimensions avec les indices de réfraction effectifs souhaités
- chauffer et étirer le modèle pour avoir les dimensions de fibres souhaitées.

1.4.3 *Propagation de la lumière dans la fibre optique*

Une onde électromagnétique est composée de deux champs : électrique et magnétique, orientés perpendiculairement et se propageant suivant la direction perpendiculaire à leur direction.

Dans la fibre, la lumière se propage par réflexion sur l'interface cœur gaine. Ceci est aussi valable dans le cas d'une courbure qui ne dépasse pas la valeur tolérée (1.4 cm de rayon pour les fibres multimodes). D'autre part, l'ouverture numérique est une propriété importante de la fibre, elle est définie comme la mesure du taux de capture de lumière de la fibre.

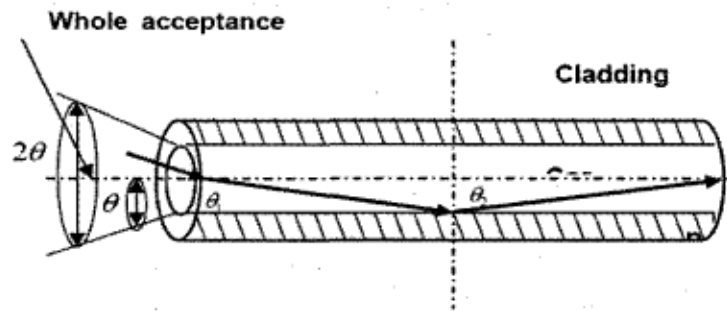


Figure 1.1 Le calcul de l'ouverture numérique

La figure 1.1 montre que pour un angle d'incidence assez étroit par rapport à l'interface air/fibre (air/cœur), le rayon d'incidence sera réfracté et l'angle que fait le rayon réfracté est égal à l'angle de réflexion (cœur/gaine) à l'intérieur de la fibre. L'angle d'acceptante (air/cœur) permet de définir un cône d'acceptante.

L'ouverture numérique est définie par le sinus du plus grand angle du cône d'acceptante, et elle est autour de 0.1 et 0.2 respectivement pour les fibres monomodes et multimodes.

$$NA = \sqrt{n_1^2 - n_2^2} \quad (1.1)$$

L'ouverture numérique permet aussi d'évaluer le rayon de courbure admissible pour la fibre. En effet, le rayon de courbure diminue pour une ouverture numérique qui augmente.

Cette donnée permet aussi de déterminer le nombre de modes à utiliser sur une même fibre (multimodes). En effet, le nombre de modes augmente avec l'ouverture numérique (ceci engendre des problèmes de dispersion que l'on discutera dans la section suivante).

1.4.4 Problèmes liés à la propagation

Connaître les défauts de la fibre est important pour pouvoir déterminer la distance que peut parcourir le signal sans devoir le régénérer. Les problèmes liés à la propagation dans la

fibres se résument en atténuations, distorsions, effets non linéaires et pertes radiatives dues aux impuretés dans la fibre.

La figure 1.2 traduit les atténuations par unité de kilomètre dans une fibre monomode en fonction de la longueur d'onde, ainsi que les deux importants mécanismes causant ces pertes : l'absorption du matériau et la diffusion de Rayleigh.

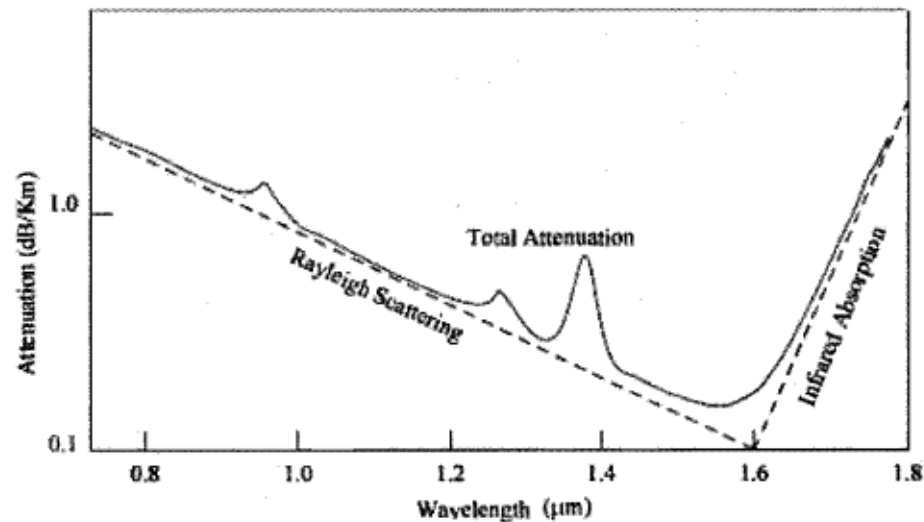


Figure 1.2 L'atténuation dans les fibres monomodes

La figure 1.2 montre que le minimum de l'atténuation (0.2 db/km) est situé autour de la région 1.55μm. Dans cette région la dispersion dans les fibres monomodes est importante. Un second minimum, égal à 0.5 db/km, est autour de la longueur d'onde 1.3 μm. Puisque la dispersion chromatique est minimale autour de cette dernière valeur de longueur d'onde, les premiers systèmes de transmission sur fibre étaient dans les années 1980 fonctionnels autour de 1.3 μm.

De nos jours, et avec l'apparition des amplificateurs EDFA ainsi que les systèmes de compensation de la dispersion chromatique, la plupart des systèmes fonctionnent à 1.55μm. (les EDFA ne fonctionnent qu'autour de 1.55μm).

1.4.4.1 Dispersion chromatique

La dispersion chromatique est la variation de la vitesse de propagation du signal optique en fonction de la longueur d'onde. Ceci est aussi connu sous le nom de Dispersion de vitesse de Groupe. Pour une fibre de longueur L , une composante spectrale du signal porté

sur une fréquence ω arrive au bout de la fibre après un délai de propagation $T = \frac{L}{V_g}$ où V_g

est la vitesse de groupe donnée par $V_g = \left(\frac{d\beta}{d\omega}\right)^{-1}$

Avec β est la constante du mode propagation

Par conséquent, une autre composante spectrale se propageant avec une autre vitesse de groupe V_g arrive dispersée dans le temps.

Le taux d'étalement du pulse dû à la dispersion chromatique est donné par la formule :

$$\Delta T = \frac{dT}{d\omega} \Delta\omega = \frac{d}{d\omega} \left(\frac{L}{V_g} \right) \Delta\omega = L \frac{d^2\beta}{d\omega^2} \Delta\omega = L\beta_2 \Delta\omega \quad (1.2)$$

Le facteur $\beta_2 = \frac{d^2\beta}{d\omega^2}$ est le paramètre de la « dispersion de la vitesse du groupe » et donne une mesure du degré de l'étalement d'une impulsion se propageant le long d'une fibre.

L'équation (1.2) peut aussi être écrite en fonction de la longueur d'onde :

$$\Delta T = \frac{d}{d\lambda} \left(\frac{L}{V_g} \right) \Delta\lambda = DL\Delta\lambda \quad (1.3)$$

$$\text{D'où } D = \frac{d}{d\lambda} \left(\frac{1}{V_g} \right) = -\frac{2\pi C}{\lambda^2} \beta_2$$

(D est le paramètre de dispersion exprime par ps/(km.nm))

La dispersion chromatique résulte de l'interaction de deux phénomènes. Premièrement, l'indice de réfraction de la silice dépend de la longueur d'onde des différentes composantes spectrales parcourant la fibre à différentes vitesses de groupe.

D'autre part, le deuxième phénomène appelé « la dispersion du guide d'onde » est dû au fait que la constante modale de propagation dépend aussi de la longueur d'onde.

Le paramètre D s'écrit donc comme la somme de ces deux effets : $D = DM + D_w$

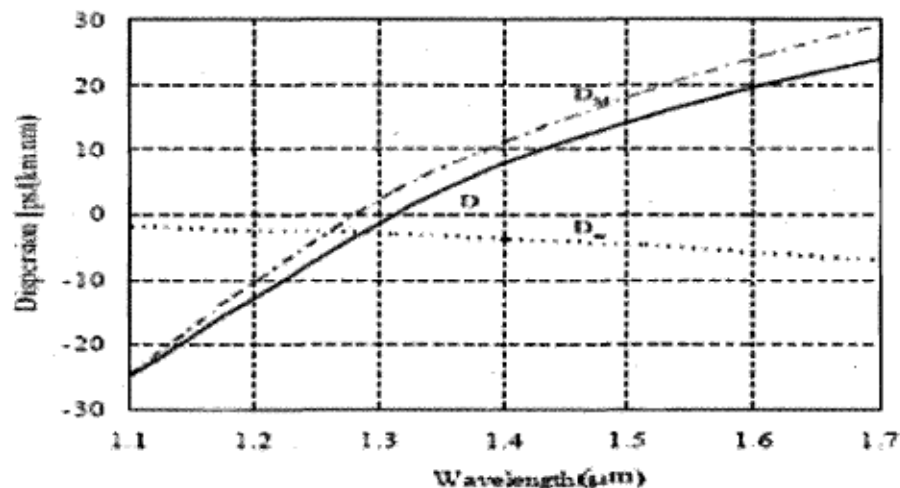


Figure 1.3 Effet de la dispersion pour les fibres monomodes

On constate, d'après la figure 1.3 que dans la région autour du 1.3 (région où le signal subit une forte atténuation), la dispersion est nettement moins élevée que dans la région spectrale de 1.55 μm.

Cette limitation peut être compensée en ajustant le profil d'indice de réfraction de la fibre. Ceci fait modifier l'indice de dispersion du guide et par suite permet de réaliser une

longueur d'onde à dispersion nulle autour de 1.55 μm (ces fibres sont appelées « Dispersion shifted fibres »)

Enlever complètement l'effet de dispersion conduit à des effets non linéaires, rendant l'utilisation de ses fibres modifiées impossibles avec des systèmes WDM. (là où l'on injecte plusieurs canaux étroitement espacés dans la même fibre). Ceci a conduit au développement d'autres types de fibres appelées fibres à dispersion non nulles « Non-Return to Zero Dispersion Shifted Fiber », qui sont caractérisées par un indice de dispersion D entre 1 et 6 ps/(km.nm) au lieu de 17 ps/(km.nm) pour le cas d'une fibre monomode normale opérant 1.5 μm . Ceci redonne la possibilité aux différentes ondes (portées sur différentes longueurs d'onde) de parcourir la fibre avec des différentes vitesses de groupe.

Cependant, il existe des effets de dispersion d'ordre supérieur limitant le lien optique même avec l'utilisation de ces fibres. Ceci est dû au fait que la dispersion ne peut jamais être nulle dans toute la région du spectre concentrée autour de la longueur d'onde à dispersion nulle. L'effet de la dispersion d'ordres supérieurs est d'autant plus prononcé que l'impulsion est plus brève.

Ces effets sont modélisés par le paramètre S appelé « pente de la dispersion ».

$$S = \left(\frac{2\pi C}{\lambda^2}\right)^2 \beta_3 + \left(\frac{4\pi C}{\lambda^3}\right)^2 \beta_2 \quad (1.4)$$

$$\text{Où } \beta_3 = \frac{d \beta_2}{d\omega} = \frac{d^3 \beta}{d\omega^3}$$

L'impact de la dispersion chromatique peut être réduit en utilisant des diodes lasers à ouvertures spectrales étroites et des modulateurs externes.

Les deux solutions les plus utilisées pour réduire la dispersion sont les fibres de compensation de dispersion DCF et les réseaux de Bragg gazouillées (Chirped Bragg gratings).

Les DCF sont des fibres à grandes valeurs de dispersion (de signe contraire à celui de la fibre de transmission) et sont introduites dans la chaîne (le lien) optique pour compenser la dispersion et l'approcher de la valeur nulle. Un inconvénient connu de cette dernière solution est les pertes d'insertion introduites dans le lien.

Les réseaux de Bragg gazouillés introduisent des différents délais à différentes longueurs d'onde et peuvent aussi être inscrits dans la fibre pour compenser la dispersion chromatique.

L'effet de la dispersion augmente avec le carré du débit (tout en considérant que les lasers sont à ouvertures très étroites). La figure 1.4 montre que pour un débit de 10 Gb/s, un système de régénération reste requis tout les 60 km mais seulement tout les 4 km pour un débit de 40Gb/s.

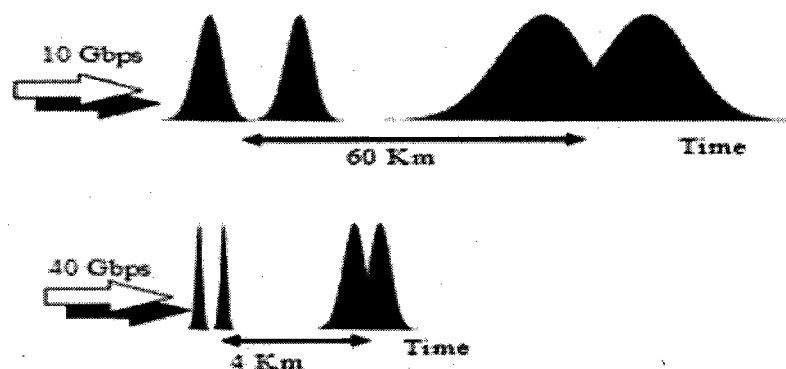


Figure 1.4 Effet de la dispersion chromatique en fonction du débit

1.4.4.2 Dispersion de mode de polarisation

Pour une longueur d'onde donnée, l'énergie d'un signal optique occupe deux modes de polarisations orthogonales au cours de sa propagation le long de la fibre.

Des imperfections comme les pressions latérales asymétriques, les changements de diamètre et de forme de cœur de fibre, etc., créent la biréfringence qui se traduit en une différence entre les indices de réfraction effectifs des deux modes (orthogonaux). Il se crée deux directions de polarisation, l'une dite rapide et l'autre lente.

À cause de la variation de la biréfringence, les deux modes se propagent à différentes vitesses, ce qui conduit à la rotation de l'orientation de polarisation du signal. Cet effet est appelé la DMP ou la dispersion de mode de polarisation.

À l'encontre de la dispersion chromatique, la DMP est un phénomène non régulier, puisque les perturbations qui causent cet effet varient avec le temps.

Un moyen pour caractériser la DMP qui est une fonction de la valeur moyenne du délai du groupe et est donnée par la relation $\Delta\tau \approx D_{PMD} \sqrt{L}$

D_{PMD} , mesuré en $(\frac{ps}{\sqrt{km}})$ est le paramètre moyen de la DMP

Vu la dépendance de la DMP par rapport au temps, la modélisation de cet effet devient complexe.

Pour simplifier la modélisation, la fibre est divisée en un grand nombre de segments. Dans chacun de ces segments, le degré de biréfringence reste constant, mais change aléatoirement de segment en segment.

Pour la PMD de premier ordre, la forme d'onde de sortie est reliée à l'entrée par

$$P_2(t) = \gamma P_1(t + \tau_0 + \frac{\Delta\tau}{2}) + (1 - \gamma) P_1(t + \tau_0 - \frac{\Delta\tau}{2}) \quad (1.5)$$

Avec τ_0 est le délai de groupe indépendant de la polarisation, et γ est l'énergie relative émise pour les deux états.

Les fibres modernes sont conçues pour minimiser la DMP, qui peut être moins de 0.1

$$(\frac{ps}{\sqrt{km}})$$

Alors que les fibres qui sont déjà en place dans les réseaux terrestres (depuis les années 1980) souffrent d'une grande valeur de la $D_{PMD} = 2(\frac{ps}{\sqrt{km}})$.

Remplacer ces fibres est une solution coûteuse. La solution la plus adéquate est de chercher des méthodes de compensation de ces distorsions.

Le problème qui se pose pour ces fibres d'anciennes générations est que la DMP fluctue aléatoirement avec le temps et peut dépasser ces valeurs moyennes.

1.4.4.3 Effets non linéaires

Les fibres optiques sont considérées comme un média de transmission linéaire pour les faibles puissances (quelques mW). Pour des débits élevés et des puissances de transmissions élevées, les non-linéarités deviennent des problèmes qui imposent des limitations aux performances du système.

Deux catégories d'effets non linéaires sont brièvement discutées dans les sections suivantes : celles qui découlent de la dépendance entre l'indice de réfraction et l'intensité du champ appliqué et celles dues aux effets de diffusions dans la fibre.

i. Modulation non linéaire de phase

L'indice de réfraction effectif de la silice a une faible dépendance par rapport à l'intensité et y est exprimé par

$$n = n_0 + n_2 I = n_0 + n_2 \frac{P}{A_{eff}} \quad (1.6)$$

Où n_0 est l'indice normal de la silice, n_2 est le coefficient non linéaire d'indice, P la puissance optique et A_{eff} est la section effective de la fibre. Cette non-linéarité est appelée l'effet Kerr

ii. Auto Modulation de Phase

La constante de propagation β est liée à la puissance par la formule :

$$\beta' = \beta + \gamma P \quad (1.7)$$

où β est la constante de propagation relative à l'indice de propagation effectif constant, γ est le coefficient de non-linéarité et P la puissance optique.

Pour une fibre de longueur L , le terme γ produit un saut de phase donné par :

$$\Phi_{NL} = \int_0^L (\beta' - \beta) dz = \int_0^L \gamma P(z) dz \quad (1.8)$$

La phase varie donc au cours du temps puisque la puissance en dépend aussi.

iii. Modulation Croisée de phase

Dans les systèmes WDM, plusieurs canaux optiques sont transmis en même temps dans une même fibre. Le saut de phase d'un canal non linéaire ne dépend pas seulement de

l'intensité de ce même canal, mais aussi des canaux adjacents transmis en même temps : ceci est appelé la modulation croisée de phase ou XPM.

La XPM se produit seulement quand deux impulsions à deux différents canaux se recouvrent dans le temps, ceci ne peut se réaliser que pendant une fraction de la période de l'impulsion puisqu'ils se propagent avec des vitesses différentes

iv. Mélange à quatre ondes

Le mélange à quatre ondes est un effet non linéaire de troisième ordre pour les fibres en silice, et ressemble aux effets d'inter modulation dans les systèmes électriques.

En effet, trois champs optiques se propageant en même temps donnent naissance à un quatrième (produit d'inter modulation) qui est relié aux trois autres par la relation :

$$f_4 = f_1 \pm f_2 \pm f_3 \quad (1.9)$$

Des effets de diaphonies peuvent avoir lieu si la nouvelle fréquence correspond à l'un des autres. Sur le plan pratique, plusieurs de ces combinaisons n'ont pas lieu car ils ne satisfont pas la condition générale de phase.

v. Diffusion Stimulée de Raman

La diffusion de Raman se produit lorsqu'une onde optique incidente est diffusée par les molécules de la silice. Par conséquent, une onde ayant une longueur d'onde plus grande est créée. La différence d'énergie entre ces deux ondes (l'onde incidente et l'onde créée) est absorbée par la fibre.

La fréquence de la lumière diffusée impose le rythme des oscillations des molécules de silice. L'amplitude de l'onde diffusée augmente avec ces oscillations, ce qui peut amplifier toute autre onde portée sur la même longueur d'onde.

Ce processus peut donc être vu comme une transformation d'énergie d'une longueur d'onde à une autre.

1.5 Méthodes de compensation de la dispersion chromatique

L'emploi des fibres à compensation de dispersion (FCD) présente la méthode de compensation de la dispersion chromatique la plus utilisée. Cette méthode consiste à insérer à l'un des bouts de la fibre de transmission de longueur Z_1 un tronçon de FCD de longueur Z_2 . Cette dernière fibre est caractérisée par un effet de dispersion inverse à celui de la fibre de transmission. Ainsi, le signal parcourt la distance totale $Z_1 + Z_2$ pour retrouver sa forme initiale.

Les pertes d'insertion dans les FCD ne sont pas négligeables. On a donc intérêt à concevoir des FCD courtes (Z_2 petite par rapport à Z_1) mais avec un montant élevé de dispersion négative (la dispersion d'ordre 2 de la fibre de transmission est généralement positive).

Si on considère le second et le troisième ordre de la dispersion, les FCD doivent satisfaire la condition suivante :

$$\beta_2 Z_1 + \beta_2 Z_2 = 0 \text{ et } \beta_3 Z_1 + \beta_3 Z_2 = 0 \quad (1.10)$$

Ceci est valable pour une pré-égalisation ou une post-égalisation.

Il existe une deuxième méthode assez populaire. Celle-ci consiste en une pré-égalisation. L'effet opposé de dispersion est introduit avant la transmission par l'intermédiaire des réseaux de Bragg gazouillés ou les modulateurs à phase quadratique.

Cependant, ces techniques de compensation sont limitées par la technologie de production de ces composants, ainsi que la bande spectrale adéquate de fonctionnement.

La méthode que nous proposons est totalement différente et se base sur un phénomène physique que nous décrivons dans la section suivante.

1.6 Effet Talbot

1.6.1 Reproduction intégrale spatiale

En champ proche, la formule de diffraction, appelée aussi diffraction de Fresnel, correspond au produit de convolution du champ électrique initial par le noyau de Fresnel :

$$h(x_0, y_0) = \frac{\exp\left(i \frac{2\pi}{\lambda} z\right)}{i\lambda z} \bullet h(x_1, y_1) \otimes \exp\left(i \frac{\pi}{\lambda z} (x_0^2 + y_0^2)\right) \quad (1.11)$$

où le noyau de Fresnel est :

$$\exp\left(i \frac{\pi}{\lambda z} (x_0^2 + y_0^2)\right) \quad (1.12)$$

Dans l'expression de la formule de la diffraction de Fresnel, donnée par l'équation (1.11), on voit que pour avoir une reproduction intégrale, traduite par une égalité stricte entre le champ de départ et celui d'arrivée, respectivement $h(x_1, y_1)$ et $h(x_0, y_0)$, le noyau de Fresnel doit être égal à la distribution de Dirac.

Autrement dit, pour neutraliser le produit de convolution, il faut avoir un second terme qui correspond à l'élément neutre du produit de convolution, à savoir le Dirac.

Dans ces conditions, la transformée de Fourier du champ d'arrivée sera égale à celle du champ de départ à une constance de phase près (amplitude maintenue à cause de la conservation d'énergie) :

$$H_0(u, v) = H_1(u, v) \cdot \lambda z \exp(-i\pi\lambda z(u^2 + v^2)) = \text{const} \cdot H_1(u, v) \quad (1.13)$$

Cette condition impose que le terme en exponentielle dans l'équation (1.13) soit égal à une constante, ce qui est impossible dans le cas général, tout simplement parce qu'une fonction exponentielle est loin d'être constante !

Dans une première étape, prenons la transformée de Fourier du noyau de Fresnel, la fonction : $\lambda z \exp(-i\pi\lambda z(u^2 + v^2))$.

La variation de sa phase est représentée par la figure 1.5 :

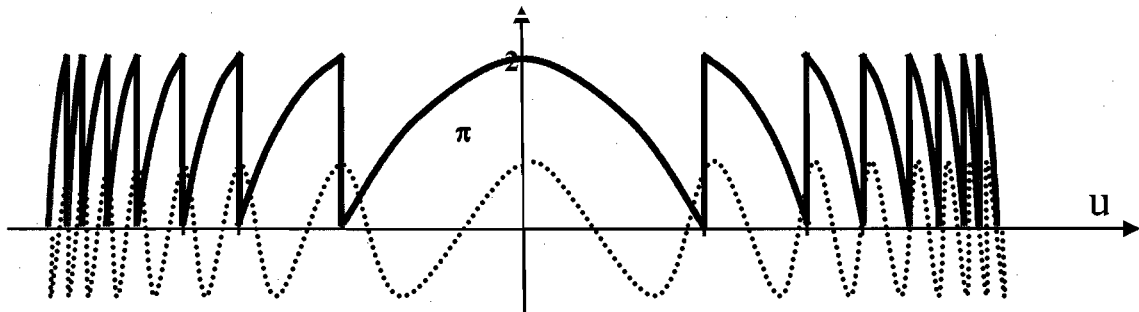


Figure 1.5 Variation de la phase du noyau de Fresnel (la partie réelle est en pointillés)

Il est clair que pour certaines distributions, telle qu'une fonction sous forme d'un train d'impulsions de Dirac, particulièrement réparties, la convolution (la multiplication dans le plan de Fourier) est neutre.

Ce résultat peut être généralisé. En effet, les fonctions neutres par rapport au produit de convolution par le noyau de Fresnel ont une forme beaucoup plus générale :

On voit dans la figure 1.6 que non seulement l'amplitude des impulsions de Dirac peut varier (amplitude 0 veut dire qu'un Dirac est manquant) sans incidence sur le résultat de la convolution, mais aussi la phase.

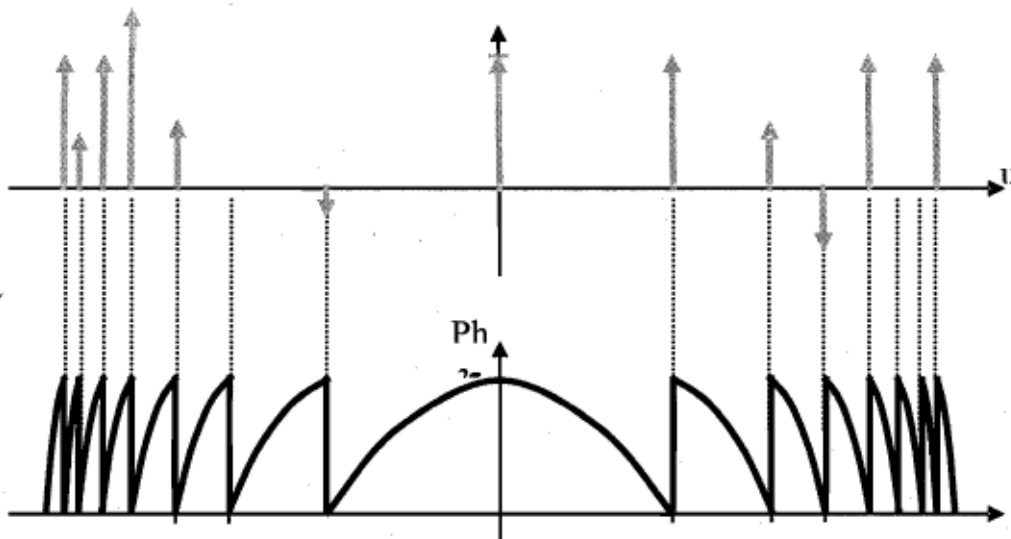


Figure 1.6 Distribution en ensemble d'impulsions de Dirac a amplitude différente, et invariante par produit de convolution par le noyau de Fresnel

On peut aussi modifier l'emplacement de ces Diracs tout en respectant la condition de phase, ces distributions particulières ont une forme encore plus générale.

Les fonctions périodiques présentent des cas plus particuliers de ces distributions. (représentées en pointillés sur la figure 1.7).

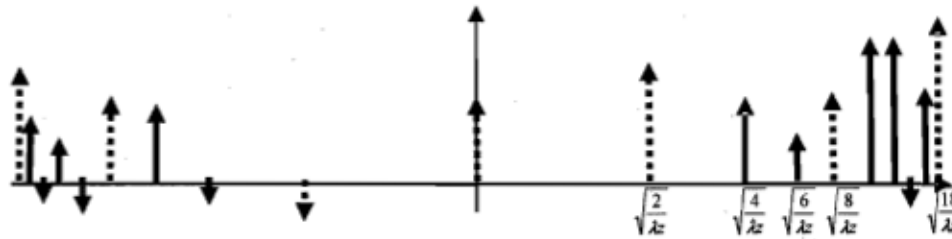


Figure 1.7 Cas général des Distribution en ensemble d'impulsions de Dirac périodiques et invariants par produit de convolution par le noyau de Fresnel

1.6.2 Effet Talbot

L'auto imagerie, aussi appelée l'effet Talbot, est un phénomène assez connu en optique. Cet effet consiste en la reproduction d'une distribution périodique dans des endroits périodiques le long de l'axe de propagation de l'onde.

La distance séparant deux distributions identiques (images) successives est appelé la distance Talbot et est égale à

$$Z_T = \frac{2d^2}{\lambda}$$

où Z_T est la distance Talbot, λ est la longueur du signal et d la période spatiale de la distribution.

1.6.3 Effet Talbot fractionnaire spatial

L'effet Talbot fractionnaire est le cas général de l'effet Talbot. Il est observé quand la distance d'observation est une fraction de la distance Talbot :

$$z = \frac{p}{q} Z_T \quad (1.14)$$

Avec p et q deux entiers premiers entre eux.

Si on considère un champ périodique initial $h(x) = h(x,0)$. Le champ diffracté observé à la

distance $z = \frac{p}{q} Z_T$ est exprimé par la somme (15) :

$$h(x, z) = \sum_{a=0}^{q/2-1} T(a, p, q) h\left(x - \frac{d}{2} + \frac{2ad}{q}\right) \quad (1.15)$$

Les coefficients de Talbot sont donnés par la relation (1.16)

$$T(a, p, q) = \frac{2}{q} \sum_{b=0}^{q/2-1} \exp\left[-i\pi\left(2\frac{b^2}{q}p + b\right)\right] \times \exp\left(i\pi\frac{4ab}{q}\right) \quad (1.16)$$

Le champ diffracté $h(x,z)$ d'un objet périodique à la fraction z de la distance Talbot est le résultat de la superposition de répliques déplacées de l'élément original, et pondérées par les coefficients Talbot décrits par l'équation (16).

1.6.4 Effet Talbot temporel

L'effet Talbot temporel est un phénomène d'auto-imagerie, qui se réalise quand un signal périodique se propage à travers un média dispersif, à une distance Z_T appelé distance Talbot.

Si l'effet de la dispersion de vitesse de groupe est dominant, alors la distance de Talbot

$$Z_T \text{ sera égale à } Z_{T2} = \frac{d^2}{\beta_2 \pi}.$$

où d est la période temporelle et Z_{T2} est la distance de Talbot relative à la dispersion de second ordre.

Un cas particulier de l'effet Talbot est observé quand la distance d'observation est une fraction de la distance Talbot :

$$Z = \frac{p}{q} Z_T \quad (1.17)$$

Ceci est connu sous le nom de l'effet Talbot fractionnaire (par analogie à l'effet de Talbot fractionnaire spatial). Le résultat observé est différent dépendamment de la valeur de p et q qui sont deux entiers premiers entre eux.

Si le signal parcourt la moitié de la distance de Talbot, il regagnera sa forme initiale, mais sera déplacé (temporellement) de la moitié de la période ($d/2$).

D'une façon générale, si le signal parcourt une distance égale à $Z = \frac{Z_T}{2m}$ (où m est un entier), le signal reconstruit aura la période divisée par m (si on se limite à l'intensité du signal).

Si maintenant, on prend en considération les effets de dispersion de troisième ordre, la distance de Talbot est donnée par la formule 1.18.

$$Z_{T3} = \frac{3}{2} \frac{d^3}{\beta_3 \pi^2} \quad (1.18)$$

où Z_{T3} est la distance Talbot relative à la dispersion chromatique de troisième ordre.

De même, l'effet Talbot fractionnaire peut aussi être observé pour les effets de dispersion d'ordres supérieurs. Pour les effets de troisième ordre, on peut reproduire à un déplacement près le même signal périodique à différentes fractions de la distance Talbot, précisément à la moitié, le $1/3$ et le $1/6$ de cette distance. En général, ceci est valable pour $mZ_T/6$ (où m est un entier positif quelconque).

Dans ce cas le signal est translaté par le produit de la période temporelle et l'ordre choisi ($1/2$, $1/3$ ou $1/6$).

Passons maintenant la modélisation de la propagation d'un signal optique à travers une fibre, qui est un milieu non- linéaire, avec pertes, isotrope, homogène et dispersif. La variation de l'enveloppe complexe (noté $u(t)$) est déterminée par l'équation non- linéaire de Schrödinger (équation 19), sous l'hypothèse de l'approximation de la variation lente de l'enveloppe (« Slowly Varying Envelop Approximation » SVAE).

$$i \frac{\partial u}{\partial z} + \frac{i}{2} \alpha u - \frac{1}{2} \beta_2 \frac{\partial^2 u}{\partial T^2} - \frac{i}{6} \beta_3 \frac{\partial^3 u}{\partial T^3} + \gamma |u|^2 u = 0 \quad (1.19)$$

où u est l'amplitude complexe du champ électrique qui varie dans l'espace (premier terme) au cours du temps (troisième et quatrième termes), z est la coordonnée longitudinale de la fibre, $T = t - \beta_1 z$ est le temps par rapport à une trame de référence qui bougerait à la vitesse de groupe $v = 1 / \beta_1$ (t étant le temps physique), α est le coefficient d'atténuation et γ le paramètre de non-linéarité relatif à l'auto modulation de phase.

Dans le cas de la fibre où la dispersion chromatique est le phénomène physique dominant, l'équation (1.19) se résout dans le domaine de Fourier et la solution est donnée par l'équation (1.20) si on ne tient pas compte de l'atténuation (α) et les effets non linéaires (γ) ainsi que la dispersion chromatique d'ordres supérieurs à 4.

$$U(w) = U(w,0) \exp\{i2\pi D(w)z\}$$

$$\text{avec } U(w) = \left(\frac{\beta_2}{2} w^2 + \frac{\beta_3}{6} w^3 \right) \quad (1.20)$$

Pour tenir compte de la dispersion chromatique d'ordre 1 (β_1) il suffit de considérer une fenêtre de temps se déplaçant avec la vitesse de groupe. Si on considère l'effet Talbot

de dispersion de deuxième et de troisième ordre en remplaçant Z_{T2} et Z_{T3} dans l'équation (1.20) on obtient

$$U_d(w, z) = \sum_m U\left(\frac{m}{d}, 0\right) \exp\{i2\pi D_m\} \delta\left(w - \frac{m}{d}\right) \quad (1.21)$$

$$\text{Avec } D_m = \left(\frac{1}{Z_{T2}} + \frac{m}{Z_{T3}}\right) m^2 z$$

ici m est un entier.

Le phénomène d'auto imagerie ne peut être observé que s'il existe deux entiers a et b tel que

$$Z_T = aZ_{T2} = bZ_{T3}$$

Ce qui est équivalent à : $\frac{a}{b} = \frac{3}{2} \frac{\beta_2}{\beta_3} \frac{d}{\pi}$

Le cas de l'effet Talbot fractionnaire donne la possibilité de combiner le second et le troisième ordre de l'effet Talbot.

Par exemple, si la distance globale est $z = Z_{T2}/2 = Z_{T3}/6$, le signal périodique est translaté simultanément par la moitié d'une période (deuxième ordre de l'effet Talbot) et par le un sixième d'une période temporelle (troisième ordre de l'effet Talbot).

1.7 Solution proposée

1.7.1 Architecture

Le signal optique arrive déformé à cause de la dispersion chromatique après une certaine distance de propagation Z_1 . Cette déformation est beaucoup plus prononcée quand les impulsions sont plus brèves. L'idée consiste à périodiser le signal obtenu après la

distance Z_1 et à le faire propager une fois de plus à travers une deuxième fibre standard de longueur Z_2 tel que $Z_T = Z_1 + Z_2$. Le signal reçu n'est rien d'autre qu'une réplique du signal initial. Il suffit donc d'appliquer une simple troncature (d'une période) pour récupérer le signal initial.

La figure 1.8 illustre l'architecture du système de compensation proposé.

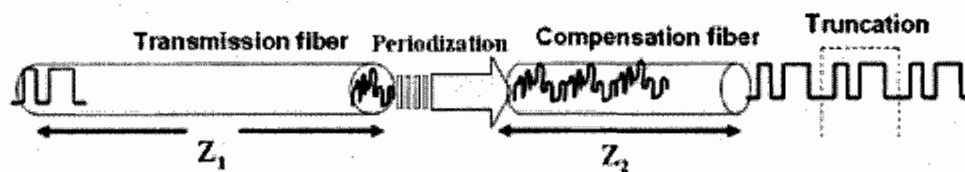


Figure 1.8 Architecture du système proposé

1.7.2 Implémentation de la périodisation

L'étage de périodisation présente la partie la plus complexe du système. Cette opération peut être réalisée par la mise en cascade multiétage soit d'interféromètres de Mach-Zehnder IMZ ou de réseaux de Bragg à long pas RBLP.

Pour l'étage de périodisation utilisant les IMZ, le signal est divisé (répliqué) en deux. Chaque réplique parcourt une branche. Sachant qu'il existe un temps de délai entre les branches de chaque interféromètre, la recombinaison produit à partir du signal incident, deux répliques identiques et distantes. En mettant en cascade plusieurs étages et en choisissant les bonnes valeurs du temps de délai, le signal à la sortie devient périodique.

La figure 1.9 montre l'étage de périodisation implémenté avec 4 IMZ avec des différents temps de délai.

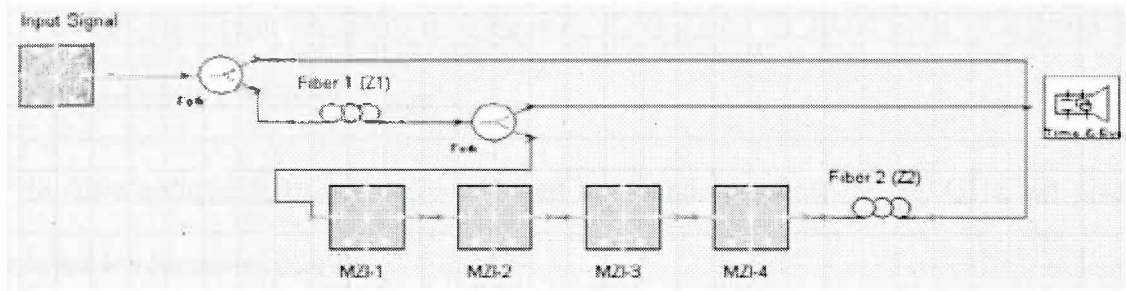


Figure 1.9 Vue générale de la solution proposée

La méthode présente de nombreux avantages. Elle permet de récupérer un signal totalement déformé, irrécupérable par n'importe quelles autres méthodes, en utilisant l'auto-imagerie. Elle utilise une fibre optique standard et s'applique à tout type de fibres ou milieu dispersif. De plus, elle peut traiter la dispersion d'ordres élevés et montre une grande flexibilité et degré de liberté concernant la périodisation et les ordres de Talbot Fractionnaire.

1.7.3 Simulations

La simulation du fonctionnement du système vise à étudier ses performances. Elle a été réalisée sous des conditions de fonctionnement réelles. Une séquence binaire pseudo aléatoire à un débit de 40Gb/s est injectée dans une fibre monomode. Le système opère dans la bande des 1550nm. Une séquence de longueur (2^n-1) a été choisie de manière à assurer que tous les motifs binaires de longueur n soient simulés. Cette modélisation est nécessaire pour simuler les systèmes souffrant de l'interférence entre symboles.

Des EDFA à gain de 20 dB sont placées entre les sections de la fibre choisie à différentes longueurs, pour les différents montages expérimentaux (2000, 4000 et 6000

Km). La dispersion pour les fibres de longueurs Z_1 et Z_2 est de $15.69 \mu\text{s/m}^2$. La pente de dispersion est égale à 50.1051 M s/m^3 .

Un filtre optique de troisième ordre ayant une bande passante de 100 GHz, est placé juste avant le récepteur optique.

Les résultats développés dans cette section correspondent à la modulation RZ. Ces résultats ont aussi été testés et validés avec les autres techniques de modulation telle que la NRZ.

Les performances du système sont quantifiées, soit en termes de la sensibilité du récepteur ou de la pénalité de puissance optique. La sensibilité du récepteur détermine la puissance minimale à l'entrée de ce dernier, qui garantit le taux d'erreur binaire (TEB) acceptable (dans la plage de 10^{-12} à 10^{-20}). La puissance du signal est parfois peu significative. On utilise la pénalité de puissance optique qui définit l'intervalle de puissance entre les niveaux de référence, qui garantit un TEB acceptable.

La figure 1.10 illustre l'ouverture du diagramme de l'œil du signal de sortie se propageant à travers une fibre de 1500 Km. Le diagramme de l'œil donne une première évaluation des performances et un aperçu de la nature des imperfections. Dans le cas de la figure 1.10, on voit bien que l'ouverture de ce dernier est assez écartée pour garantir une détection correcte.

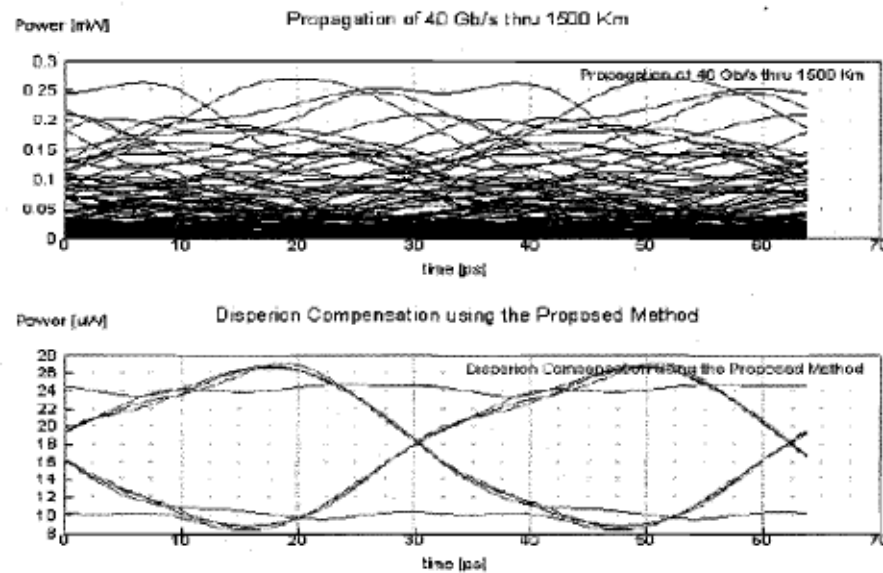


Figure 1.10 Diagramme de l'œil du signal de sortie pré dispersé

Le taux d'erreur binaire représente la probabilité de l'identification incorrecte d'un bit par le circuit du récepteur.

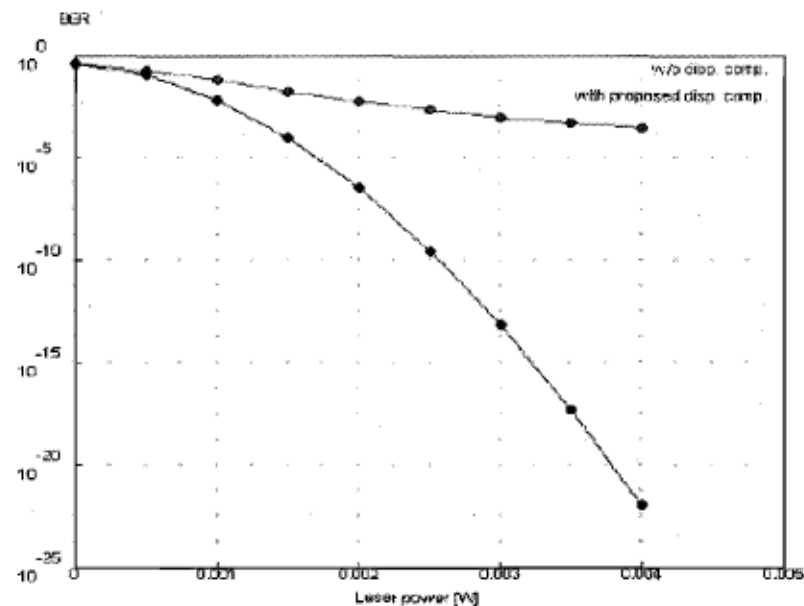


Figure 1.11 Mesure du TEB pour différents niveaux de puissance du laser avant et après l'utilisation de la méthode proposée.

La figure 1.11 montre le TEB, avant et après l'application de la méthode proposée pour une longueur de fibre égale à 2000 Km. Cette figure montre clairement le gain en puissance d'émission apportée par cette dernière.

Comme a été expliquée dans les sections précédentes, l'effet Talbot fractionnaire est observable à une distance $Z = \frac{p}{q} Z_T$ où Z_T est la distance Talbot.

L'effet de l'erreur au niveau de la détermination de la distance de l'observation Z a été simulé avec l'applet en prenant $Z = \left(\frac{p}{q} + e \right) Z_T$.

L'applet montre à travers la figure 1.12 que l'erreur tolérée (au niveau de la longueur z) avant que le signal commence à se déformer atteint le 5%. La figure 1.12 a) montre qu'une erreur de 0.2% n'influe pas sur le signal, qui commence à dévier à partir de 5% d'erreur (figure 1.12 b))

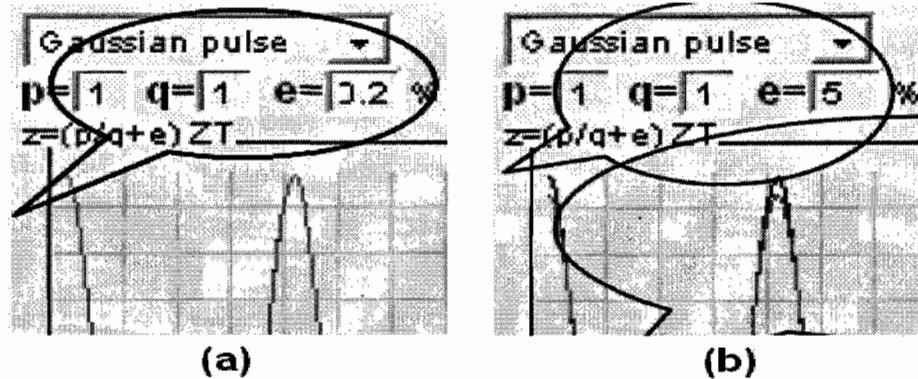


Figure 1.12 Influence de l'erreur de la distance d'observation (longueur totale de la fibre) sur le signal de sortie

L'effet Talbot fractionnaire peut remédier, à la fois, à la dispersion du second et du troisième ordre. Il a été expliqué dans les sections précédentes que la distance d'observation doit être, dans ce cas, tel qu'il existe deux entiers a et b vérifiant : $Z_T = aZ_{T2} = bZ_{T3}$

Ce qui est équivalent à : $\frac{a}{b} = \frac{3 \beta_2 d}{2 \beta_3 \pi}$.

Par exemple, pour une distance de Talbot, d'ordre 2, Z_{T2} égale à 400Km et une distance de Talbot, d'ordre 3, Z_{T3} égale à 997 Km, la distance commune pour la compensation prévue est égale à $Z_T = 400 \times 997 = 389\,800$ Km, qui est de l'ordre de la moyenne de la distance Terre-Lune !

La solution est donc de chercher une distance d'approximation Z' assez suffisamment courte (pour être réalisée en pratique) et respectant une erreur tolérée.

Pour le même exemple, on remarque que $5 \times Z_{T2} = 2000$ Km et que $2 \times Z_{T3} = 1994$, qui sont deux valeurs assez proches.

On peut donc prendre $a' = 5$ et $b' = 2$ qui sont deux valeurs acceptables et vérifiant la condition suivante :

$$\left| \frac{a}{b} - \frac{a'}{b'} \right| < tol ; \quad or \quad \left| \frac{a}{b} - \frac{a'}{b'} \right| = 0.0012 < tol = \frac{1}{100}$$

Pour une différence du rapport inférieure à la valeur tolérée 1%, a' et b' peuvent être des valeurs de substitution aux valeurs a et b sans affecter significativement le signal observé à la distance z .

1.8 Conclusion

Le défi pour la compensation de la dispersion chromatique du second et du troisième ordre dans les systèmes à haut débit, est l'implémentation des solutions avec des composants tout optique, qui ne dégradent pas les performances du lien optique.

La méthode proposée se base sur l'effet physique, dit effet Talbot, qui s'applique dans le domaine optique de Fresnel. Elle implique des systèmes tout optiques et n'impose aucune conversion optoélectronique.

Ses performances ont été vérifiées avec un débit de 40 Gb/s avec des fibres monomodes. Ce débit est très souhaité dans les communications optiques.

La méthode proposée offre plusieurs autres avantages. Elle offre une totale restauration de la forme du signal qui a été totalement modifié par l'effet de la dispersion chromatique, et une liberté totale pour le choix de la période et des distances de Talbot fractionnaires (le rapport p/q peut être inférieur comme il peut être supérieur à 1). Cette méthode est totalement indépendante du débit choisi et offre aussi la possibilité de réduire la puissance du laser émetteur. Aucune imposition sur le type de fibre à utiliser n'étant faite, cette méthode a montré son efficacité avec des fibres monomodes ordinaires.

La tolérance pour le choix de la longueur de la fibre atteint le 5%, qui est une valeur assez confortable et rend le dimensionnement du système assez flexible.

Alors que ce travail vise seulement la compensation de la dispersion chromatique et non pas la dispersion du mode de polarisation et les effets non linéaires, il peut être facilement combiné avec d'autres méthodes pour atteindre cet objectif.

Chapter 2 - Introduction

For a better understanding of this thesis as a whole, its sections are organized as follows: The present chapter presents an introduction outlining the context and major objectives of the work, a literature review of existing methods related to the subject, a definition of the issue studied, the originality of the work and our scientific contribution. Next, there is a short description of the problems regarding data transmission in an optical fiber link, namely, attenuation, chromatic dispersion (CD), polarization mode dispersion (PMD) and non-linearity.

Chapter 2 offers an overview of optical fiber systems (transmitter, transmission medium and receivers), including the components and devices put into play. Chapter 3 outlines the physical background of the phenomenon to be compensated, dispersion. First, however, light propagation is analyzed to introduce this phenomenon inherent in propagation. Next, a more detailed description of fiber impairment is presented in detail including attenuation, chromatic dispersion (CD), polarization mode dispersion (PMD) and non-linearity. The proposed solution called “**Talbot Effect Chromatic Dispersion Compensation (TEChDC)**” is described in Chapter 4. This description follows a theoretical analysis of the Talbot effect and its related mathematical equations, which we used as a basis for the desired compensation. Results are presented in Chapter 5, and Chapter 6 contains the summary and a conclusion regarding future work.

2.1 Context and main objective

In high speed digital communication systems, the effect of each symbol transmitted over a time dispersive channel extends beyond the time interval required to represent that symbol. This causes interference between the neighboring symbols, which eventually leads to a distortion of the received signal. This inter-symbol interference (ISI) is a major obstacle to reliable high speed data transmission over optical fibers.

Like any transmission medium, optical fiber suffers from impairments limiting the bandwidth-distance product (in GHz·km). The latter term often appears in the context of optical fiber communications and will be used in the present document. The (bandwidth·distance) product, which is normalized to 1 km, is a useful figure of merit for predicting the effective fiber bandwidth for other lengths and concatenated fibers [1].

Because of the world's growing need for more communication bandwidth, constant progress is reported in the building of newer fibers capable of handling the rapid increase in traffic. Building an optical fiber link is a major investment, however, and is very expensive to implement. For example, the optical fiber cables installed during the 1980s consist of more than 50 million kilometers of "standard" single-mode fiber (SSMF). By the end of 1988 in North America alone, over 10 million kilometers of fiber had been installed, and more than 90 percent of long distance telephone traffic was carried on optical fibers. Since old optical fibers cannot be easily replaced with newer ones, innovative methods of exploiting the available bandwidth are crucial. Even today, standard single-mode fibers are substantially cheaper than the more advanced fibers [2].

Accordingly, the main objective of this thesis is to increase the bandwidth distance product, thereby reducing cost and error while maintaining the existing single-mode fiber-based communication infrastructures. Particular attention is given to Chromatic Dispersion. TEChDC is suitable for both pre- and post equalization depending on the application. It has many advantages, including complete freedom to choose the period, the high-order Talbot distances; no need to increase the number of repeaters, which results in major cost savings; it is independent from the bit rate sent originally, which means it can handle higher bit rates; and no special fiber is required.

2.2 Literature findings

When it comes to chromatic dispersion, any fiber length can be compensated for, since the required equalizer can be built. For heterodyne detection, the compensation can be done at the intermediate frequency (IF) by using microstrip lines [3], microwave waveguides [4] and monolithic microwave integrated circuits (MMICs) [5] whose phase responses can be designed to counteract those of the fiber. Equalization can also be performed by using a homodyne receiver, but at the cost of a substantial increase in complexity [6]. Equalization can also be performed by using fractionally-spaced tapped delay line equalizers, as shown in [7]¹. Compared with microstrip lines and waveguides, they offer the advantages of being tunable (or even adaptive) and capable of equalizing other linear distortions such as PMD and the non-ideal receiver response. Owing to the nature of a SSMF in the 1550 nm band, the coefficients of the equalizer are complex-valued, that is, they must produce a gain and phase shift. Alternatively, a quadrature hybrid can be used to generate the in-phase and

¹ Only simulation results were presented.

quadrature components of the signal. Thus, the equalizer at IF can be built from two filter banks with real-value coefficients. At the baseband, more hardware is required where four cross-coupled filter banks are needed to equalize the in-phase and quadrature electrical signals. However, the filters require only a bandwidth that is equal to, rather than twice, that of the baseband signal, as in the pass-band equalizer. Despite the potential for equalization in coherent receivers, the research effort decreased significantly in this area, mainly because of the practical difficulties of building a coherent receiver. Instead, research focused on equalization in direct detection receivers.

In [8], an 8-tap linear equalizer, a DFE with only one feedback tap and a DFE with 8 feed-forward taps and 1 feedback tap, were experimentally investigated to examine the electrical mitigation of PMD-induced signal distortion. The latter was shown to exhibit the lowest residual penalty with a maximum value of nearly 5 dB at a 100 ps differential group delay. At moderate distortion levels corresponding to a DGD as high as 70 ps, the penalty of the linear equalizer was less than 3 dB and was comparable to that of the second DFE.

One of the first adaptive 10 Gb/s optical receivers was reported in [9]. The receiver incorporates an 8-tap fractionally-spaced transversal filter that was used to compensate for PMD. Adaptation was performed by monitoring the eye diagram with a pseudo-error monitor (PEM) chip. The PEM chip contains two decision devices: the first is the main detector used for the normal detection of the received data bits, and in the second detector the decision threshold was detuned to generate pseudo-errors. These pseudo-errors can be correlated to the actual errors for determining eye quality. This technique allows bit error rate measurement in a range where conventional methods are too time-consuming. The entire adaptation process was controlled by a microprocessor. Also, an adaptive 5-tap

fractionally-spaced transversal filter used to compensate for PMD was reported in [10]. An eye monitor chip provided a measure of the eye opening, which was used by the control system to direct the adjustment of tap weights.

To accommodate fast PMD fluctuations that can occur from mechanical vibrations [11], the authors in [12] proposed using the least-mean-square (LMS) algorithm to adaptively adjust the equalizer coefficients. System level simulations were performed on a 7-tap linear equalizer. The results showed that the LMS algorithm can cope with the fastest expected time-varying distortions. The principle of operation was demonstrated experimentally by using a 4-tap transversal filter and several SiGe ICs. Only the first tap was adaptively controlled, while the others were set to a fixed value. Nevertheless, LMS adaptation is not easy to implement with analog signal processing techniques close to the speed limit of the electronics. Therefore, most of the adaptive equalizers reported so far depend on some sort of variation of the differential steepest descent algorithm [13]. Quality signals can be derived from error monitor chips [14] or eye-opening monitor chips [15] that are fed into the adaptation control processor. As well, there have been reports on utilizing the error count of a forward error correcting chip (FEC) to provide a low-cost adaptive solution [16, 17]. These simpler-to-implement algorithms, however, come with a substantial speed penalty compared with the LMS algorithm.

As for maximum likelihood detection equalizers, no experimental work has been reported till now for 10 Gb/s, mainly because of implementation complexity, especially if the equalizer must be adaptive. Nevertheless, theoretical discussions and system level simulations reveal the superiority of maximum likelihood detection to all other equalization

methods, with the potential to more than double the distance limited by chromatic dispersion [18, 19, 20, 21, 22].

It has been demonstrated that nonlinear equalization using a decision feedback equalizer (DFE) is required to reduce the power penalty caused by CD and PMD to acceptable levels [23]. The only 40-G bits/s DFE reported to date was mentioned by Nakamura *et al.* [24]. Hazneci and Voinigescu [25] reported a 49-G bits/s transversal filter implemented in $0.18\ \mu\text{m}$ SiGe BiCMOS. The filter has a tap spacing of 6.75 ps, and cable equalization at 40 and 49 G bits/s was demonstrated. The equalizer makes use of a traveling-wave topology, with Gilbert cell tap multipliers distributed along the length of the input and output transmission lines. The nominal power consumption is 750 mW .

A 1 tap 10 G bits/s FBE implemented in an AlGaAs/GaAs high electron mobility transistor technology was described by Mäoller *et al.* [26]. The IC consumes 600 mW, and equalization of PMD with DGDs up to 1.2 bit periods was demonstrated. A 5 tap 10 G bits/s analog equalizer implemented in a $0.25\ \mu\text{m}$ SiGe process was reported by Azadet *et al.* [27]. This IC targets equalization of both multi-mode fiber (MMF) and SMF, and equalization of PMD with DGD equal to half of a bit period was demonstrated.

Kanter *et al.* [28] reported a self-adaptive 10 tap FFE for equalization in a 10 G bits/s optical system. The stated objective of the equalizer is to increase the length of optical links that use electro-absorption modulators (EAMs). Wu *et al.* [29] reported a 7 tap (50 ps tap spacing), 10 G bits/s transversal equalizer for equalization of inter-modal dispersion in MMF. The IC was implemented in a $0.18\ \mu\text{m}$ SiGe BiCMOS process and consumes 40 mW . This equalizer makes use of a traveling-wave topology, with delays implemented using artificial L-C transmission lines and gain cells composed of Gilbert cell multipliers.

As recently reported by *Chongjin Xie et al* [30], optical duobinary modulation has attracted much attention for its compact spectrum and good transmission performance. It has been shown that a non-return-to-zero (NRZ) duobinary format can tolerate about three times more chromatic dispersion than ordinary NRZ, and that return-to-zero (RZ)-duobinary is more tolerant of nonlinearity than ordinary RZ in highly dispersed pseudo-linear transmission systems. A commercially available duobinary transmitter with a 2.5-GHz duobinary electrical filter generated a 9.953-Gb/s NRZ-duobinary signal. A pulse carver was positioned after the duobinary transmitter to produce a 33% duty-cycle RZ-duobinary. Different lengths of fibers induced the required chromatic dispersion.

The OSNR was measured in 0.1-nm noise bandwidth. It shows that the optimum optical bandwidth for back-to-back NRZ-duobinary is about 10 GHz (one time bit rate), which is smaller than NRZ (about 14 GHz difference). The optimum optical filter bandwidth is about 27 GHz for RZ-duobinary, which is close to that of conventional RZ. Shrinking the optical filter bandwidth can reduce amplified spontaneous emission (ASE) noise in the receiver, so decreasing the filter bandwidth can improve system sensitivity as long as the filter does not induce significant signal loss and distortions. Eye diagrams for the RZ-duobinary system with 8- and 71-GHz optical filter bandwidths at different amounts of chromatic dispersion were shown. With the wide-filter bandwidth, there is almost no signal information in the eye diagram when the system has about 3085-ps/nm chromatic dispersion. With the 8-GHz filter bandwidth, the eye diagram of the back-to-back RZ-duobinary looks similar to that of the NRZ-duobinary.

Lothar Möller et al, [31] demonstrated that at the receiver, an improvement of the back-to-back (b-t-b) performance of optical duobinary signals at 10 Gb/s. The required optical

signal-to-noise ratio for a bit-error rate of 1×10^{-3} was found to be as low as 10.8 dB in b-t-b operation. The receiver was tested with two commercially available 10-Gb/s duobinary transmitter samples. Excellent chromatic dispersion tolerance was maintained with the novel receiver design.

H. Gnauck et al, [32] experimentally compared non-return-to-zero and return-to-zero ON-OFF keying with a number of recently proposed modulation formats for 1980-km 42.7-Gb/s single-channel transmission over a standard single-mode fiber. Substantial performance improvements are obtained with the new formats. In back-to-back measurements, all 33% and 67% RZ formats (including single-detector RZ-DPSK) had a similar performance, reaching a bit-error rate (BER) of 1.0×10^{-3} at an OSNR of 14.5–15.0 dB (measured in a 1.0-nm resolution bandwidth and referred to 0.1 nm). NRZ performance was about 1 dB poorer, while RZ-DPSK with balanced detection was about 2.5 dB better. The BER of the various OOK signals after transmission as a function of the power launched into each SSMF span was shown. When the launched power is low (-3 dBm), the system is almost linear. The performance for all formats is similar and largely set by the received OSNR of 14.9 dB. As the power is increased, dramatic performance differences among formats become apparent. The NRZ format, as expected, is the least robust in terms of nonlinearity. Furthermore, for the NRZ, it was necessary to adjust the chromatic post-compensation at each power level for optimum performance.

2.3 Originality

To the best of our knowledge, TEChDC method for chromatic dispersion compensation based on the Talbot effect is being exploited for the first time. The interest of this phenomenon lies in the integral reproduction of the signal along the propagation axis,

referred to as “self-imaging”. Once drastically deformed, a periodic optical signal recovers its initial shape after traveling one or a multiple of the Talbot distance. Thus, when the initial signal is periodized, its total deformation during propagation is of no importance if the fiber length is equal to one or a multiple of the Talbot distance. The originality of this work stems from this observation.

2.4 Thesis contribution

This thesis explores the possibility of applying the concept of optical pre- and post equalization to 40 Gb/s signals that are transmitted over SSMF. Previously known electrical and/or optical schemes [33, 34] are limited only to pre-chirping/DCF, which are limited to achieve modest improvements and/or are bulky and expensive to implement as will be discussed later on. Moreover, major signal deformations go beyond the capacity of these methods.

TEChDC is suitable for both pre- and post equalization depending on the application. It has many advantages, a few of which are:

- The signal received may be totally altered.
- There is complete freedom to choose the period, the high-order Talbot distances.
- There is no need to increase the number of repeaters, which results in major cost savings.
- It is independent from the bit rate sent originally, which means it can handle bit rates in excess of 40 G bit/s.
- No special fiber is required. Standard single mode fibers can be used.

Our method is based on the Talbot Effect. This latter is a self-imaging phenomenon that occurs when a periodic signal propagates through a dispersive medium at a given distance named Talbot distance Z_T . Therefore, the key element and main idea in the TEChDC is the regeneration of a periodic signal where one period is similar to the initial signal. This property is the main reason for using the temporal Talbot effect to optically compensate for the chromatic dispersion. While periodization creates the power of the system, it is also the source of its complexity. The distorted optical signal obtained from a transmission fiber of length Z_I passes through a periodization stage. As detailed in chapter 4, this operation can be performed by a multistage cascaded Mach-Zehnder interferometer (MZI) or cascaded long period fiber grating (LPFG). Using a MZI-based periodization stage, the input signal is split in two. Each part travels along a leg. Because of the time delay between MZI legs, the recombination produces two distanced identical images. When cascading several stages, if an appropriate time delay for each stage is chosen, the outgoing signal becomes periodic. Finally, the periodized signal propagates a second time over another standard fiber of a complementary length of Talbot distance (or half of any appropriate fractional distances).

The TEChDC solution is applied not only to the first order dispersion but also to the combination of second and third order chromatic dispersion. Indeed, both second and third order dispersion can be handled either separately or simultaneously by TEChDC. However, this leads to an optimization of the length of the correcting fiber. Both Talbot distances Z_{T2} and Z_{T3} are calculated, leading to a common Talbot distance Z_T , which may be infinite if calculated rigorously. However, we showed that reasonable quasi-common Talbot distances can be found. For this purpose, an algorithm was developed to easily calculate the integer parameters a and b in the following equation: $Z_T = aZ_{T2} = bZ_{T3}$.

To assess the performance of the TEChDC under more realistic transmission impairments, the following case was considered. A 40-Gb/s scenario system was carried out with different system effects. The system ran over a Standard single-mode fiber (SSMF with 2000, 4000 and 6000 km fiber lengths) and operated in the 1550-nm band. The simulation results show that the TEChDC is capable of carrying high data through long distances as demonstrated and explained in Chapter 5.

To prove the feasibility of the TEChDC architecture, an applet was created to simulate all possible conditions including second and third order dispersion. The applet calculates the error, that is, the tolerance that helps determine the length of the fiber.

2.5 Problematic issues

Generally, an optical fiber consists of a central core, surrounded by a cladding layer whose refractive index is slightly lower than that of the core. The optical fiber acts as a dielectric waveguide to confine light within its surfaces and guides the light in a direction parallel to its axis. This confinement of light is achieved using the phenomenon called a total internal reflection. Total internal reflection is achieved when the angle of incidence of light is greater than the critical angle [35].

As with any other transmission medium, signal loss and distortion in an optical fiber are important degradation factors. The loss of signal is attributed to *attenuation* in the fiber as the signal propagates through it. The distortion of signal is due to *dispersion* in the fiber, which causes optical signal pulses to broaden as they travel along it. Dispersion is our main concern in this thesis, during which we propose a novel approach for solving the issue. Along with attenuation and dispersion, fibers also add *nonlinear effects*. Fiber

nonlinearities can be classified into two categories based on their origin. One category of nonlinearity arises from the Kerr effect, which is the intensity-dependent variation in the refractive index of a fiber. This produces effects such as *self-phase modulation* (SPM), *cross-phase modulation* (XPM) and *four-wave mixing* (FWM). The other category arises from the nonlinear inelastic scattering processes. These are *stimulated Raman scattering* (SRS) and *stimulated Brillouin scattering* (SBS). These factors are briefly discussed in the following subsections.

2.6 Attenuations

While light propagates along the fiber, its power decreases exponentially with distance owing to fiber attenuation. Attenuation plays a major role in determining the maximum non-amplified transmission distance between a transmitter and a receiver or the distance between the in-line amplifiers. The main loss mechanisms are material absorption, Rayleigh scattering, and radiative losses of the optical energy.

Material absorption includes the intrinsic absorption of silica, the material used to manufacture the fiber, and the extrinsic absorption owing to impurities in the fiber. The material absorption of pure silica is negligible in the entire 0.8-1.6 μm band (ultraviolet absorption) used for optical communication systems. Infrared absorption dominates the fiber loss beyond 1.6 μm , making the fiber unusable.

2.7 Chromatic dispersion (CD)

Chromatic dispersion is the variation in the speed of propagation of a lightwave signal with wavelength. This phenomenon is also known as group velocity dispersion (GVD), since dispersion occurs because group velocity is a function of the wavelength.

Chromatic dispersion results from the interplay of two phenomena. The first is that the refractive index of silica is frequency-dependent. Therefore, different frequency components travel at different speeds in the silica. This component of chromatic dispersion is called material dispersion. The other component is called waveguide dispersion, which results from the dependence of the modal propagation constant on the wavelength.

Systems operating in this wavelength range, however, are attenuation-limited. As a result, there is considerable interest today in optical communication systems that operate in the 1.55 μm band owing to the low loss in this region and well-developed EDFA technology [36].

2.8 Polarization-mode dispersion (PMD)

The signal energy at a given wavelength occupies two orthogonal polarization modes. In ideal fibers with a perfect rotational symmetry, the two modes are degenerate with equal propagation constants, and any polarization state that is injected into the fiber propagates unchanged. However, real fibers contain imperfections such as asymmetrical lateral stresses, non-circular cores and variations in the refractive-index profiles. These imperfections break the circular symmetry of the ideal fiber creating *birefringence*, which is the difference between the effective refractive indices of the two modes. As a result, the modes propagate with different velocities. The resulting difference in propagation times, $\Delta\tau$ (differential group delay (DGD)), causes pulse-spreading. As well, the variation of birefringence along the length of the fiber induces a rotation of the polarization orientation. This is called *polarization mode dispersion* (PMD).

In contrast to chromatic dispersion, which is a relatively stable phenomenon along a fiber, the PMD varies randomly along the same fiber. The main reason for this is that the perturbations causing the birefringence effects vary with the temperature. In practice, this shows up as a random, time-varying fluctuation in the value of the PMD at the fiber output. Therefore, statistical predictions are needed to account for PMD. A useful means of characterizing the PMD for long fiber lengths is in terms of the mean value of the differential group delay.

2.9 Nonlinear optical effect

For practical purposes, the optical fiber can be treated as a linear medium, as long as the fiber is being used at a reasonable power level (a few mW). However, at high bit rates such as 10 Gb/s and above, and/or at higher transmitted powers, nonlinearity becomes an important issue that can place significant limitations on system performance. For WDM systems, the nonlinear effects can become important even at moderate powers and bit rates.

There are two categories of nonlinear effects: nonlinearity due to the dependence of the refractive index on the intensity of the applied electric field, and nonlinearity due to scattering effects. These nonlinear effects are briefly discussed in the following section.

2.9.1 Nonlinear phase modulation

The refractive index of silica has a weak dependence on optical intensity. In silica, the value of n_2 ranges from 2.2 to $3.4 \times 10^{-8} \mu m^2/W$. This nonlinearity in the refractive index is known as *Kerr nonlinearity* and results in a carrier-induced phase modulation of the propagating signal, called the *Kerr effect*. It can cause *self-phase modulation* (SPM), *cross-phase modulation* (XPM) and *four-wave mixing* (FWM).

2.9.2 Self-phase modulation (SPM)

Because the local refractive index is a function of the optical intensity of the propagating signal, the mode propagation constant becomes dependent on the optical intensity as well.

Since this nonlinear phase modulation is self-induced, the nonlinear phenomenon responsible for it is called SPM. As phase fluctuations translate into frequency fluctuations, SPM causes frequency chirping of the optical pulses, which is a source of error.

2.9.3 Cross-phase modulation (XPM)

In WDM systems, where several optical channels are transmitted simultaneously inside an optical fiber, the nonlinear phase shift for a specific channel depends not only on the power of that channel but also on the power of the other channels. Moreover, the phase shift varies from bit to bit, depending on the bit pattern of the neighbouring channels. This nonlinear phenomenon is known as XPM. Like SPM, XPM may lead to erroneous reception of the transmitted bits sequence.

2.9.4 Four-Wave Mixing (FWM)

FWM is a third order nonlinearity in silica fibers caused by the third order nonlinear susceptibility of silica. FWM resembles inter-modulation distortion in electrical systems. If three optical fields with carrier frequencies f_1 , f_2 , and f_3 are propagating simultaneously in a fiber, the fiber nonlinearity causes them to mix, producing a fourth inter-modulation term that relates to the other frequencies by the equation $f_4 = f_1 \pm f_2 \pm f_3$. FWM is an additional source of ISI.

2.10 Conclusion

We began this chapter by describing the context and main objective of the present work. It is widely recognized that modern society is in constant need of bandwidth owing to technological advancements and such recent Internet innovations as video on demand, e-learning and numerous other applications. Optical fiber communication is one of the best means possible for carrying the huge amounts of data required to meet present-day as well as future expectations. Nevertheless, OFC faces a major obstacle that will prevent it from realizing its full potential.

A literature survey was presented describing the latest solutions to such issues; these solutions are limited to the achievement of modest improvements and/or are bulky and expensive to implement. The major problems facing OFC (attenuation, CD, PMD and non-linearity) are described in greater detail in Chapter 3. In chapter 4, we present the TEChDC scheme and discuss its merits in details. We believe that the TEChDC provides the optical community a way to overcome the above obstacles. Simulation results are performed and discussed in Chapter 5. The results show that the TEChDC resolves the issue of signal degradation over a long distance and provides enough bandwidth using the current installed optical fibers.

Chapter 3 - Optical Fiber Transmission Systems

3.1 Introduction

The goal of an optical fiber communication system is to transmit the maximum number of bits per second over the maximum possible distance with the fewest errors. A typical digital fiber optic link is depicted in Figure 2.1.

Data encoded as electrical pulses are recoded instead as optical pulses. Electrical data signals are converted to optical signals via a transducer. “1” is transmitted as a pulse of light while a “0” has no light output. This modulation is referred to as “ON-OFF keying.”

The use of light as a method of communication can be dated to antiquity if we define optical communications more broadly. People used mirrors, fire beacons, or smoke signals to relay a single piece of information.

The idea of using glass fiber to carry an optical communications signal was conceived during the time of Alexander Graham Bell; however, almost a century passed (in 1966, Charles Kao and George Hockham at Standard Telecommunications Laboratories in England published their famous landmark theoretical paper [37]), before better glasses and low-cost electronics made the idea useful in practice. Modern fiber-optic communications began during the 1970s, when the GaAs semiconductor laser was invented and optical fiber loss could be reduced to 20 dB/km in the wavelength region near $1\mu\text{m}$ [38].

During the last four decades, optical communications in public networks evolved from a curiosity to the dominant technology. Among the thousands of developments and inventions that contributed to this evolution, five major inventions stand out as milestones [31]:

- Invention of the LASER (in the early 1960's)
- Development of low loss optical fiber (1970's)
- Invention of the fiber Bragg grating (late 1970's)
- Invention of the optical fiber amplifier (late 1980's)
- Development of WDM technique (1990's)

3.2 Overview

An optical communications system consists, on the whole, of an optical source, transmitter, medium and receiver. In the digital optical transmission system, the data bit rate per channel is assumed to be in the range of multi G b/s (up to 40 G b/s/channel are currently feasible). In the transmitter, a time-division multiplexer (MUX) combines several parallel data channels into a single data stream with a high bit rate. Then, a driver stage generates the current required for driving the laser diode directly or the voltage required to drive an external modulator indirectly. Non return-to-zero (NRZ) and return-to-zero (RZ) are the most commonly applied modulation formats because of their implementation simplicity at very high speeds.

Similar to frequency division multiplexing in radio systems, *wavelength division multiplexing* (WDM) can be used to increase the transmission capacity beyond that limited

by the speed of electronics. The idea of WDM is to simultaneously transmit data at multiple carrier wavelengths over a fiber. Interaction among these different channels is minimized by placing these wavelengths sufficiently apart from each other. WDM can expand the capacity of the link into the Terabit/s region, well beyond the capabilities of electrical transceivers [39, 40].

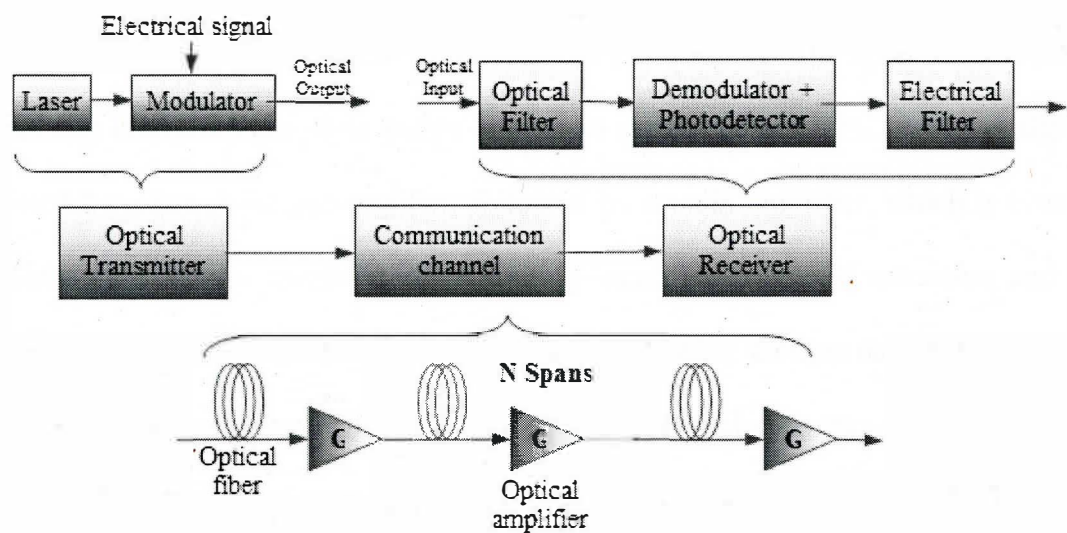


Figure 3.1 General optical fiber system transmission system layout

Traditionally, the optical link span was limited by fiber attenuation, and repeaters had to be placed wherever the optical power dropped below a certain level. To regenerate an optical signal with a conventional repeater, optical-to-electrical conversion, electrical amplification, retiming, reshaping and, finally, electrical-to-optical conversion are necessary. This is expensive for a high-speed multi-wavelength system; therefore, optical amplifiers such as Erbium Doped Fiber Amplifiers (EDFA) are used instead. Transparent to bit rates and modulation formats, optical amplifiers offer the advantage of easy system upgrading by changing the equipment at the ends of the link. Another advantage is that the

optical amplifiers can amplify signals at many wavelengths simultaneously. However, the link now becomes limited by other fiber impairments such as chromatic dispersion, polarization mode dispersion, and the nonlinear effects in the fiber. For long-haul applications, dispersion compensating modules (DCMs) such as Dispersion Compensation Fiber (DCF) are placed periodically along the link to compensate for the chromatic dispersion (CD).

At the end, an optical de-multiplexer routes each wavelength to its designated electrical receiver. In the latter, a photo-detector (which can be either a P-I-N diode or an avalanche photodiode) converts the optical pulses into small current pulses. This low-level signal is amplified by a low-noise preamplifier, followed by a main amplifier, which is either an automatic gain control amplifier or a limiting amplifier. A clock extraction and data regeneration circuit recovers the timing information from the random data and samples the data stream at the right moment. Finally, a serial to parallel converter de-multiplexes the retimed serial data to a lower rate, where the data is processed by other circuitry [28].

3.3 System concepts

Fiber optic communications systems are deployed worldwide and have certainly revolutionized current and future telecommunications infrastructures. At present, virtually all telephone conversations, cellular phone calls, and internet packets must pass through pieces of optical fibers from source to destination. While initial deployments of optical fiber are intended mainly for long-haul or submarine transmissions, lightwave systems are currently in virtually all metro and access networks and are considered the backbone of Local Area Networks (LANs).

A fiber-optic system can generally be viewed as a system with three main components: a transmitter (dashed box), a transmission medium (the rest), and a receiver (dashed box) as shown in Figure 2.2. A regenerator may be used if the distance between the transmitter and the receiver is very long, causing the signal to be drastically deformed and attenuated before reaching the receiver. As a model, it is similar to the copper wire system that fiber-optics replaces. The difference is that fiber-optics use light pulses to transmit information down a fiber instead of electronic pulses to transmit information down copper lines. In the following sections we study the three main components in the fiber-optic chain to offer a better understanding of how the system works in conjunction with wire-based systems.

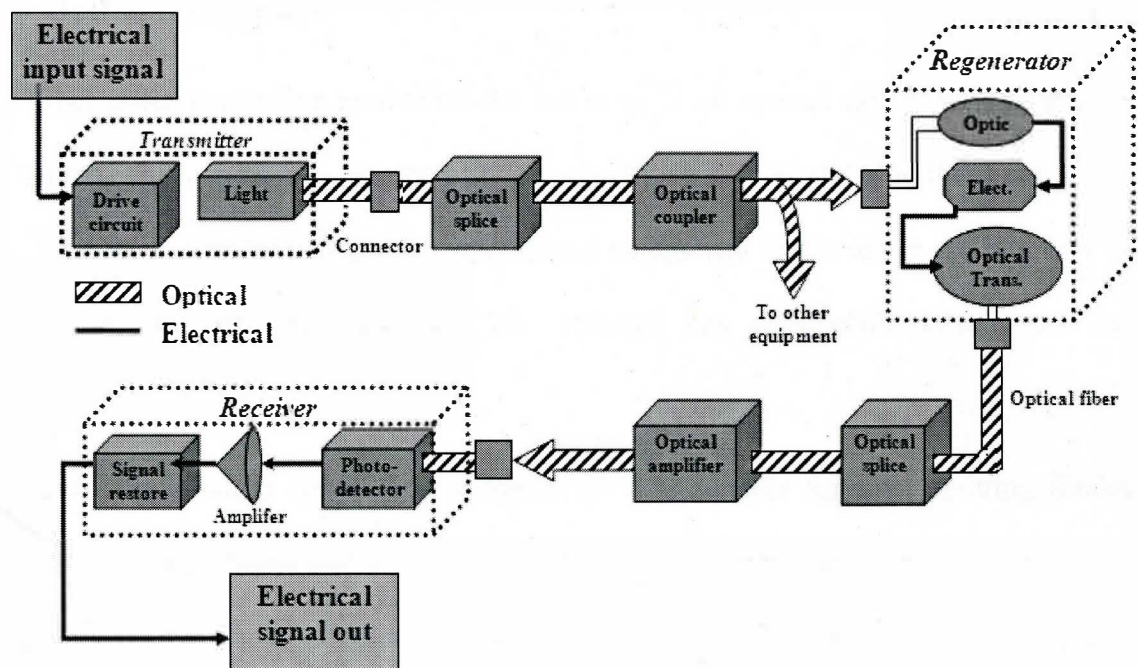


Figure 3.2 General view of an optical fiber link

- A serial bit stream in electrical form is presented to a modulator, which encodes the data properly for fiber transmission.

- A light source Light-Emitting Diode (LED) or laser is modulated by the modulator and the light is focused into the fiber.
- The light travels down the fiber (and suffers loss reducing its intensity).
- At the receiver end the light is incident onto a detector and converted to electrical form.

The signal is then amplified and fed to another detector, which isolates the individual state changes and their timing. It then decodes the sequence of state changes and reconstructs the original bit stream [41].

3.4 Optical transmitters

A fiber optic transmitter modulates the intensity of an optical carrier generated by a light source. This can be done in one of two ways: by directly modulating the input power to the light source, or by using a separate optical component that changes the intensity of the light leaving the light source. Each approach has its specific advantages and disadvantages.

Direct modulation is simple and inexpensive. It is suitable for light emitting diodes (LEDs) and semiconductor lasers, because their light output increases with the drive current passing through the semiconductor device once a certain threshold bias current is exceeded in the case of the laser. The input signal modulates the drive current, so the output optical signal is proportional to the input electrical signal. However, LEDs take time to respond to changes in the drive current. Semiconductor lasers are much faster, but their optical properties change slightly with the drive current, causing a slight “chirp” in the wavelength as the signal switches ON and OFF. External modulation is needed for high speed systems

(> 2.5 Gb/s) to minimize undesirable nonlinear effects such as chirping. A variety of external modulators are available either as separate devices or as integral parts of laser transmitter packages [41].

3.4.1 *Light-emitting diode*

A Light-Emitting Diode (LED) is essentially a P-N junction solid-state semiconductor diode that emits light when a current is applied through the device. The essential portion of the Light Emitting Diode is the semiconductor chip. This chip is divided into two parts or regions separated by a boundary called a junction. The P-region is dominated by positive electric charges (holes) and the n-region is dominated by negative electric charges (electrons). The junction serves as a barrier to the flow of the electrons between the p and n-regions. This is somewhat similar to the role of the band-gap because it determines how much voltage must be applied to the semiconductor chip before the current can flow and the electrons move across the junction into the p-region. Band-gaps determine how much energy is needed for the electron to leap from the valence band to the conduction band. As an electron in the conduction band recombines with a hole in the valence band, the electron makes a transition to a lower-lying energy state and releases energy in an amount equal to the band-gap energy. This energy is released in photons. Since the recombinations do not always generate emitted photons, the non-radiative recombinations heat the material. In an LED, the emitted photons may give infrared or visible light [41].

3.4.2 *Lasers*

Semiconductor lasers are very similar to Light-Emitting Diodes (LED) in structure. Laser diodes are a p-n junction semiconductor that converts the electrical energy applied

across the junction into optical radiation. In both laser diodes and LEDs, the wavelength of the output radiation depends on the energy gap across the p-n junction. However, the output from a laser diode is highly coherent and can be collimated, while the output from an LED has many phases and is radiated in different directions [41].

3.4.3 Mach-Zehnder interferometer modulators

The Mach-Zehnder interferometer (MZI) (named after physicists Ernst Mach and Ludwig Zehender) is used to split an optical signal into two components, directs them down two separate paths, and then recombines them. A phase delay between the two optical signals causes them to interfere when recombined, giving an output modulated intensity. Such a device can modulate the optical power from 100% (constructive interference) to 0% (destructive interference).

MZIs as illustrated in Figure 2.3 are used in a wide variety of applications within optics and optical communications. The basic principle is that there is a balanced configuration of a splitter and a combiner connected by a pair of matched waveguides. When a phase shift is created between the signals in the two matched waveguides interference, it produces differences in the amplitude of the output signal in the recombination process. Thus, an intensity modulator based on an MZI converts changes in phase to changes in signal amplitude. The principle is very simple:

- The signal entering the device is split through a “Y” splitter into two directions. In a properly constructed device half of the signal goes in each direction and polarization is not affected.

- When there is no phase delay (both arms of the interferometer are equal in length), the signal is recombined at the “Y” junction (coupler) immediately before the light exits the device. Since the signals in each arm are coherent, they are reinforced during recombination.
- When there is a phase delay of 180° , the output will be zero [41].

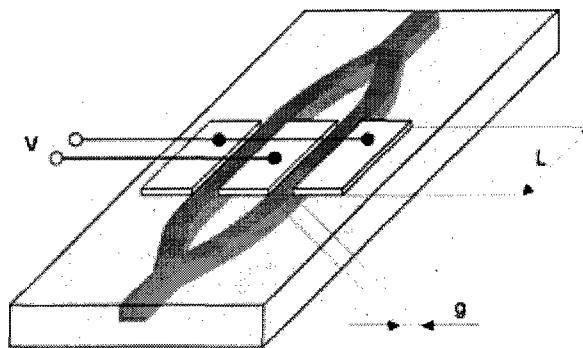


Figure 3.3 Modulator using Mach-Zehnder Interferometer (L: length, g: width and V: voltage)

3.5 Optical transmission medium

The optical fiber is the transmission medium. An ideal transmission medium would have no effect on the signal it carries, but any medium inevitably has some effects.

In a fiber, the two principal limiting effects on the signal are attenuation of the signal strength and pulse spreading (dispersion). Both depend on how far light travels through the fiber. Attenuation reduces the intensity of the optical signal. Pulse spreading limits the data rate and/or increases the bit error rate (BER) of the digital signal and/or reduces the signal to noise ratio of an analog signal. Both attenuation and dispersion in the glasses used to

make the fiber have low values in the wavelength ranges between 1250 and 1650 nanometers [41].

3.5.1 Optical amplifiers

An optical amplifier can boost the strength of optical signals so they can travel farther through optical fibers. They amplify light directly in optical form without converting the signal to electrical form [42].

3.5.2 Repeaters and regenerators

The repeater and *regenerator* (see section 6 for more details) first convert the optical signal to electrical form, then amplify it and deliver the electrical signal they generate to another transmitter. That transmitter then generates a fresh optical version of the signal. Regenerators can clean up the effects of dispersion and distortion on optical signals [41].

3.5.3 Optical splices

Normally, optical fibers are connected to each other by either connectors or splicing, that is, joining two fibers together to form a continuous optical waveguide. The generally accepted splicing method is arc fusion splicing, which melts the fiber ends together with an electric arc. For quicker fastening jobs, a “mechanical splice” may also be used [41].

3.5.4 Optical splitters and couplers

In an optical network there are many situations where signals must be combined and/or split in multiple ways. Splitters are designed to split an optical signal into two or more components. Fiber optic couplers are optical devices that connect three or more fiber ends, dividing one input between two or more outputs, or combining two or more inputs into one

output. The cable type accepted by fiber optic couplers may be single-mode or multi-mode. Single-mode describes an optical fiber that allows only one mode to propagate. The fiber has a very small core diameter of approximately 8 μm . It permits signal transmission at extremely high bandwidth and allows for very long transmission distances [41].

3.5.5 Optical receivers

Receivers are the final elements in any communication systems. They convert a signal transmitted in one form into another form. For example, a radio receiver detects weak radio waves in the air and processes them electronically to generate sound that can be heard. Fiber optic receivers detect the optical signal emerging from the fiber and transfer the data in the form of an electrical signal. A photo-detector generates an electrical current from the light it receives. Electronics in the receiver then amplify that signal and process it to decode the signal. After long distances and for the purpose of improved reception, a preamplifier precedes the photo-detector [38].

3.5.6 Optical filters

An optical filter is a device which selectively transmits light having certain properties (often, a particular range of wavelengths, that is, range of colors of light), while blocking the remainder [38].

3.5.7 Photo-detectors

The fundamental mechanism behind the photo-detection process is optical absorption. The main objective of the photo-detector is to receive the optical signal, remove the data from the optical carrier and output it as a modulated electrical photocurrent through the photoelectric effect. The requirements for a photo-detector are fast response, high

sensitivity, low noise, low cost and high reliability. Its size should be compatible with the fiber-core size [38].

3.6 Conclusion

Chapter 2 provided an overview and some key historical milestones that changed the way fiber is applied today. We described the system concept and the system components necessary for an optical transmitter, receiver (such as LED), lasers, Mach-Zehnder, filters and photo-detectors. We also described the components of an optical transmission medium: the amplifier, repeaters, generator and splices. Special attention was given to the Mach-Zehnder and the way it works since we will use it later to perform our periodization steps. The above description offers an overall view of the system we will be working on and facilitates an understanding of the approach used in the rest of our work.

Chapter 4 - Optical fiber and light propagation

An optical fiber is a very thin strand of silica glass in geometry that resembles a human hair. In reality it is a very narrow, very long glass cylinder with special characteristics. It consists of two parts: the core and the cladding. The core is a narrow cylindrical strand of glass and the cladding is the tubular jacket surrounding it. The core has a (slightly) higher refractive index than the cladding. This means that the boundary (interface) between the core and the cladding acts as a perfect mirror. If a short pulse of light from a source such as a laser or an LED is sent down a narrow fiber, it will be changed (degraded) by its passage down the fiber. It will emerge (depending on the distance) much weaker, lengthened in time (“smeared out”) and distorted in other ways.

4.1 Conventional fibers

Like other waveguides, an optical fiber guides waves in distinct patterns called transverse *modes*, which describe the distributions of light energy across the waveguide. The precise patterns depend on the wavelength of light transmitted and on the variations in refractive index across the fiber core. There are three basic types of fiber, namely:

- Multi-mode Step-Index
- Multi-mode Graded-Index
- Single-Mode (Step-Index)

The difference between fiber modes lies in the way light travels along the fiber. There is a core diameter of 50 microns (μm) for multi-mode fibers and a cladding diameter of 125 μm (these are the dimensions of standard glass fibers used in telecommunications). (Fiber size is normally quoted as the core diameter followed by the cladding diameter. Accordingly, the fiber is identified as 50/125.) The cladding surrounds the core. The cladding glass has a different (lower) refractive index from that of the core, and the boundary forms a partially reflecting interface.

Light is transmitted (with very low loss) down the fiber by reflection from the boundary between the core and the cladding. This phenomenon is called “total internal reflection.” Perhaps the most important characteristic is that the fiber bends around corners to a radius of only a few centimeters without any loss of light. The lowest loss occurs at 1.55 microns, and there is also a minimum loss at 1.31 microns wavelengths [38].

4.1.1 Multi-mode step-index fiber

Fiber that has a core diameter large enough for the light used to find multiple paths is called a “multi-mode” fiber as shown in Figure 3.1.

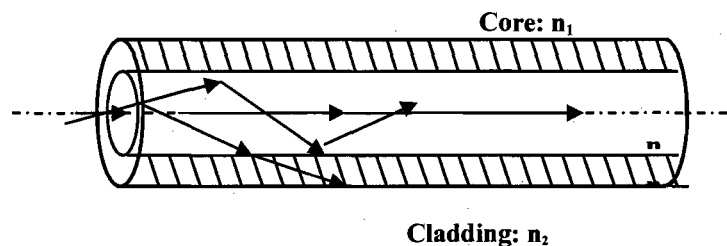


Figure 4.1 Multi-mode step-index fiber

For a fiber with a core diameter of 62.5 microns using light of wavelength 1300 nm, the number of modes is around 400 depending on the difference in refractive index between the core and the cladding. The problem with a multi-mode operation is that some of the paths taken by particular modes are longer than others. This means that light arrives at different times according to the path taken. As a result, the pulse tends to disperse (spread out) as it travels through the fiber. This effect is one cause of “inter-symbol interference.” This restricts the distance that a pulse can be usefully sent over a multi-mode fiber [38].

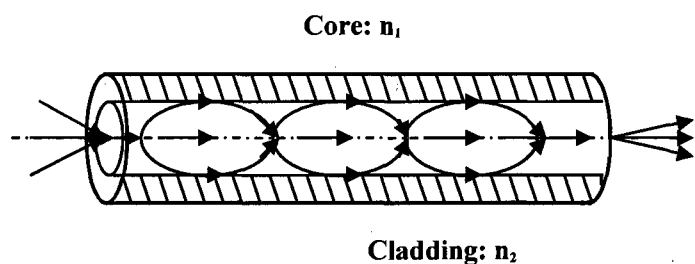


Figure 4.2 Multi-mode graded index fiber

One way around the problem of (modal) dispersion in a multi-mode fiber is to impact the glass in such a way that the refractive index of the core changes gradually from the centre to the edge. Light traveling down the center of the fiber experiences a higher refractive index than light traveling farther out towards the cladding. Thus, light on physically shorter paths (modes) travels more slowly than does light on physically longer paths. The light follows a curved trajectory within the fiber as illustrated in Figure 4.2. The purpose is to maintain the same light propagation speed on each path with respect to the axis of the fiber. Thus, a pulse of light composed of many modes stays together as it travels through the fiber, which allows for transmission over longer distances than does regular multi-mode transmission. This type of fiber is called “Graded Index” fiber. Within a GI

fiber, light typically travels in about 400 (at a wavelength of 1300 nm) or 800 modes (in the 800 nm band) [43]. A multi-mode fiber is characterized by its distance \times bandwidth product.

4.1.2 Single-mode fiber

Single-mode fibers (SMF) (also called *mono-mode fibers*) are optical fibers designed to support only a single mode per polarization direction for a given wavelength. As shown in Figure 4.3, the core diameter is typically between 8 and 9 microns, while the cladding diameter is 125 microns.

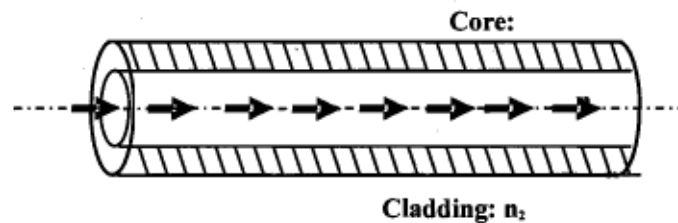


Figure 4.3 Single-mode fiber. The core diameter is typically between 8 and 9 microns while the cladding diameter is 125 microns.

The number of modes allowed in a given fiber is determined by a relationship between the wavelength of the light passing through the fiber, the core diameter of the fiber and the material of the fiber. This relationship is known as the Normalized Frequency Parameter, or V number. The mathematical description of the V number is given by:

$$V = \frac{2 * \pi * NA * r}{\lambda} \quad (4.1)$$

where NA = Numerical Aperture

r = Core fiber radius (microns)

λ = wavelength (microns)

The electromagnetic wave is tightly held to allow travel down the axis of the fiber. The longer the wavelength of light in use, the larger the diameter of fiber we can use and still have light travel in a single mode. The core diameter used in a typical single-mode fiber is nine microns. It is not quite as simple as this in practice. A significant proportion (up to 20%) of the light in a single-mode fiber actually travels in the cladding. For this reason the “apparent diameter” of the core (the region in which most of the light travels) is somewhat wider than the core itself. The region in which light travels in a single-mode fiber is often called the “mode field”, and the mode field diameter is quoted instead of the core diameter. The mode field varies in diameter depending on the relative refractive indices of the core, and cladding the core diameter is a compromise. The core cannot be made too narrow because of losses at bends in the fiber. When the core is very narrow, the mode spreads more into the cladding. As the core diameter decreases compared to the wavelength (the core becomes narrower or the wavelength gets longer), the minimum radius for bending the fiber without loss increases. If a bend is too sharp, the light simply moves out of the core into the outer parts of the cladding and is lost [43].

Single-mode optical fiber is an optical fiber in which only the lowest order bound mode can propagate at the desired wavelength. Single-mode fibers are best at retaining the fidelity of each light pulse over longer distances and exhibit no dispersion caused by multiple spatial modes; thus, more information can be transmitted per unit time giving single-mode fibers a higher bandwidth in comparison with multi-mode fibers. A typical

single-mode optical fiber has a core radius of 5 to 10 μm and a cladding radius of 120 μm . At present, data rates of up to 10 gigabits per second are possible at distances of over 60 km with commercially available transceivers.

4.2 Non-conventional fiber

4.2.1 Photonic crystal fiber

Photonic Crystal Fiber (PCF) or “Holey” fiber is the optical fiber having a periodic structure of cylindrical holes running along the length of the optical fiber as shown in Figure 4.4. PCF structures were modified with the introduction of such fibers including air-silica fiber, photonic band-gap fiber and hollow core photonic crystal fiber. The air-silica fiber is the most basic structure and has a silica background and periodic air holes surrounding the silica core. Thus, the core has the high refractive index of the traditional optical fiber. As a result, Total Internal Reflection (TIR) dominates the guiding mechanism, whereas, in photonic band-gap fibers, air holes are filled with materials that have a higher refractive index than its core material [44]. Obviously, this violates the condition for TIR. However, light is still guided via a different mechanism, the so-called Bragg scattering of constructive or destructive scattering. Finally, the hollow core photonic crystal fiber is the air-silica fiber with larger air holes in the core region [45]. As a result, the core has a lower refractive index than the cladding, making the guiding mechanism is similar to that of the photonic band-gap fiber.

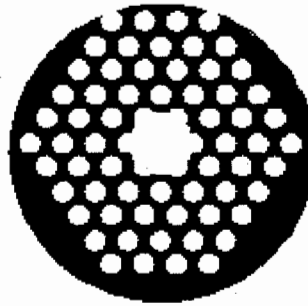


Figure 4.4 Photonic crystal fiber cut-view

Holey fibers operating under the TIR principle show some significant advantages compared with their conventional counterparts. For instance, they can be exclusively fabricated out of a single dielectric, thus avoiding interfaces between different materials that may undermine the fiber's performance. The dependence of the cladding's effective index on wavelengths permits the manifestation of only a finite number of modes at relatively high frequencies owing to the reduction of the difference between the refractive indices of the core and the cladding for increasing frequencies [46]. Furthermore, it has been theoretically shown and experimentally verified that holey fibers with a triangular lattice of air holes can exhibit endlessly single-mode operation provided the diameter of the cladding's air holes and the centre-to-centre spacing of two adjacent holes (lattice constant) are properly chosen [46].

The variation of the cladding's effective index can be turned to optimal advantage as far as the fiber's dispersion properties are concerned. The wide tailoring of the fiber's design in terms of air hole sizes, shapes and arrangements offers much freedom, and their proper combination can tune the fiber's dispersion curve. The influence of the design parameters on the dispersion properties of holey fiber has been extensively studied relative to both the

classical triangular air hole-silica core lattice and other configurations that include additional features, e.g. air hole rings of varying diameters, air holes with elliptical cross-sections or doped-silica cylindrical cores [46, 47, 48, 49]. Several types of holey fiber were designed that exhibit favorable dispersion properties such as zero-dispersion at the 1.55 μm operation wavelength, and ultra-flattened group-velocity dispersion curves of zero, positive or negative dispersion over a significant wavelength regime [50, 51].

4.2.2 *Liquid crystal fiber*

Nematic liquid crystals are anisotropic materials consisting of rod-like molecules whose axis coincides with the optical axis of the anisotropy. The liquid crystal director indicates the local alignment direction, which usually varies with the volume of the liquid crystal. When confined in closed cylindrical cavities in the absence of external stimuli, the liquid crystal's director distribution is determined by the physics of elastic theory and the anchoring conditions at the cavity's surface [47, 48]. In the application of a static electric field the director's orientation can be controlled, since the liquid crystal directors tend to align their axis in accordance with the applied field. In an alternative approach, the properties of nematic liquid crystals can be tuned thermally owing to the dependence of refractive index values on temperature. The above features are responsible for their utilization in a number of proposed photonic crystal-based optoelectronic devices [52, 53, 54, 55].

4.2.3 *Plastic optical fiber*

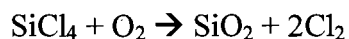
Plastic optical fiber (POF) is an optical fiber made of plastic; traditionally, PMMA (acrylate) is the core material, and fluorinated polymers are the cladding material. The

cores of plastic fibers are relatively larger than those of glass fibers (2 mm). The material is a type of plastic and therefore quickly absorbs the light traveling through the material. Its lowest loss occurs in the red, rather than the infra-red, part of the spectrum. Applications for plastic fibers are limited to short-range data transmission. Compared with glass fibers, plastic fibers are less expensive in the overall optical link owing to the lower cost of the connector and splicing used in POF.

4.3 Fiber fabrication

The fiber fabrication process consists of two major stages. The first produces a *preform*, a cylinder of silica of 10 to 20 cm diameter and about 50 to 100 cm in length. This preform consists of a core surrounded by a cladding with a desired refractive-index profile, a given attenuation and other characteristics; in other words, this is a desired optical fiber, but on a much larger scale.

The second stage consists of *drawing* the made preform into an optical fiber of the size desired. The preform is made by vapor-phase oxidation during which two gases, SiCl_4 and O_2 , are mixed at a high temperature to produce silicon dioxide (SiO_2):



Silicon dioxide, or pure *silica*, is usually obtained in the form of small particles (about $0.1 \mu\text{m}$) called “soot.” This soot is deposited on the target rod or tube. The depositing of the silica soot, layer upon layer, forms a homogeneous, transparent *cladding* material. To change the value of a cladding's refractive index, some dopants are used. For example, fluorine (F) is used to decrease the cladding's refractive index in a depressed-cladding configuration.

The soot for the *core* material is made by mixing three gases - SiCl_4 , GeCl_4 , and O_2 - which results in a mixture of SiO_2 and GeO_2 . The degree of doping is controlled by simply changing the amount of GeCl_4 gas added to the mixture. The same principle is used for doping other materials.

Since deposition is made by the application of silica layers one on top of the other, the manufacturer can control the exact amount of dopant added to each layer, thus controlling the refractive-index profile. The vapor-phase oxidation process produces extremely pure material whose characteristics are under the absolute control of the manufacturer.

4.4 Propagation of light in optical fibers

The fiber itself is one of the most significant components in any optical fiber system. Since its transmission characteristics play a major role in determining the performance of the entire system, a number of questions that may arise concerning optical fibers are: What is the structure of the fiber? How does light propagate through the fiber? What is the nature of light traveling through the fiber?

4.4.1 Nature of light and its propagation characteristics

The view of the nature of light has varied throughout the history of physics. Light is the basis of our most important sensory function. It was generally believed that light consisted of a stream of tiny particles emitted by luminous sources. These particles were pictured as traveling in straight lines. However, the answer to the question of what light “really is” varies depending on the situation. Light is usually described in one of three ways: rays, electromagnetic waves and photons.

Fresnel accurately explained the electromagnetic nature of light in 1815, when he showed that the approximately rectilinear propagation character of light could be interpreted on the assumption that light was a wave motion and that the diffraction fringes could therefore be accounted for in detail. Later on, in 1864, Maxwell theorized that light waves must be electromagnetic in nature. The observation of polarization effects, furthermore, indicated that light waves are transverse (i.e., the wave motion is perpendicular to the direction in which the wave travels) [38]. Figure 4.5 illustrates the electromagnetic wave spectrum of light.

4.4.2 Light as an electromagnetic wave

An electromagnetic wave consists of an electric field and a magnetic field; both fields have a direction and a strength (or amplitude). Within the electromagnetic wave the two fields (electric and magnetic) are oriented at precisely 90° to one another as illustrated in Figure 4.6.

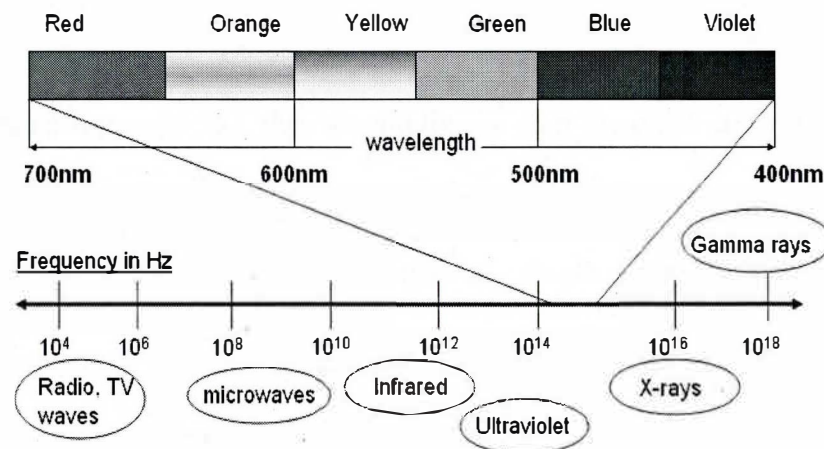


Figure 4.5 Electro-magnetic wave spectrum

The fields move (by definition at the speed of light) at a 90° direction to both of them. In three dimensions one may consider the electric field to be oriented on the x-axis, and the magnetic field on the y-axis. The direction of travel would then be along the z-direction.

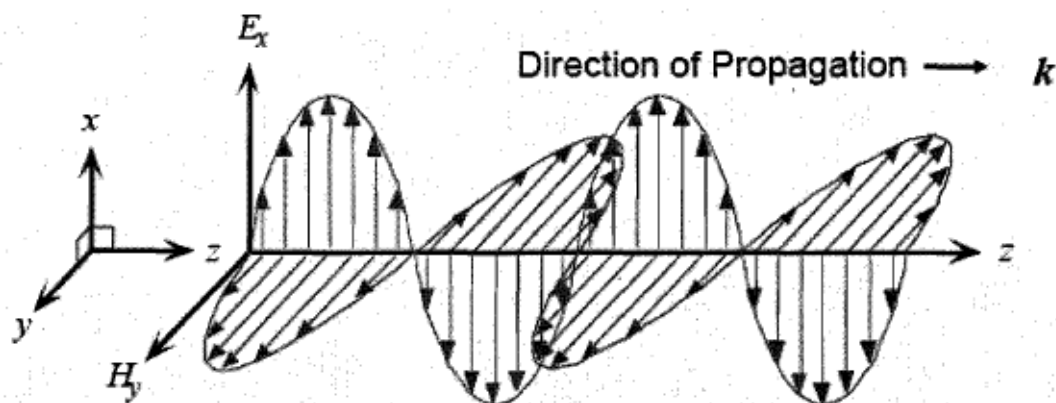


Figure 4.6 Electric and magnetic fields are orthogonal to each other and to the direction of propagation

As the electromagnetic wave travels, the field at any point in space oscillates in direction and strength. Figure 4.6 shows the electric and magnetic fields separately, yet occupying the same space. In fact, they should lie one over the other and are only depicted this way for the purpose of clarity. The z-direction in Figure 4.6 may be considered to represent passing time or a wave traveling in space at a single instant in time.

If the electromagnetic wave is observed from a stationary viewpoint, we see that the field is oriented at the start from bottom to top (increasing values of x). Sometime later the field direction has reversed. Still later, the field direction has reversed again and is now as it was originally [38].

4.4.3 Light propagation in multi-mode fiber

Fiber types including multi-mode fibers will be discussed in section 4. The key feature of light propagation in a fiber is that the fiber may bend around corners. As long as the bend radius is not too tight (1.4 cm is about the minimum for most multi-mode fibers and waveguides [38]), the light will follow the fiber and propagate without loss due to the bends as shown in Figure 4.7.

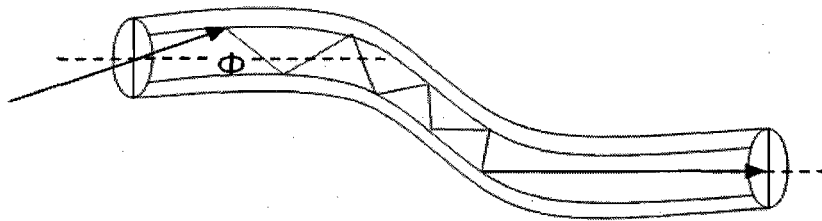


Figure 4.7 Light propagation in a multi-mode fiber

This observable fact is called “total internal reflection.” A ray of light entering the fiber is guided along the fiber because it reflects from the interface between the core and the (lower refractive index) cladding. Light is said to be “bound” within the fiber.

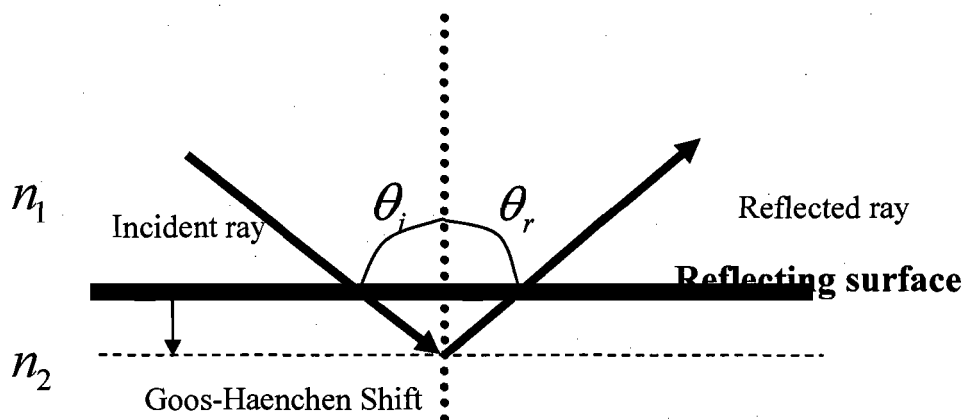


Figure 4.8 The Goos-Haenchen shift causes a phase shift of the reflected ray as if reflected from a reflecting surface very slightly deeper in the cladding layer

If we consider the propagation of a “ray” in a multi-mode step index fiber, “the angle of incidence is equal to the angle of reflection.” This is illustrated in Figure 4.8. This means that $\theta_i = \theta_r$.

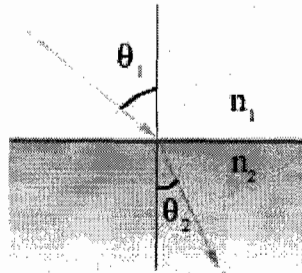


Figure 4.9 Refraction

The important thing to realize about propagation along a fiber is that not all light can propagate this way. The angle of incidence of the ray at the core-cladding interface must be quite small or else the ray will pass through into the cladding and (after a while) will leave the fiber. The geometric interpretation of light can be handled more rigorously by electromagnetic theory. In this case, Maxwell equations combined with boundary conditions should be considered.

4.4.4 Geometrical optics laws and parameters

4.4.4.1 Snell's law

To understand ray propagation in a fiber one more physics law is needed. This is known as Snell's law. Referring to Figure 4.9:

$$n_1 \sin(\theta_1) = n_2 \sin(\theta_2) \quad (4.2)$$

where n denotes the refractive index of the material, one notices that:

1. Angle θ_1 is the angle between the incident ray and an imaginary line normal to the plane of the core-cladding boundary.
2. When light passes from a material of a higher refractive index to a material of a lower index the (refracted) angle θ_2 becomes larger.
3. When light passes from a material of a lower refractive index to a material of a higher index, the (refracted) angle θ_2 becomes smaller [38].

4.4.4.2 Critical angle

If we consider Figure 4.10, we notice that as angle θ_1 becomes larger and larger so too does angle θ_2 .

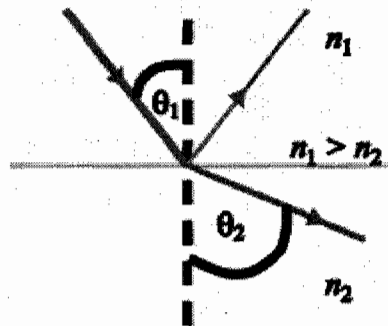


Figure 4.10 Critical angle

At some point θ_2 will reach 90° while θ_1 is still considerably less than that. This is called the “critical angle.” When θ_1 is increased further, refraction ceases, and the light is entirely reflected rather than refracted. Thus light is perfectly reflected at an interface between two materials of different refractive index if and only if:

- The light is incident on the interface from the side of higher refractive index.

- Angle θ is greater than a specific value called the “critical angle”.

If we know the refractive indices of both materials then the critical angle can be very easily derived from Snell's law. At the critical angle we know that θ_2 equals 90° and $\sin(90) = 1$ and therefore:

$$n_1 \sin(\theta_1) = n_2, \quad (n_2 < n_1) \quad (4.3)$$

Therefore

$$\sin(\theta_1) = \frac{n_2}{n_1} \quad (4.4)$$

Another point to consider here is that when light meets an abrupt change in refractive index (such as at the end of a fiber), not all the light is refracted. Usually about 4% of the light is reflected back along the path from which it came depending on the end surface finish.

When we consider rays entering the fiber from the outside (into the end-face of the fiber) we notice a further complication. The refractive index difference between the fiber core and the air causes any arriving ray to be refracted. This means there is a maximum angle for a ray arriving at the fiber end face at which the ray will be bound in a propagating mode [38].

4.4.4.3 Numerical aperture

One of the most often quoted characteristics of an optical fiber is its “Numerical Aperture.” The NA is intended as a measure of the light-capturing ability of the fiber. However, it is used for many other purposes. It may, for example, affect the amount of loss that we may expect in a bend of a particular radius etc.

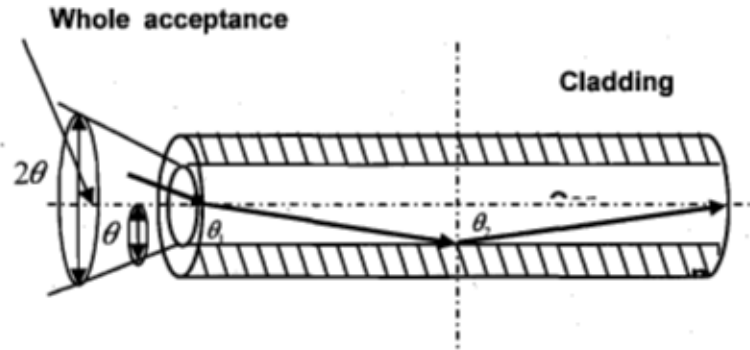


Figure 4.11 Calculating the Numerical Aperture

Figure 4.11 shows a ray entering the fiber at an angle close to its axis. This ray will be refracted and will later encounter the core-cladding interface at an angle allowing it to be reflected. This is because angle θ_2 will be greater than critical angle θ_c . The angle is greater because we are measuring angles from a normal to a core-cladding boundary, not a glancing angle to it. It is clear there is a “cone” of acceptance (illustrated in Figure 4.11). If a ray enters the fiber at an angle within the cone, it will be captured and propagate as a bound mode. If a ray enters the fiber at an angle outside the cone, it will leave the core and eventually leave the fiber itself.

The Numerical Aperture is the *sine* of the largest angle contained within the cone of acceptance. Looking at Figure 4.11, the $NA = \sin(\theta)$. The NA is also given by the following:

$$NA = \sqrt{n_1^2 - n_2^2} \quad (4.5)$$

where n_1 = refractive index of the core and n_2 = refractive index of the cladding.

Another useful expression for NA is: $NA = n_1 \sin(\theta_1)$. This relates the NA to the RI of the core and the maximum angle at which a bound ray may propagate (angle measured

from the fiber axis rather than its normal). The typical NA for single-mode fiber is 0.1. For multi-mode fiber, NA is between 0.2 and 0.3 (usually closer to 0.2). NA is related to a number of important fiber characteristics as follows:

1. It is a measure of the ability of the fiber to gather light at the input end (as discussed above).
2. NA is a measure of the contrast in RI between the core and the cladding, thus it is a good measure of the light guiding properties of the fiber. The higher the NA the tighter (smaller radius) bends in the fiber can be before loss of light becomes a problem.
3. The higher the NA , the more modes there are. Rays can reflect at greater angles and consequently there are more of them. This means that the higher the NA , the greater the dispersion of this fiber (in the case of MM fiber).

In SM fiber a high RI contrast usually implies a high level of dopant in the cladding. Since a significant proportion of optical power in SM travels in the cladding, there is a markedly increased amount of attenuation owing to the higher level of dopant. Thus (as a rule of thumb), the higher the NA of SM fiber, the higher the attenuation of the fiber [38].

4.4.4.4 Refractive index

Refractive index (RI) is the ratio of the velocity of light in a vacuum to the velocity of light in a medium. It is referred to as the medium's refractive index, denoted by the letter n given by:

$$n(RI) = C/V \quad (4.6)$$

where C is the speed of light in a vacuum and V is the velocity of light in the material.

The velocity of light in a vacuum is 3.0×10^8 m/s or about 186,000 miles/s. The refractive index of a transparent substance or material is defined as the relative speed at which light moves through the material with respect to its speed in a vacuum. By *definition*, the refractive index of a vacuum is defined as having a value of 1.0, which serves as a universally accepted reference point.

4.5 Fiber impairments

Non-idealities of optical fiber place restrictions on the distance that can be tolerated without introducing signal regenerators, in-line optical amplifiers and DCMs. These non-idealities can be broadly classified into attenuation that causes a loss in the signal power, distortion that causes pulse broadening and therefore ISI, and fiber nonlinearity that causes self-phase modulation, cross-phase modulation and four-wave mixing.

Radiative losses occur when a fiber is subject to either macroscopic bends (bends with radii that are large, compared with the fiber diameter) or random microscopic bends.

Figure 4.12 illustrates the loss spectrum of conventional single-mode fibers and the relative contributions of the two most important loss mechanisms: material absorption and Rayleigh scattering.

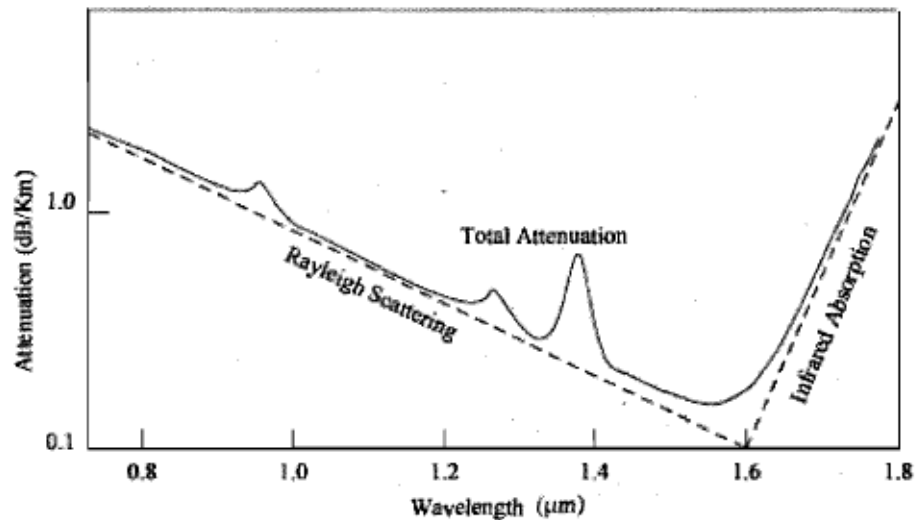


Figure 4.12 Attenuation for single-mode fiber

The fiber exhibits a minimum loss of approximately 0.2 dB/km in the wavelength region near 1.55 μm . However, SSMFs have a high dispersion in this wavelength window, limiting the performance of high-speed systems. A secondary minimum occurs close to 1.3 μm , where the fiber loss is below 0.5 dB/km. Since the chromatic dispersion is close to 1.3 μm minimum, this low-loss window was adopted for light-wave systems that were built in the 1980s. Today, optical amplifiers such as the Erbium-Doped Fiber Amplifier (EDFA) can substantially mitigate attenuation to the extent that the link is no longer considered power-limited. However, EDFAs operate only in the 1.55 μm window. As a result, long-haul systems favour this band, despite the higher dispersion effect, over the 1.3 μm band.

4.5.1 Signal distortion

4.5.1.1 Chromatic dispersion

Chromatic dispersion is the variation in the speed of propagation of a light-wave signal with wavelength. This phenomenon is also known as *group velocity dispersion* (GVD), since the dispersion is the result of group velocity being a function of the wavelength. For a single-mode fiber of length L , a specific spectral component at a frequency ω arrives at the other end of the fiber after a propagation delay of $T = \frac{L}{v_g}$, where v_g is the *group velocity*,

given:

$$v_g = \left(\frac{d\beta}{d\omega}\right)^{-1} \quad (4.7)$$

where β is the mode propagation constant. Because of the dependence of group velocity on frequency, the different spectral components of the data pulses travel with different velocities along the fiber, arriving at the fiber output dispersed in time. The amount of pulse broadening owing to chromatic dispersion, as illustrated in Figure 4.13, can be quantified as [38]:

$$\Delta T = \frac{dT}{d\omega} \Delta\omega = \frac{d}{d\omega} \left(\frac{L}{v_g}\right) \Delta\omega = L \frac{d^2\beta}{d\omega^2} \Delta\omega = L\beta_2 \Delta\omega \quad (4.8)$$

The factor $\beta_2 = \frac{d^2\beta}{d\omega^2}$ is the GVD parameter, which provides a measure of the degree to

which a pulse broadens in time as it travels along an optical fiber.

In optical communication, it is customary to specify the range of wavelengths emitted by the source, $\Delta\lambda$, instead of $\Delta\omega$. Following such a convention, equation (4.8) is rewritten as:

$$\Delta T = \frac{d}{d\lambda} \left(\frac{L}{v_g} \right) \Delta\lambda = DL\Delta\lambda \quad (4.9)$$

$$\text{where the factor: } D = \frac{d}{d\lambda} \left(\frac{1}{v_g} \right) = -\frac{2\pi C}{\lambda^2} \beta_2$$

D is called the *dispersion parameter* and is expressed in $ps/(km.nm)$.

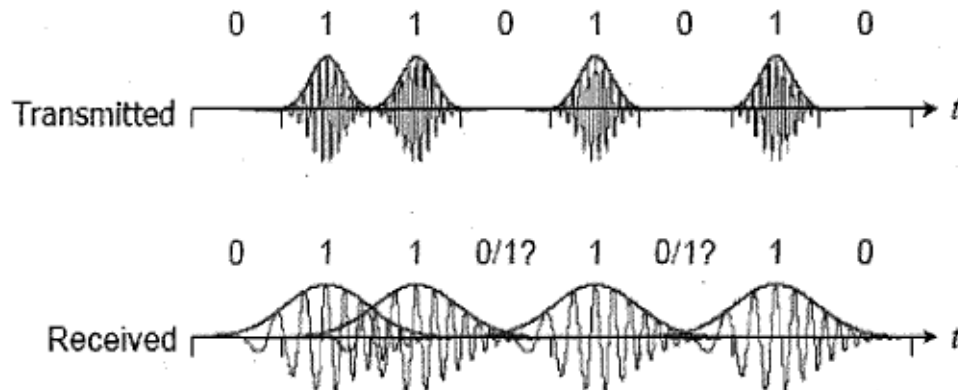


Figure 4.13 CD Effect - spreading the signal pulses [56]

Chromatic dispersion results from the interplay of two phenomena. The first is that the refractive index of silica is frequency-dependent and, therefore different frequency components travel at different speeds in the silica. This component of chromatic dispersion is called *material dispersion*. The other component is called *waveguide dispersion*, which

results from the dependence of the modal propagation constant on the wavelength. As a result, D is written as the sum of two terms:

$$D = DM + D_w \quad (4.10)$$

where DM is the *material dispersion* and D_w is the *waveguide dispersion*.

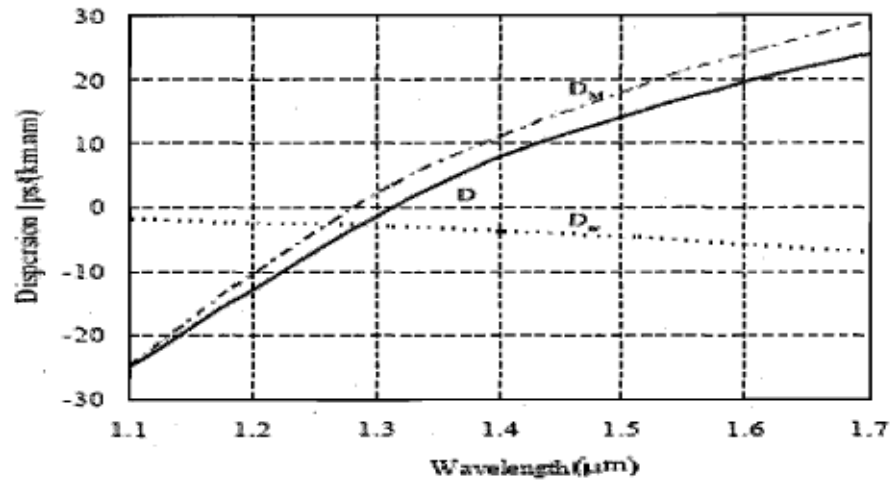


Figure 4.14 Total dispersion, D , and relative contributions of material dispersion, DM , and wave guide dispersion, D_w , for a SSMF

Figure 4.14 illustrates the relative contributions of DM and D_w for a SSMF, whose dispersion effects are small in the $1.3 \mu\text{m}$ band.

However, systems operating in this wavelength range are attenuation-limited. As a result, there is considerable interest today in optical communication systems that operate in the $1.55 \mu\text{m}$ band because of the low loss in this region and the well developed EDFA technology. But in this band, communication is chromatic dispersion-limited ($D \approx 17 \text{ ps}/(\text{km} * \text{nm})$). This limitation can be reduced if the zero dispersion wavelength is

shifted to $1.55 \mu\text{m}$, which can be accomplished by modifying the waveguide dispersion by changing the refractive index profile of the fiber. Fibers with this property are called *dispersion-shifted fibers* (DSFs). However, they are not suitable for use with WDM systems because of the severe penalties resulting from four-wave mixing and other nonlinearities. These penalties are reduced if some chromatic dispersion is present in the fiber, because the different interacting waves then travel with different group velocities.

This has led to the development of Non-Return to Zero Dispersion Shifted Fiber (NZDSF), which has a chromatic dispersion between 1 and 6 ps/(nm.km), or between -1 and -6 ps/(nm.km) in the $1.55 \mu\text{m}$ wavelength window. This reduces the penalties due to nonlinearities, while retaining most of the advantages of the DSFs. However, operating the optical link at the zero-dispersion wavelength does not eliminate chromatic dispersion completely. Instead, the link becomes limited by the effects of higher order dispersion. This comes about because D cannot be zero for all the wavelengths within the pulse spectrum, which is centered about the zero-dispersion wavelength. Higher order dispersion effects are governed by the *dispersion slope* S , where

$D = \frac{dD}{d\lambda}$, which is written as:

$$S = \left(\frac{2\pi C}{\lambda^2}\right)^2 \beta_3 + \left(\frac{4\pi C}{\lambda^3}\right) \beta_2 \quad (4.11)$$

where $\beta_3 = \frac{d\beta_2}{d\omega} = \frac{d^3\beta}{d\omega^3}$ is the third-order dispersion parameter.

The impact of chromatic dispersion can be reduced by utilizing external modulation instead of direct modulation for the laser diode, in conjunction with choosing lasers with narrow spectral widths. Dispersion compensation is employed when external modulation is

not sufficient to reduce the dispersion penalty. The two most popular methods used are the DCFs and chirped fiber Bragg gratings. DCFs are fibers with a high dispersion value that is chosen to negate that of the link fiber in order to achieve a net zero dispersion. One disadvantage of this approach is the loss introduced in the system. Chirped Bragg gratings are optical devices that introduce different delays at different frequencies which are utilized to counteract the effect of chromatic dispersion.

For high-speed systems that utilize SSMFs and operate in the $1.55\ \mu\text{m}$ band, chromatic dispersion is a major bottleneck. For such systems, the effect of chromatic dispersion increases by the square of the bit rate (assuming that the laser sources have a very narrow spectral width). For example, systems running at 2.5 Gb/s can cover a distance of more than 940 km on SSMF without a significant power penalty due to chromatic dispersion. At 10 Gb/s, system designers are forced to introduce dispersion compensators at approximately 60 km intervals along the link and 4 km for 40 Gb/s as shown in Figure 4.15 [1].

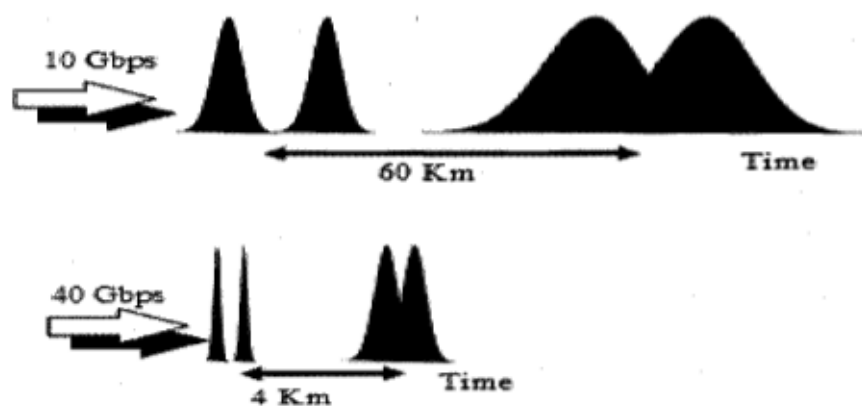


Figure 4.15 Chromatic dispersion effect with respect to bit rate and distances

4.5.1.2 Polarization-mode dispersion (PMD)

As shown in Figure 4.16, the signal energy at a given wavelength occupies two orthogonal polarization modes. In ideal fibers with a perfect rotational symmetry, the two modes are degenerate with equal propagation constants, and any polarization state that is injected into the fiber, propagates unchanged. However, in real fibers there are imperfections such as asymmetrical lateral stresses, non-circular cores and variations in the refractive-index profiles. These imperfections break the circular symmetry of the ideal fiber and create *birefringence*, which is the difference between the effective refractive indices of the two modes. As a result, the modes propagate with different velocities. The resulting difference in propagation times, $\Delta\tau$ (differential group delay (DGD)), results in pulse spreading. Also, the variation of birefringence along the length of the fiber induces a rotation of the polarization orientation. This is called *polarization mode dispersion* (PMD).

In contrast to chromatic dispersion, which is a relatively stable phenomenon along a fiber, the PMD varies randomly along a fiber. A major reason for this is that the perturbations causing the birefringence effects vary with the temperature. In practice, this shows up as a random, time-varying fluctuation in the value of the PMD at the fiber output. Therefore, statistical predictions are needed to account for PMD. A useful means of characterizing the PMD for long fiber lengths is in terms of the mean value of the differential group delay. This is described by the relations $(\Delta\tau) \approx D_{PMD} \sqrt{L}$, where D_{PMD} is measured in $(\frac{ps}{\sqrt{km}})$, which is the average PMD parameter.

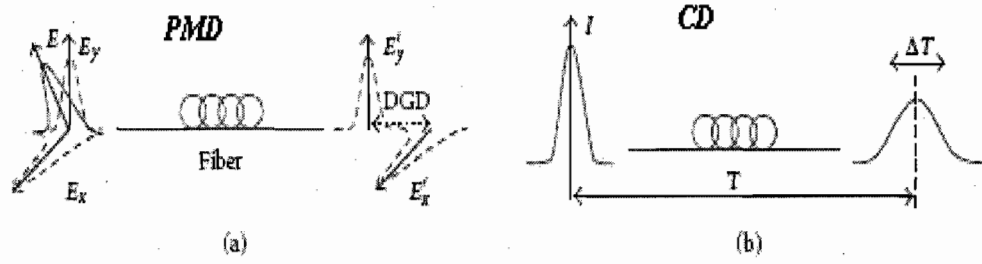


Figure 4.16 Dispersion types: a) PMD and b) CD

As a result of this statistical nature, PMD modelling becomes quite complex. The modelling is based on the concept of *principal states of polarization* (PSP) [57] and the fact that for any linear optical transmission medium that has no polarization-dependent loss, there are orthogonal input states of polarization for which the corresponding output states of polarization are orthogonal and show no dependence on wavelength to the first order. Therefore, these principal states provide an orthogonal basis set for the description of the polarization dispersion in fibers. An arbitrary optical pulse polarization can be projected on these PSPs. In a simple model, the fiber is divided into a large number of segments in which the degree of birefringence and the orientation of the principal axes remain constant but change randomly from segment to segment. If first-order PMD is taken into account, the output waveform $P_2(t)$ detected by a square law detector is related to the input power waveform $P_1(t)$ as follows [58]:

$$P_2(t) = \gamma P_1\left(t + \tau_0 + \frac{\Delta\tau}{2}\right) + (1 - \gamma) P_1\left(t + \tau_0 - \frac{\Delta\tau}{2}\right) \quad (4.12)$$

Where τ_0 is the polarization-independent group delay, $\Delta\tau$ is the DGD between the two PSPs, and $0 < \gamma < 1$ is the relative power launched in the two principal states.

Modern single-mode fibers exhibit a negligible PMD that can be less than $0.1 \left(\frac{ps}{\sqrt{km}} \right)$.

However, some of the older fiber cables, particularly those embedded in terrestrial networks, can have large D_{PMD} values as high as $2 \left(\frac{ps}{\sqrt{km}} \right)$ [59]. These can cause large receiver power penalties; for example, a mean DGD of 50 ps results in a power penalty of only 0.1 dB at 2.5 Gb/s, but causes a power penalty of 4 dB at 10 Gb/s [60]. What makes things worse for these legacy fibers is that the PMD fluctuates randomly with time and can temporarily exceed its average value by a few times. Thus, we find that older fibers can usually support a transmission of 2.5 Gb/s signals over terrestrial distances of up to 1000 km, but cannot support 10 Gb/s [60]. Replacing these fibers with new ones or placing more regenerators along the link is quite an expensive solution; a much cheaper method is to apply equalization techniques to compensate for these distortions.

In addition to the time variance, the PMD also varies with the wavelength. This variance, which is called second-order PMD, results in an optical dispersion that is a function of both the channel bandwidth and the value of the DGD over that bandwidth. Typically, first-order PMD is the dominant cause of signal distortion [59].

4.5.2 Nonlinear optical effects

Practically speaking, the optical fiber can be treated as a linear medium as long as it is used at a reasonable power level (a few mW). However, at high bit rates such as 10 Gb/s and above and/or at higher transmitted powers, nonlinearity becomes an important issue that can place significant limitations on system performance. For WDM systems, the nonlinear effects can become important even at moderate powers and bit rates.

There are two categories of nonlinear effects: those due to the dependence of the refractive index on the intensity of the applied electric field and those due to scattering effects. These nonlinear effects are briefly discussed in the following section.

4.5.2.1 Nonlinear phase modulation

The refractive index of silica has a weak dependence on the optical intensity, I (optical power per effective area in the fiber) and is given by:

$$n = n_0 + n_2 I = n_0 + n_2 \frac{P}{A_{eff}} \quad (4.13)$$

where n_0 : is the *normal refractive index* of the fiber material, n_2 : is the *nonlinear index coefficient*, P is the optical power and A_{eff} is the effective cross-sectional area of the fiber.

In silica, the value of n_2 ranges from 2.2 to 3.4 $\times 10^{-8} \mu\text{m}^2/\text{W}$. This nonlinearity in the refractive index is known as *Kerr nonlinearity* and results in a carrier-induced phase modulation of the propagating signal, called the *Kerr effect*. It can cause *self-phase modulation* (SPM), *cross-phase modulation* (XPM) and *four-wave mixing* (FWM).

4.5.2.2 Self-phase modulation (SPM)

Since the local refractive index is a function of the optical intensity of the propagating signal, the mode propagation constant becomes dependent on the optical intensity as well.

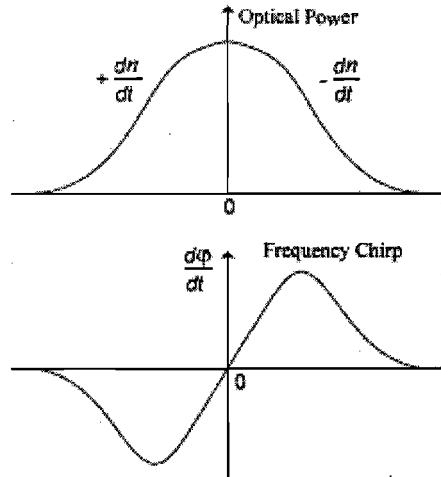


Figure 4.17 Phenomenological description of the spectral broadening of a pulse due to self-phase modulation.

The power dependent propagation constant, β' , can be written as:

$$\beta' = \beta + \gamma P \quad (4.14)$$

where β is the mode propagation constant that is derived by assuming a constant refractive constant. The nonlinear coefficient γ is defined by $\frac{2\pi n_2}{\lambda A_{eff}}$.

For a fiber of length L , the γ term produces a nonlinear phase shift given by

$$\phi_{NL} = \int_0^L (\beta' - \beta) dz = \int_0^L \gamma P(z) dz \quad (4.15)$$

The time dependence of P causes ϕ_{NL} to vary with time. Since this nonlinear phase modulation is self-induced, the nonlinear phenomenon responsible for it is called SPM. Since phase fluctuations translate into frequency fluctuations, SPM causes frequency chirping of the optical pulses. Figure 4.17 portrays an example of how the SPM causes frequency chirping. The time-varying signal intensity produces a time-varying refractive

index. As a result, the leading edge sees a positive dn/dt , whereas the trailing edge sees a negative dn/dt . This temporally varying refractive index results in a temporally varying phase change, shown by $d\phi/dt$ in Figure 4.17. Therefore, the instantaneous optical frequency differs from its initial value across the pulse. As a result, the rising edge of the pulse undergoes a red shift in frequency (towards the lower frequencies), and the falling edge of the pulse is subjected to a blue shift in frequency (towards the higher frequencies). In the wavelength region where the chromatic dispersion is negative ($D < 0$ or $d^2\beta/d^2\omega > 0$), the red-shifted leading edge of the pulse travels faster than the blue-shifted trailing edge. Therefore, a GVD-induced pulse broadening results. Yet, in the wavelength region where the chromatic dispersion is positive ($D > 0$ or $d^2\beta/d^2\omega < 0$), the red-shifted leading edge of the pulse travels more slowly than the blue-shifted trailing edge. Therefore, the SPM partly compensates for the chromatic dispersion, causing pulse narrowing.

4.5.2.3 Cross-phase modulation (XPM)

In WDM systems, where several optical channels are transmitted simultaneously inside an optical fiber, the nonlinear phase shift for a specific channel depends not only on the power of that channel but also on the power of the other channels. Moreover, the phase shift varies from bit to bit, depending on the bit pattern of the neighboring channels. This nonlinear phenomenon is known as XPM. The XPM-induced phase shift can occur only when two pulses from different channels overlap in time. Usually, the time overlap occurs

only over a fraction of the pulse period, because pulses in the different channels have different propagation velocities.

For widely spaced channels, the pulses overlap for such a short time that the XPM produces negligible effects. However, for neighboring channels, the pulses overlap long enough for the XPM effects to accumulate.

4.5.2.4 Four-wave mixing (FWM)

FWM is a third order nonlinearity in silica fibers, caused by the third order nonlinear susceptibility of silica. FWM resembles intermodulation distortion in electrical systems. If three optical fields with carrier frequencies f_1 , f_2 , and f_3 are propagating simultaneously in a fiber, the fiber nonlinearity causes them to mix, producing a fourth intermodulation product that is related to the other frequencies by the relation $f_4 = f_1 \pm f_2 \pm f_3$. Severe crosstalk can result if the newly generated frequency lies within the transmission window of the original frequencies. In addition, the generated frequencies reduce the power of the involved channels. Although several intermodulation frequencies corresponding to different plus and minus sign combinations are possible, practically speaking, most of these combinations fail to build up because of a phase matching condition that must be satisfied. In practice, a frequency combination of the form $f_4 = f_1 + f_2 - f_3$ is the most troublesome for WDM systems, since the different frequencies can become nearly phase-matched when the channel wavelengths lie close to the zero-dispersion wavelength. In fact, the case in which $f_1 = f_2$ is often the most detrimental to system performance.

The efficiency of FWM depends on fiber dispersion and channel spacing. Since chromatic dispersion varies with the wavelength, the signal waves and the generated waves

have different group velocities. This destroys the phase matching of the interacting waves and lowers the efficiency of the transference of power to the newly generated frequencies. The greater the differences in the group velocities and the wider the channel spacing, the lower the FWM. Modern WDM systems avoid FWM by adopting the technique of dispersion management, in which chromatic dispersion is kept locally high within each fiber section, while overall dispersion is kept low by the use of DCMs after each section. Commercial NZ-DSFs are designed with a dispersion of about 4 ps/(km.nm), which is large enough to suppress FWM while retaining most of the advantages of DSFs.

4.5.2.5 Stimulated light scattering

Rayleigh scattering, introduced in section 2.2.1, is an example of elastic scattering in which the frequency of the scattered light remains unchanged. In inelastic scattering, however, the energy is transferred from one light wave to another wave of a higher wavelength (or a lower energy). The energy difference appears in the form of a phonon. Optical phonons are involved in *stimulated Raman scattering* (SRS), whereas acoustic phonons are involved in *stimulated Brillouin scattering* (SBS).

4.5.2.6 Stimulated raman scattering (SRS)

Raman scattering occurs in optical fibers when a pump wave is scattered by the silica molecules. As a result, a scattered wave with a longer wavelength is created, and the energy difference is absorbed by the silica molecules. The beating of the pump frequency and the scattered light frequency creates a beat frequency that drives the oscillation of the silica molecules. Because the amplitude of the scattered wave increases in response to these oscillations, a positive feedback loop is created. If another signal is present at the longer

wavelength of the scattered wave, the signal becomes amplified and the pump wavelength signal decreases in power. Consequently, SRS can severely limit the performance of a multi-channel optical communication system by transferring energy from the short-wavelength to the long-wavelength channels. The powers in WDM channels, separated by up to 16 THz (125 nm), can be coupled through the SRS effect.

4.5.2.7 Stimulated brillouin scattering (SBS)

In a dielectric material like the silica of an optical fiber, a high electric field causes a compression of the medium, which in turn increases its refractive index. This phenomenon is called electrostriction. If two optical waves of different frequencies counterpropagate in the same material, their interference creates zones of high electrical field intensity and zones of weaker field intensity. Because of electrostriction, periodic compression zones, moving at the speed given by the optical frequency difference, are induced in the material. If this speed corresponds to the speed of sound in the material, an acoustic wave is created. An oscillating electric field at a pump frequency, Ω_p , is initially scattered by the acoustic noise that results from the unavoidable molecular vibrations within the silica. This backscattered light propagates in the opposite direction and interferes with the pump light. Because of electrostriction, an acoustic wave, at some frequency Ω , is generated.

This acoustic wave scatters the pump wave, generating a new wave at the frequency Ω_s . The new wave beats with the pump frequency, creating a frequency component at the beat frequency, $\Omega_p - \Omega_s$, which is equal to the acoustic frequency Ω . As a result, the beat frequency increases the amplitude of the acoustic wave, which in turn increases the amplitude of the scattered wave, resulting in a positive feedback loop. The scattered light gains power from the forward-propagating signals, reducing the power of the transmitted

signal. The SBS effect is confined within a single wavelength channel in a WDM system as opposed to that of SRS. As a result, the effects of the SBS accumulate individually for each channel and occur at the same power level of single channel systems. Both SBS and SRS have input power threshold levels, beyond which the intensity of the scattered light grows exponentially.

4.6 Conclusion

Chapter 4 is the core of this work in that it contains all necessary information concerning fiber types and modes (single-mode, multi-mode, photonic crystal and liquid crystal), fiber, geometrical laws such as Snell's law, critical angle, numerical aperture and refractive index, fiber fabrication and light propagation through fiber. It discusses all possible fiber impairments such as signal distortion, CD, PMD, nonlinear optical effects, nonlinear phase modulation, SPM, XPM and FWM. All the above descriptions are given in detail because of the importance of understanding all current and/or future work related to the field.

Chapter 5 - Proposed optical solution & theoretical analysis

Before describing our solution for chromatic dispersion compensation, we introduce in this section the physical elements underlying our technique. First, we briefly cover pulse propagation through the fiber, which is a dispersive and non-linear medium, the non linear Schrödinger equation, quick description of the non linearity and dispersion was introduced. Chromatic dispersion compensation in the optical domain using DCF is discussed. The temporal and fractional third order Talbot effect on which our optical solution is based is then presented.

5.1 Pulse propagation in an optical fiber

Pulse propagation through an optical fiber is widely described in several works [61]. In its easiest formulation, when the pulse width is larger than five picoseconds under the assumption of Slowly Varying Envelop Approximation (SVAE), the variation of the complex envelope $u(t)$ is governed by the Non-Linear Schrödinger Equation (NLSE):

$$i \frac{\partial u}{\partial z} + \frac{i}{2} \alpha u - \frac{1}{2} \beta_2 \frac{\partial^2 u}{\partial T^2} - \frac{i}{6} \beta_3 \frac{\partial^3 u}{\partial T^3} + \gamma |u|^2 u = 0 \quad (5.1)$$

Where α is the attenuation coefficient, $T = t - \beta_1 z$ is the related time frame, γ is the nonlinear parameter known as the Self-Phase Modulation (SPM) and $(\beta_2$ and $\beta_3)$ are, respectively, the second and third order dispersion parameters referred to as Group Velocity

Dispersion (GVD) and Third Order Dispersion (TOD). While dispersion is responsible for a temporal broadening of the signal, the SPM effect is observed in the spectral domain through a spectral enlargement. To quantify the effect of those phenomena along a transmission length, we find it practical to introduce some characteristic variables, $L_D = \frac{T_0^2}{|\beta_2|}$, $L'_D = \frac{T_0^3}{|\beta_3|}$ and $L_N = \frac{1}{\gamma P_0}$, which are, respectively, the second and third order dispersion lengths and the nonlinear lengths. In the following, we consider a lossless medium ($\alpha = 0$).

Generally, the GVD effect is more important than TOD ($L'_D \gg L_D$), and the latter is usually neglected except in ultra-short pulses ($>100\text{Gbit/s}$) and zero dispersion conditions. When $L_D \cong L_N$, both GVD and SPM effects have a comparable contribution. In this case, a Soliton-like pulse is the ideal signal shape for very long distances. This pulse is the analytical solution of the NLSE using the inverse scattering method [61]. It results from the interplay between the GVD and SPM effects. When $L_N \gg z$, the greatest contribution of the physical phenomenon occurs from chromatic dispersion. Therefore, equation (5.1) can be easily solved in the Fourier domain:

$$U(w, z) = U(w, 0) \exp\{i2\pi D(w)z\} \quad (5.2)$$

$$\text{Where, } D(w) = \left(\frac{\beta_2}{2} w^2 + \frac{\beta_3}{6} w^3 \right)$$

Both nonlinearity and dispersion effects are undesirable in an optical fiber transmission. They distort the propagated signal resulting in Inter-Symbol Interference, which limits the propagation distance. Optical transmission engineers must take these phenomena into

account in order to optimize the transmission over an optical link. Several studies led to the use of a novel modulation format, reshaping pulses and/or/using compensation stages. In this thesis, we focus on an optical transmission in which only chromatic dispersion makes a significant contribution. Other undesirable effects will not be considered. To overcome this limitation, therefore, we must introduce a compensation stage in optical links. They are qualified by pre- (respectively post-) even the compensation stage is before (respectively after) the transmission stage. The study as a whole is based on equation (5.2) showing the contribution of chromatic dispersion on the distortion of an optical pulse. As well, no conditions were established regarding the optical signal. An interesting case can be examined when the input signal is periodic. This is known as the temporal Talbot effect [62].

5.2 Chromatic dispersion compensation

The most commonly used optical methods employ Dispersion Compensation Fiber (DCF). This method introduces a dispersive behaviour along the DCF with length Z_2 , which is the exact opposite of the dispersion naturally resulting from light propagation through a standard fiber of length Z_1 . The signal covers a total distance $Z = Z_1 + Z_2$ and recovers its initial shape. Losses in DCF are not negligible. Furthermore, to obtain a short DCF, we should create a high amount of negative dispersion. If we consider both the second and third order of dispersion, the DCF must satisfy the following two equations:

$$\beta_2 Z_1 + \beta_2^{DCF} Z_2 \text{ and } \beta_3 Z_1 + \beta_3^{DCF} Z_2 = 0 \quad (5.3)$$

Pre-equalization methods use the same principle. The opposite dispersion effect is introduced before transmission by means of chirped fiber Bragg gratings or quadratic phase

modulators. Therefore, these techniques are limited by the technology providing such components and an applicable wavelength range. All electronic techniques of post-compensation are limited to a few dispersion lengths and are only functional for bit rates smaller than 10 Gb/s [63]. Effect of the CD is illustrated in Figure 5.1 below.

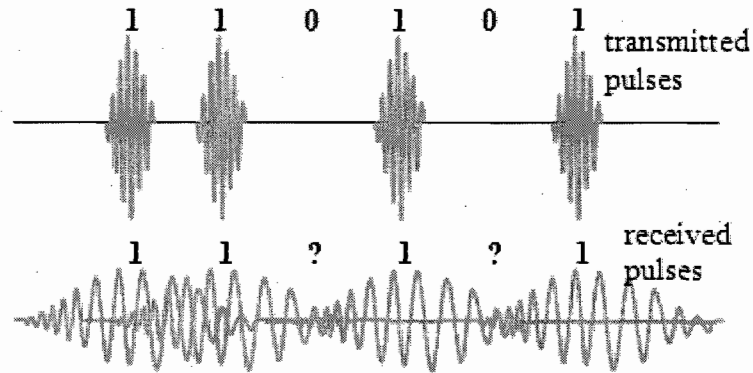


Figure 5.1 Effect of the CD of a transmitted signal

5.3 Temporal Talbot effect

Temporal Talbot effect is a self-imaging phenomenon that occurs when a periodic signal propagates through a dispersive medium at a given distance named Talbot distance Z_T [64, 65]. If the GVD effect is dominant,

$$Z_{T2} = \frac{d^2}{\beta_2 \pi} \quad (5.4)$$

where d is the period. (It must be noted here that Z_{T2} is the second order dispersion Talbot distance). A particular case of the Talbot effect is observed when the propagated distance is a fraction of the Talbot distance

$$Z = \frac{p}{q} Z_T \quad (5.5)$$

This is known as the Fractional Talbot effect. The resulting signal undergoes some modifications according to the value of p and q (p and q are both integers with no common factor). If the propagated signal is half the Talbot distance, the optical signal at the output is shifted by a half period ($d/2$). In general, if the signal is propagated in such a way that $Z = Z_T/2m$ (m is an integer), the reconstructed signal has a period divided by m . One can use the fractional Talbot effect for bit rate multiplication for pulse lasers.

If we take into account only the TOD effect, the Talbot distance

$$Z_{T3} = \frac{3}{2} \frac{d^3}{\beta_3 \pi^2} \quad (5.6)$$

(It must be noted here that Z_{T3} is the third order dispersion Talbot distance). As well, the Fractional Talbot effect can be observed for high order dispersion. Especially for TOD, we can reproduce exactly the same periodic signal at different fractional orders precisely at $1/2$, $1/3$ and $1/6$, but the signal is shifted by the product of the temporal period by the same value of the order chosen [64, 65].

Generally speaking, it is necessary to include the TOD effect, substituting Z_{T2} and Z_{T3} expressions in the equation (5.2) for a periodic signal. We then obtain:

$$U_d(w, z) = \sum_m U\left(\frac{m}{d}, 0\right) \exp\{i2\pi D_m\} \delta\left(w - \frac{m}{d}\right) \quad (5.7)$$

where $D_m = \left(\frac{1}{Z_{T2}} + \frac{m}{Z_{T3}}\right) m^2 z$, m is an integer. The self-imaging phenomenon can be

observed only if there are two integers a and b such as:

$$Z_T = aZ_{T_2} = bZ_{T_3} \quad (5.8)$$

(Global Talbot distance) that means $\frac{a}{b} = \frac{3}{2} \frac{\beta_2}{\beta_3} \frac{d}{\pi}$. This allows the cancellation of both

second and third order effects. Fractional Talbot cases make it possible to combine both second and third order Talbot effects. For example, when the global distance is $Z = Z_{T_2}/2 = Z_{T_3}/6$, the periodic signal is simultaneously translated by a half period (second order Talbot effect) and a one-per-sixth time period (third order Talbot effect). Indeed, we investigated the fractional third order Talbot distances and found that $Z = nZ_{T_3}/6$ (n is an arbitrary integer) is a very special distance. This new scientific observation is detailed in the next subsection.

5.4 Fractional third order Talbot distances

To illustrate fractional third order Talbot proprieties, we consider the example of $Z = n \frac{Z_{T_3}}{6}$, which will be used later on. We note that general cases of fractional third order Talbot will not be discussed at this level and will form the subject of future work. For $n = 1$, $\beta_2 = 0$, and $Z = \frac{Z_{T_3}}{6}$, we obtain:

$$D_m = \frac{m^3}{Z_{T_3}} Z = \frac{m^3}{6} \quad (5.9)$$

Using the following relation:

$$m^3 = 6k + m \quad (5.10)$$

Where k is an integer for any integer m .

We obtain:

$$\exp(i2\pi D_m) = \exp\left(i2\pi \frac{m}{6}\right) = \exp\left(i2\pi \frac{d}{6} \frac{m}{d}\right) \quad (5.11)$$

Equation (5.7) then becomes:

$$U_d(w, z) = \exp\left(i2\pi \frac{d}{6} w\right) \sum_m U(w, 0) \delta\left(w - \frac{m}{d}\right) \quad (5.12)$$

The result was that the propagated signal at the fractional Talbot distance $Z = \frac{Z_{T3}}{6}$ is identical to the origination signal at $Z = 0$, except for a temporal shift by $d/6$:

$$u_d(t, z = Z_{T3}/6) = u_d(t - \frac{d}{6}, 0) \quad (5.13)$$

It is obvious that the signal attaining the distance

$$Z = \frac{Z_{T3}}{3} = \frac{Z_{T3}}{6} + \frac{Z_{T3}}{6} \quad (5.14)$$

is twice shifted by the amount $\frac{d}{6}$. As expected for the half Talbot distance, $Z = \frac{Z_{T3}}{2}$, we obtain a shift of $\frac{d}{2} = 3\frac{d}{6}$. This interesting result shows that we can obtain the exact initial periodic signal, considering only third order dispersion at different Fractional third order Talbot distances $Z = n\frac{Z_{T3}}{6}$, except for a shift of $(m \text{ modulo } 6) \frac{d}{6}$, where modulo denotes the rest of the integer division.

An example of Talbot effect is illustrated in Figure 5.2 below.

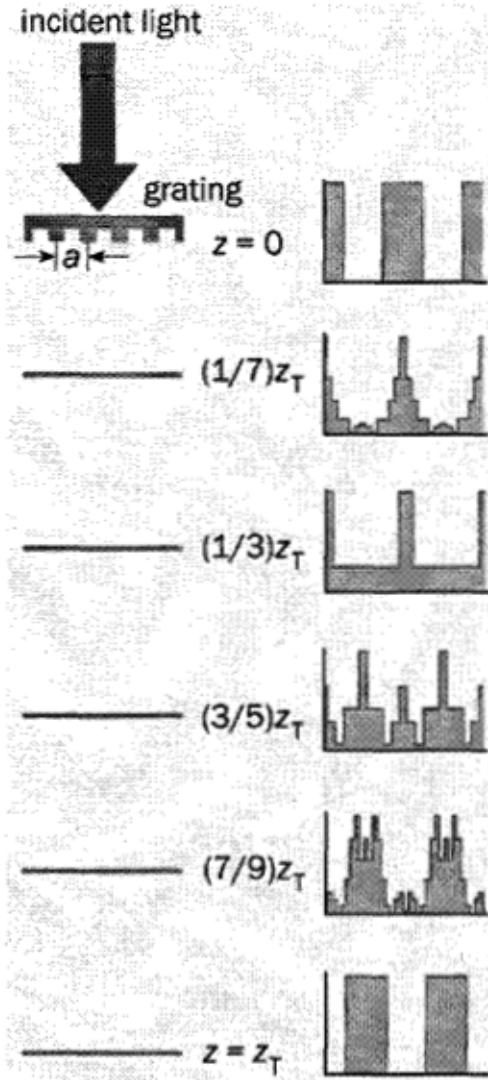


Figure 5.2: Talbot effect example.

5.5 Proposed optical solution

5.5.1 Optical nature

Because chromatic dispersion is an optical phenomenon, the most appropriate method is expected to be of an optical nature. Indeed, the most mature technique for chromatic dispersion compensation is the use in the optical domain of dispersion compensating fibers

(DCFs) having a dispersion characteristic that negates that of the original fiber. But DCFs are expensive and bulky; for every 80-100 km of SSMF, several kilometers of DCF are required and could cost as much as the fiber for which it compensates [2]. Since the DCF is added to compensate for what is already installed, its length does not add to the total length of the link. Instead, the DCF sits at one end of the link on a drum. This adds to the total attenuation of the link (the DCF has a typical attenuation of 0.5 dB/km) so that additional amplification may be needed. Furthermore, the narrow core of the DCF makes it more susceptible to fiber nonlinearity effects. The DCF is also polarization-sensitive.

5.5.2 Principle

We propose an optical solution based on the Talbot Effect to compensate for chromatic dispersion. In what follows, we advance and analyze the first optical post-compensation of chromatic dispersion using a temporal Talbot effect.

Briefly, if we let

$$Z = Z_1 + Z_2 \quad (5.15)$$

and substitute this into equation (5.2), separating terms, we get:

$$U_d(w, z) = U(w, 0) \exp\{i2\pi D Z_1\} \sum_m \delta\left(w - \frac{m}{d}\right) \exp\{i2\pi D_m Z_2\} \quad (5.16)$$

The first two terms $(U(w, 0) \exp\{i2\pi D Z_1\})$ can represent the propagation of a non-periodic signal U along the distance Z_1 ; next, the summation term $(\sum_m \delta(w - \frac{m}{d}))$ can be referred to a periodization stage, and finally, the last term in the equation $(\exp\{i2\pi D_m Z_2\})$ refers to the propagation of the periodized signal along the distance Z_2 . It is obvious that if

$$Z_1 + Z_2 = Z_T \quad (5.17)$$

one can regenerate a periodic signal where one period is similar to the initial signal. This property is the main reason for using the temporal Talbot effect to optically compensate for chromatic dispersion. Figure 5.3 illustrates the scheme of the proposed TEChDC system. While periodization creates the power of the system, this operation is also the source of its complexity. The distorted optical signal obtained from a transmission fiber of length Z_1 passes through a periodization stage. As detailed in the next subsection, this operation can be performed by a multistage cascaded Mach-Zehnder interferometer (MZI) or cascaded long period fiber grating (LPFG). Using MZI based periodization stage; the input signal is split into two. Each part travels along a leg. Time delay between MZI legs in such a way the recombination produces two distanced identical images. Cascading several stages, if we choose appropriate timing delay for each stage, the outgoing signal becomes periodic. At last, the periodized signal propagates a second time over another standard fiber of a complementary length of Talbot distance (or a half or any appropriate fractional distances).

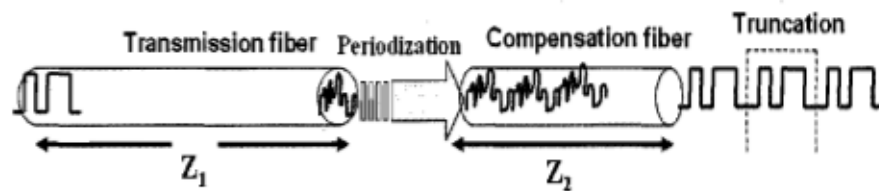


Figure 5.3 Schematic model of the proposed TEChDC

post-compensation model

5.5.3 Periodization process

The periodization process is considered the engine of the whole idea. When a deteriorated signal is received after passing through fiber Z_1 (as shown in Figure 5.3), it is

entered into the periodizer, from whose output we obtain a periodized signal. This periodized signal is then injected into fiber Z_2 . There are two possible alternatives for implementing the periodization process:

5.5.3.1 Mach-Zehnder interferometer (MZI)

The periodization stage is implemented by using four Mach-Zehnder interferometers with different time delays as shown in Figure 5.4. The choice of the 4 Mach-Zehnder periodizer is the best compromise to have enough periodicity with reasonable power consumption.

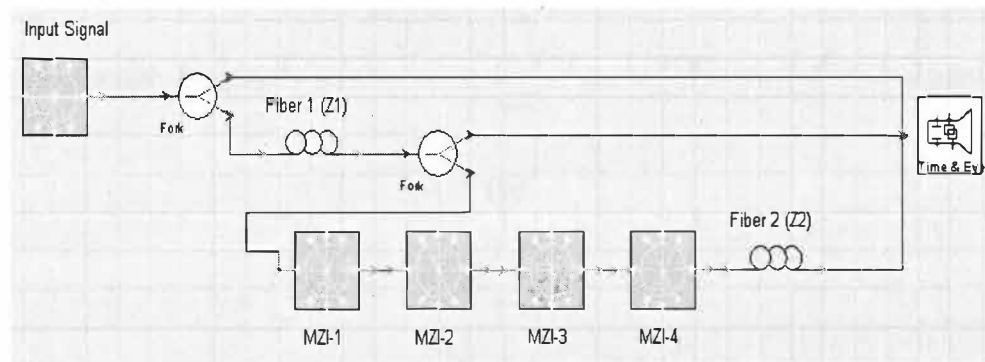
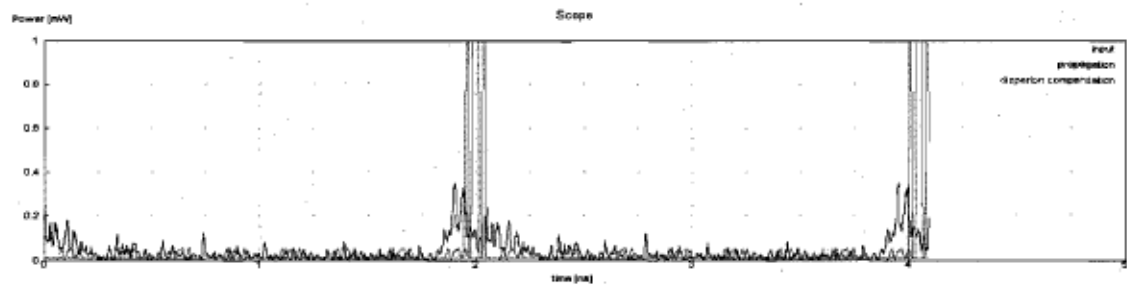
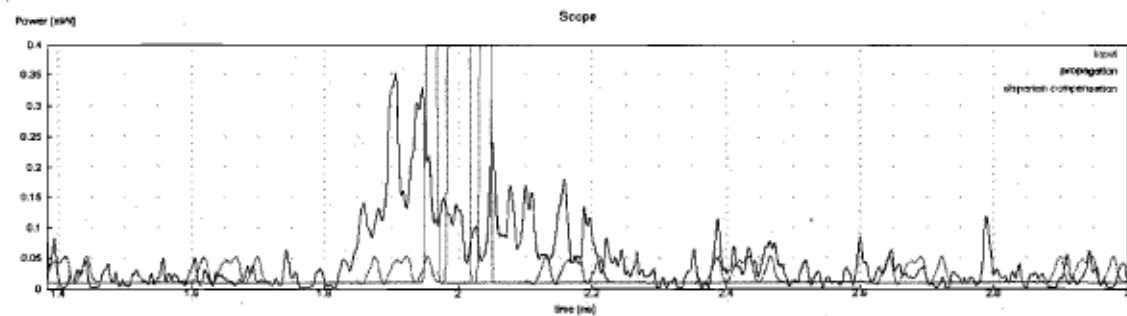


Figure 5. 4 A periodizer implemented using four MZIs

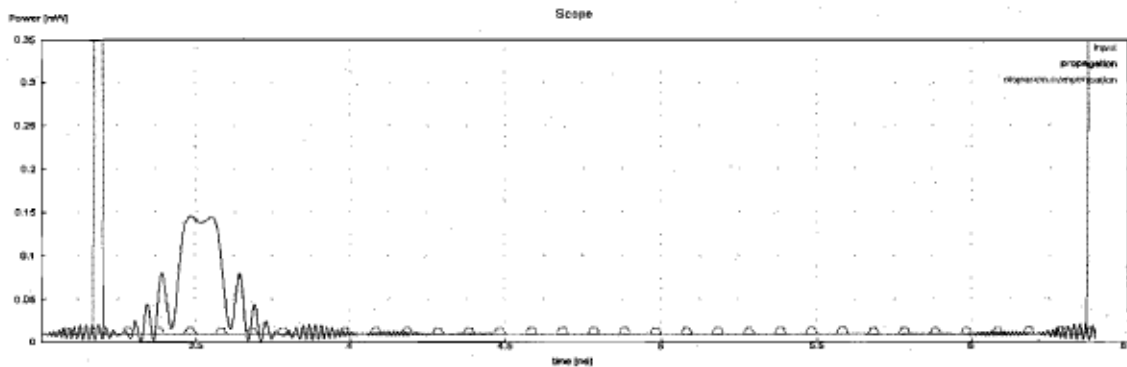
Once implemented, Figure 5.5 a) shows the profiles of two input pulse signals and their propagation results.



(a)



(b)



(c)

Figure 5. 5 Periodizer outputs for a) general view, b) same signal as in a) and c) another signal with a detailed view of the periodized signal

Figure 5.5 b) is a close-up of the same signals shown in a). The cascaded MZI-based system performs the periodization of any input signal including the deteriorated signal.

Figure 5.5 c) illustrates different input signals where there is different dispersion on the signal and different periodization periods.

5.5.3.2 Long period fiber grating (LPFG)

The periodization process is also possible using a cascaded Long Period Fiber Grating (LPFG). An LPFG is a device used for mode coupling between the core and the co-propagating cladding modes of an optical fiber. In general, the cladding mode has a lower propagation constant than the core mode. Therefore, the optical pulse coupled to the cladding mode by an LPFG propagates faster than the uncoupled core mode. By using another LPFG in series, the pulse in the cladding mode can be coupled back to the core mode. Hence, two optical pulses that are identical but separated in time can be obtained from a single pulse, but within a single piece of fiber. The time delay, ΔT , between the pulses is simply calculated as:

$$\Delta T = \frac{L}{C} \Delta m_{eff} \quad (5.18)$$

where L is the separation between the LPFGs, C is the speed of light in a vacuum, and Δm_{eff} is the differential effective group index (DEGI) of the two modes. Thus, by cascading a series of LPFGs, multiple identical optical pulses can be generated from a single short optical pulse. The schematic diagram for the realization of a true time delay is illustrated in Figure 5.6. The inset figures show the measured near-field intensity patterns of the fundamental core mode and a DCF cladding mode.

If we use N LPFGs in series, we can have $(2N - 1)$ pulses from a single pulse. The separations among the pulses are determined by the separations of the LPFGs. Therefore, N

cascaded LPFGs will constitute $(N - 1)$ delay elements and multiplicative $(2N - 1)$ optical pulses. Each delay element consists of two identical but separated LPFGs. Note that only pulse trains in the core mode are taken after the last grating of the cascaded LPGs. The other $2N$ pulses in the cladding mode, after passing the last grating, are generally absorbed or scattered at the cladding surface [38].

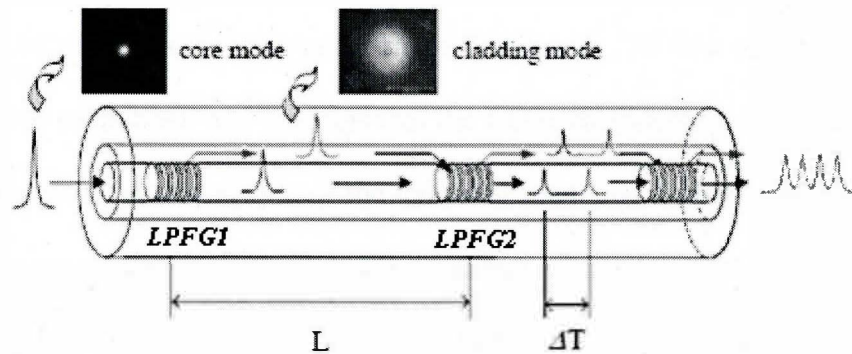


Figure 5. 6 Schematic diagram of realization of a true time delay with a cladding mode using cascaded LPFGs

5.5.4 Advantages

The new method developed for the chromatic dispersion of post-compensation based on the Talbot effect has many advantages, including the following:

- The signal received may be totally altered.
- It offers complete freedom to choose the period, the high order Talbot distances.
- There is no need to increase the number of repeaters, which results in major cost savings.

- It is independent from the bit rate sent originally, meaning that it can handle bit rates in excess of 40Gbit/s.

No special fiber is required. Standard single mode fibers can be used.

5.6 Conclusion

Chapter 5 contains two major sections, theoretical analysis and proposed optical solution; it is one of the most important parts of this thesis. The first section describes the pulse propagation in an SMF and explains that the CD is considered a major concern to be dealt with in the OFC. A description of the temporal/fractional Talbot effect is also given. The second section describes the basics and principles of the TEChDC. The TEChDC for combating the CD is based entirely on the Talbot effect. This technique relies on the reproduction of a totally altered signal. The alteration is in turn the effect of the CD after the signal has traveled a certain distance, Z_1 . The same signal is then propagated through a periodizer (to obtain a periodized signal), then injected through Z_2 to be Z_T in total. The periodization process can be obtained using either MZM or long period grating. These methods and some of their advantages are discussed in the Conclusion.

Chapter 6 - Simulation results

6.1 Introduction

To assess the performance of the TEChDC under more realistic transmission impairments, the following case is considered. A 40-Gb/s scenario system was carried out with different system effects. The system ran over a Standard single-mode fiber (SSMF with 2000, 4000 and 6000 km fiber lengths) and operated in the 1550-nm band. Inline EDFAs of 20-dB gain each were placed between every two sections to compensate exactly for section attenuation. An optical third-order Bessel filter having a bandwidth of 100 GHz was placed immediately before the receiver p-i-n diode. Different types of inputs and modulation formats such as return-to-zero (RZ), non-return-to-zero (NRZ), RZ Duo-binary and NRZ Duo-binary were available. The NRZ modulation format results are presented, but other formats are available as well.

6.2 Setup description

In general, an optical communication system consists of an optical source, transmitters, modulators, fiber and receivers. Since the major components are already outlined in the main thesis, a quick explanation of their operation is given along with their role within the simulator. Various limiting parameters associated with each photonic or optoelectronic device are also introduced. Figure 6.1 depicts the system setup used during the simulation.

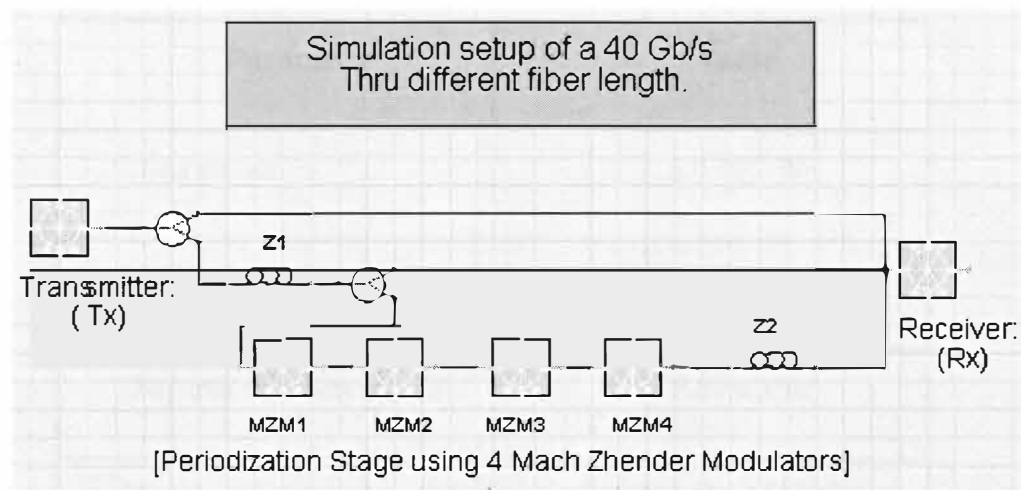


Figure 6.1 General view of the TEChDC

In brief descriptions, a fundamental understanding of the optical transmitters used in the simulation package is based on the laser source, modulation, line coding formats and pulse formats. A 40-Gb/s PRBS is used as the test signal. While closely resembling a random sequence, a PRBS of length $(2^n - 1)$ ensures that all the bit patterns of length n , except an all-zero pattern, are available. This is particularly important in the study of systems suffering from ISI, since the distortion is bit-pattern dependent. Choosing the PRBS length depends on the amount of pulse spreading expected. The following table describes the parameters used during the simulation.

Tableau 6-1: Parameters used in the simulation

Parameter	Value
Laser power	$5.0 \cdot 10^{-3} \text{ W}$
Modulation type	NRZ
Dispersion parameter, D	$15.69 \mu \text{ s/m}^2$
Dispersion slope, S	50.1051 M s/m^3
Laser wavelength, λ	1550 nm
Fiber Type	SSMF
Fiber length	2000-6000 km
Fiber core area	80 pico m^2
Tau_1	12.2 femto
Tau_2	32.0 femto

A laser was used in which data is encoded in return-to-zero (RZ), non-return-to-zero (NRZ), RZ Duo-binary and NRZ Duo-binary formats corresponding to the experimental setup described in the applet. In this study, only bursty data is assumed at the input level. Continuous data is not considered in this study.

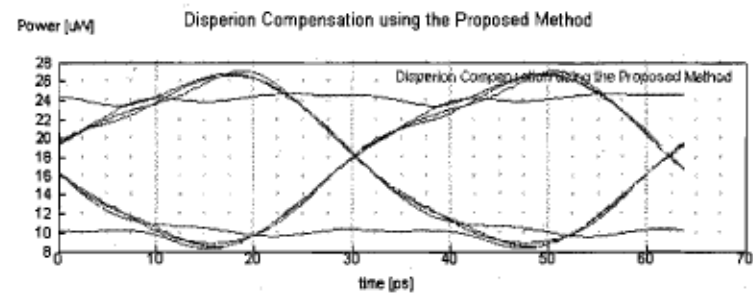
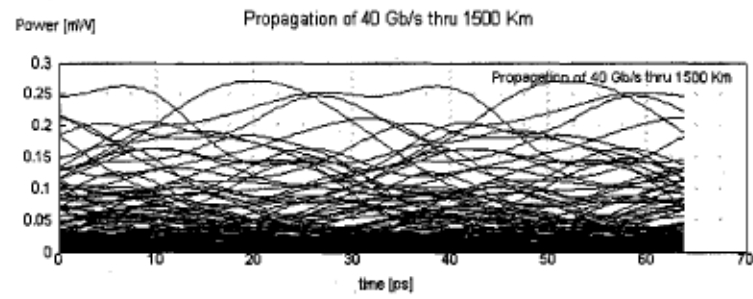
Because SSMFs are the most commonly used fibers, they were employed in the simulations of one span of fiber propagation. We investigated several setups for different fiber lengths, although all other fiber parameters remained the same. The SMF used has the following characteristics: length: (ranging from 2000 km to 6000 km) for Z_1 and the (ranging from 22 to 132 km) for Z_2 , a core area of 80 p (pico) m^2 , and a dispersion and dispersion slope of $15.69 \mu \text{s/m}^2$ and 50.1051 M s/m^3 respectively with $\text{Tau}_1 = 12.2$ femto and $\text{Tau}_2 = 32.0$ femto (10^{-15}).

At the receiver, the signal is filtered in the optical domain by a third order Bessel filter with 100-GHz bandwidth and in the electrical domain by a fourth order Bessel low-pass filter with a 3-dB and a cutoff frequency of 0.7 GHz.

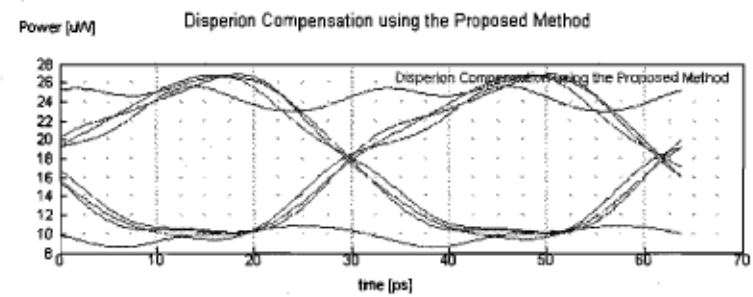
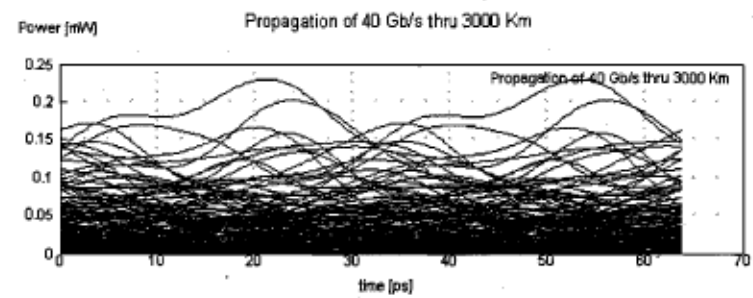
6.3 Simulation of 40 Gb/s results

The performance of the system is quantified in terms of receiver sensitivity or optical power penalty. Receiver sensitivity is defined as the optical power at the receiver that is required to achieve a certain bit-error-rate (BER, typically ranging from 10^{-12} to 10^{-20}). When the absolute values of the received optical power are not important, the optical power penalty can be used instead. The optical power penalty is defined as the required increase in the optical power needed to achieve a certain BER relative to a reference zero-penalty case.

The 40 Gb/s was transmitted through different fiber lengths as shown in the diagrams in Figure 6.2. We opted for the eye diagram, since it is a useful tool for the qualitative analysis of a signal used in digital transmission. An eye diagram offers at-a-glance evaluation of system performance and can offer insight into the nature of channel imperfections.



a)



b)

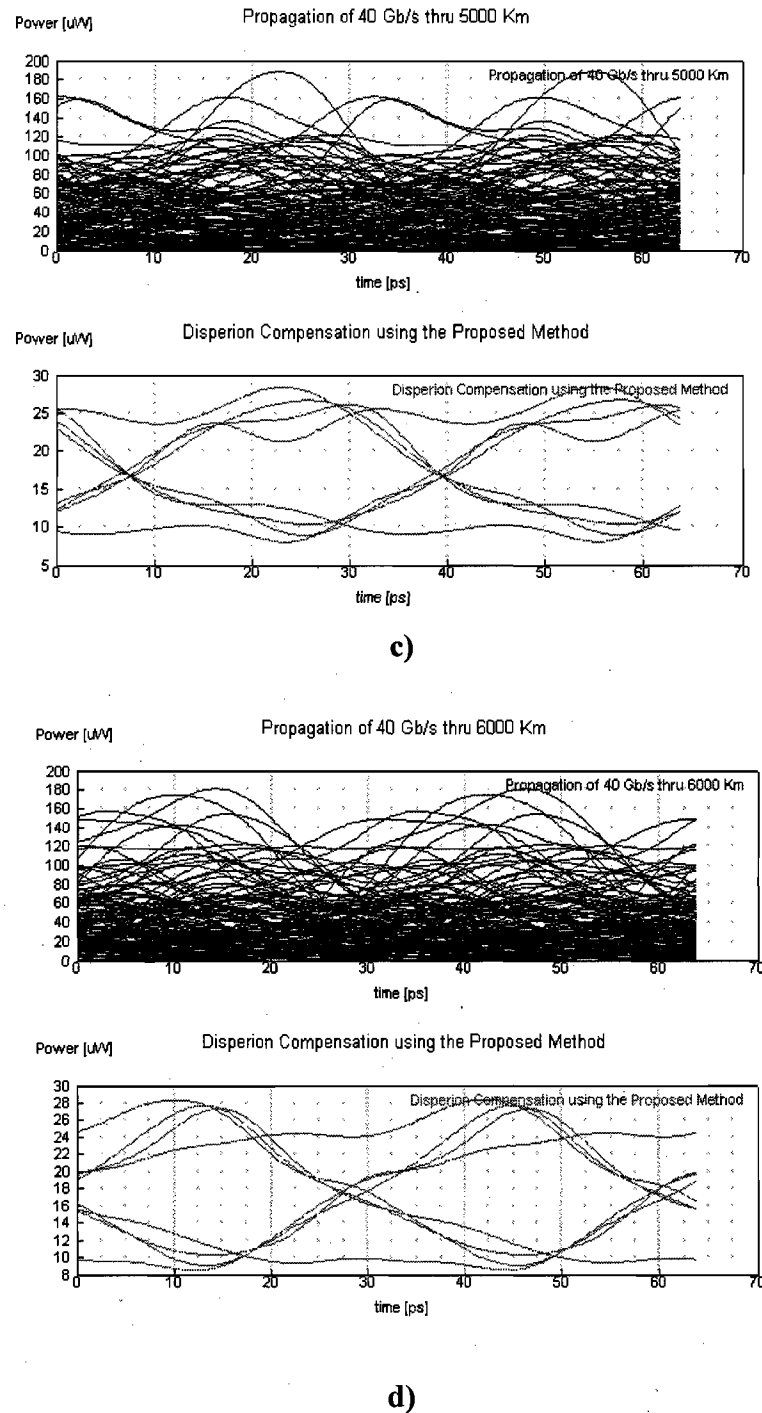


Figure 6.2 Simulated receiver eye diagrams of noise-free pre-distorted 40-Gb/s

Figure 6.2 a) illustrates the eye diagram opening of 40-Gb/s through a fiber length of 1500 km. It is obvious that the eye diagram is spacious for a better sampling of the signal, which is a reasonable indication that the transmission was carried out faithfully. It is also

very clear that the edge where the zero crossing takes place is almost negligent, the horizontal and vertical openings are both wide enough. The slope indicating sensitivity to timing error is extremely small and curved, which is in turn a clear indication that the signal is likely to be sampled without error. Figure 6.2 b) indicates that after transmitting the signal through an SSMF of 3000 km in length, the eye diagram still holds its global shape for a better signal sampling. As for Figure 6.2 c) and d), and after the 5000 and 6000 km that is considered an enormous distance, the eye diagram begins to deteriorate after 6000 km.

6.4 Bit Error Rate (BER)

The digital receiver performance is governed by the BER. The latter is the probability that a bit is identified incorrectly by the decision circuit of the receiver. In fiber optic communication systems, the error rates usually range from 10^{-12} to 10^{-20} . This value depends on the signal-to-noise ratio at the receiver. Under the assumption of a Gaussian probability density function (PDF), the probability of error for a *one* or *zero* is simply calculated as:

$$P_{1,0} = \frac{1}{2} \operatorname{erfc} \left(\frac{|\mu_{1,0} - I_{th}|}{\sqrt{2}\sigma_{1,0}} \right) \quad (6.1)$$

where $\mu_{1,0}$ and $\sigma_{1,0}$ are the mean and standard deviations of the *one* and *zero*, respectively, and I_{th} is the decision threshold. $P_{1,0}$ is the probability of receiving a bit of value 1 when a bit of value 0 was sent. To take into account the bit pattern effects due to ISI, (1) is calculated for each 1 and 0 in the PRBS, and the BER is merely calculated as the average of all those calculations,

$$BER = \frac{1}{2N} \sum_{k=1}^N \operatorname{erfc} \left(\frac{|\mu_k - I_{th}|}{\sqrt{2}\sigma_k} \right), \quad (6.2)$$

where N is the number of symbols in the PRBS.

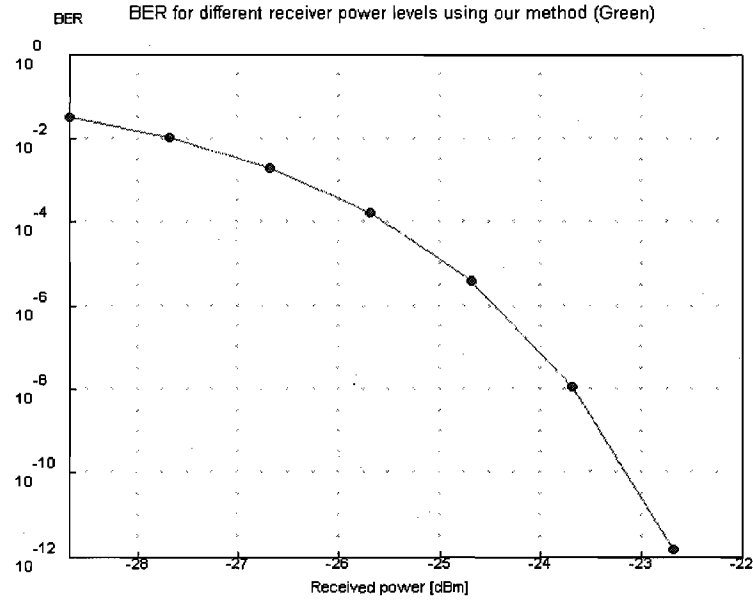


Figure 6.3 Receiver performance when transmitting a 40 Gb/s through 5000 km using the TEChDC method

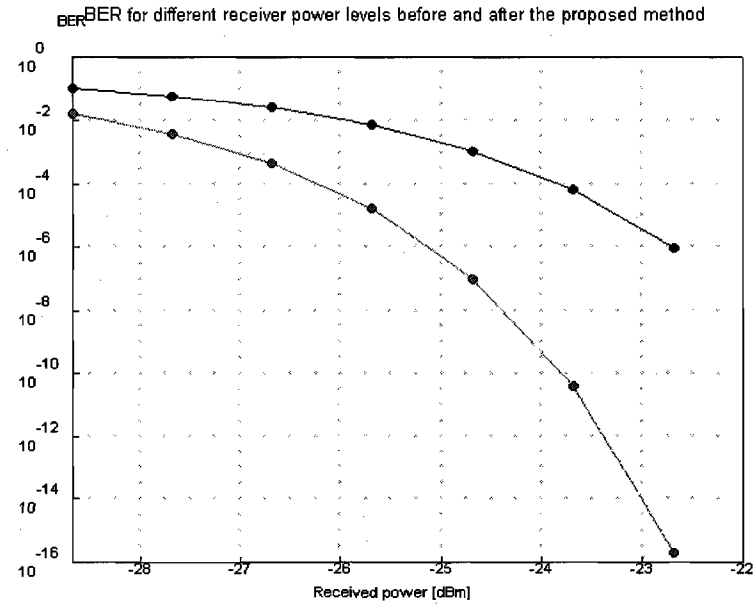
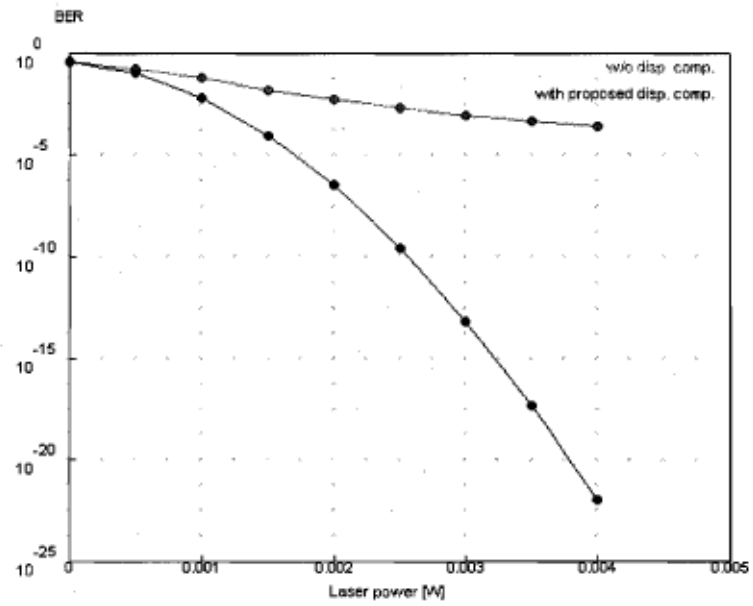
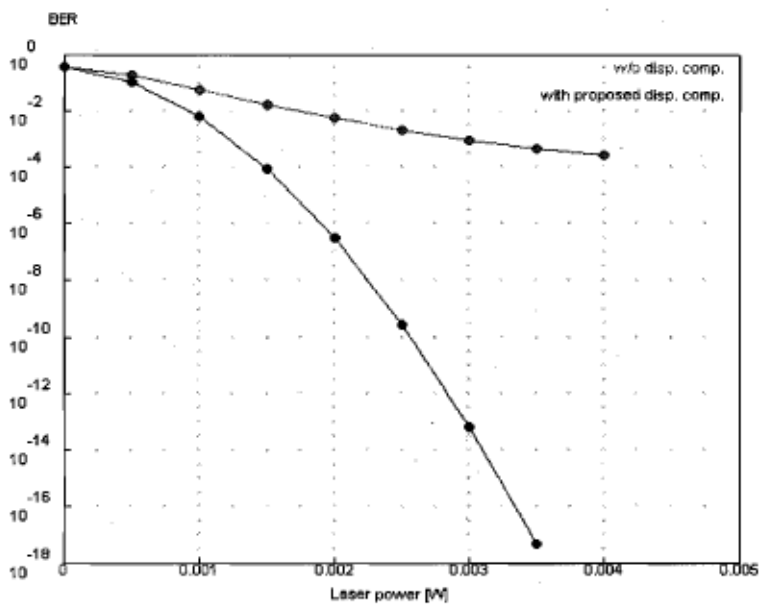


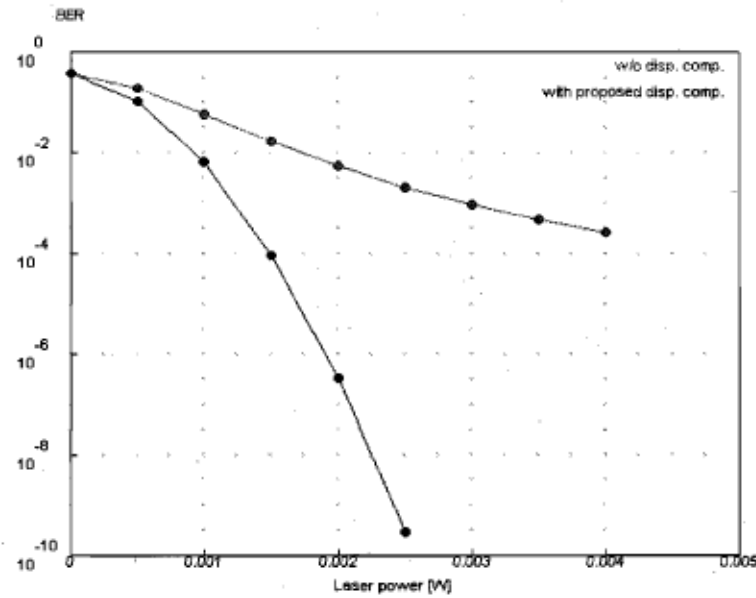
Figure 6.4 Comparing receiver sensitivity before and after applying the TEChDC method through 5000 km



a) 2000 km



b) 4000 km



c) 6000 km

Figure 6.5 a, b, c) Receiver performance for different fiber lengths in terms of BER with respect to laser power

Figure 6.3 compares receiver sensitivity before and after the TEChDC method was applied, Figure 6.4 illustrates the BER in terms of the laser power used to transmit data with a rate of 40-Gbs through the indicated fiber lengths. Figures 6.5 a), 6.5 b) and 6.5 c) shows clearly that a significant reduction of the laser power was used to achieve the desired BER. Figures 6.5 a), 6.5 b) and 6.5 c) clearly demonstrate that the values of the laser power necessary to attain such low BER is in the order of 0.004, 0.003 and 0.0025 W respectively.

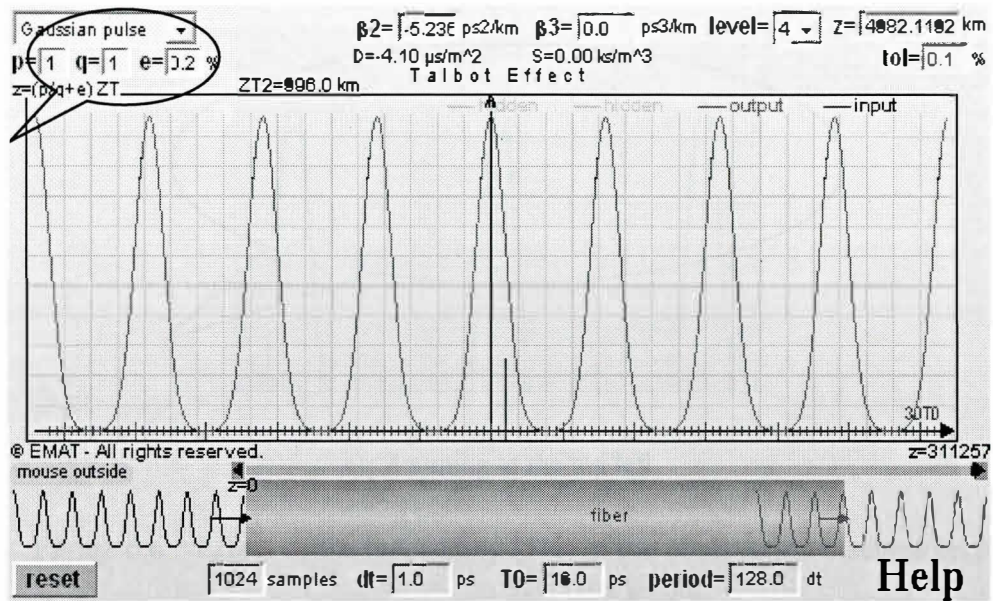
6.5 Robustness of the TEChDC method with respect to fiber length

The TEChDC method is based on the solid theory of the Talbot effect, which is a self-imaging phenomenon that occurs when a periodic signal propagates through a dispersive medium at a given distance termed Talbot distance Z_T . If the Group Velocity Dispersion

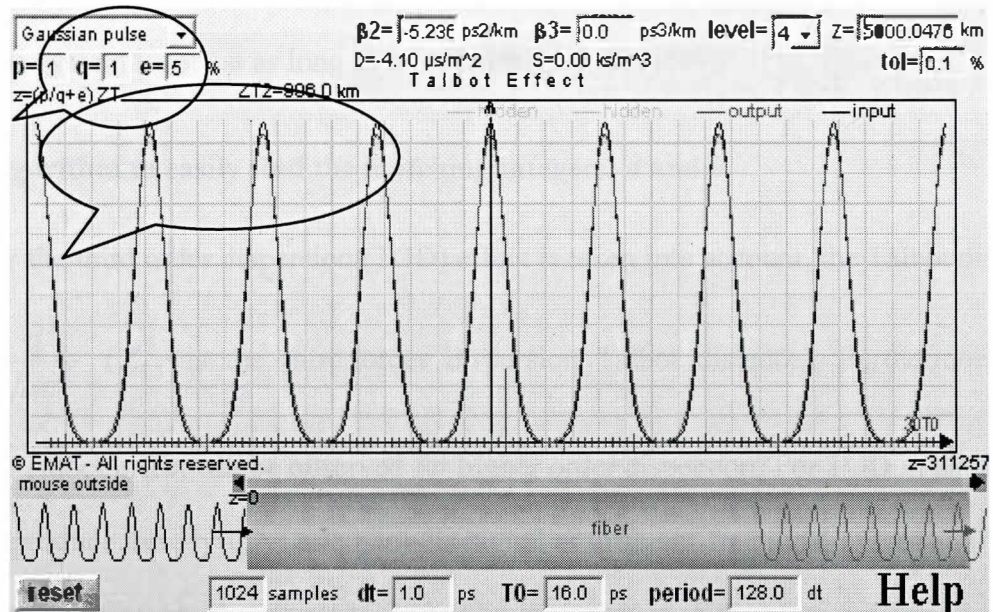
(GVD), or chromatic dispersion of second order, is dominant, then $Z_{T2} = \frac{d^2}{\beta_2 \pi}$, where Z_{T2} is referred to as the second order dispersion Talbot distance, d is the period and β_2 is the second order dispersion coefficient. A particular Talbot effect is observed when the propagated distance is a fraction of Talbot distance $Z = \frac{p}{q} Z_T$. Here Z_T is equal to Z_{T2} . This is known as the Fractional Talbot effect. The resulting signal undergoes some modifications according to the value of p and q (p and q are both integers with no common factor). A calculation including errors was added to the applet where the error e of the fiber length affects the observation distance Z as follows:

$$Z = \left(\frac{p}{q} + e \right) Z_T \quad (6.3)$$

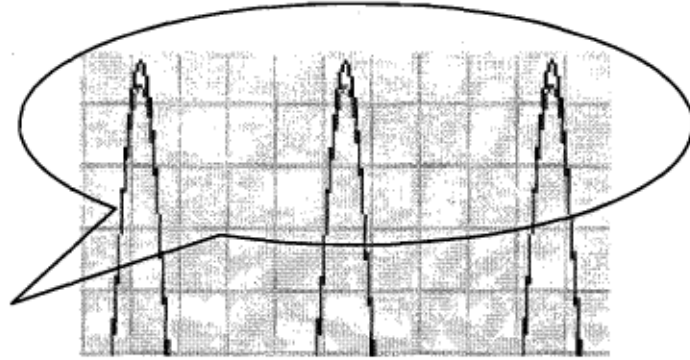
An example of errors is given in the top left corner of Figures 6.4 b) and c). Figure 6.5- a) points out that the effect of the error is not observable until the error reaches 5% of the total fiber length as shown in Figure 6.5 b). Figure 6.5 c) illustrates the case in which we focus on the top left edges of the signal where the signal deviation starts to take place.



a): Applet simulating the effect of the error at the level of the observation distance Z (x-axis is time and y-axis is amplitude)



b): Input and output signal for an observation distance with a 2% relative error (x-axis is time and y-axis is amplitude)



c): Zooming at the top left

Figure 6.6 Effect of the inaccuracy (5%) of the observation distance on the received signal

By zooming the selected top corner of Figure 6.6 b), one obtains Figure 6.6 c). It is clear that the compensated signal (output) and the input signal are not significantly different. The received signal starts to diverge from the input signal when the error reaches 5%. Error tolerance in the fiber length is acceptable if it is less than 5% of the total fiber length. The system is robust as long as error is insignificant (5%).

6.6 Algorithm to easily find the matching integers: a and b

If only the third order dispersion (TOD) effect is taken into account, the Talbot distance is $Z_T = \frac{3}{2} \frac{d^3}{\beta_3 \pi^2}$ (Z_{T3} is the third order dispersion Talbot distance). Furthermore, the Fractional Talbot effect can be observed for higher order dispersion. For TOD in particular, we can reproduce exactly the same periodic signal at different fractional orders at $1/2$, $1/3$ and $1/6$ specifically, but the signal is shifted by the product of the temporal period by the same value of the order chosen. For a given distance Z the spectrum of the periodic signal observed at this distance is:

$$U_d(\omega, z) = \sum_m U\left(\frac{m}{d}, 0\right) \exp\{i2\pi D_m\} \delta\left(\omega - \frac{m}{d}\right) \quad (6.4)$$

Where $D_m = \left(\frac{1}{Z_{T2}} + \frac{m}{Z_{T3}}\right) m^2 z$, and m is an integer

when both second and third order dispersion are involved, self-imaging will be observed only if there are two integers a and b such as:

$$Z_T = aZ_{T2} = bZ_{T3} \quad (6.5)$$

(Global or common Talbot distance) which means $\frac{a}{b} = \frac{3\beta_2}{2\beta_3} \frac{d}{\pi}$. This makes it possible

to cancel both second and third order effects.

Let us take an example: $Z_{T2} = 400$ km and $Z_{T3} = 997$ km. In this case, the two co-primary integers a and b are $a = 997$ and $b = 400$. In other words, these two values make it possible to express the common Talbot distance as follows: $Z_T = 997 \times 400$ km = 400×997 km = 398 800 km. This deals with a huge distance, which is approximately the average distance between the earth and the moon.

However, we note that: $5 Z_{T2} = 2 000$ km and $2 Z_{T3} = 1994$ km, which are two relatively close distances. So $a' = 5$ and $b' = 2$ are acceptable matching integer values if a certain tolerance, tol , is permitted. Indeed,

$$\frac{a}{b} = \frac{997}{400} = 2.4925 \quad \text{and} \quad \frac{b}{a} = 0.4012 \quad (6.6)$$

$$\text{Thus: } \left| \frac{b'}{a'} - \frac{b}{a} \right| = |0.4 - 0.4012| = 0.0012 < \frac{1}{100} = tol \quad (6.7)$$

Therefore, if a tolerance $tol = 1\%$ is permitted, the integers a' and b' are acceptable matching values. We denote r the ratio a'/b' ($r=a'/b'$). The coefficient a' and b' are calculated according to the following relation:

$$\left| \frac{1}{r} - \frac{b}{a} \right| < tol \quad (6.8)$$

Let us take $Z_{T3} > Z_{T2}$ (which is the general case) and $tol = 1/L$ (for example if $tol = 5\%$ then $L = 20$). $Z_{T3} > Z_{T2}$ means that $r > 1$ and $b/a < 1$:

$$0 < \frac{b}{a} < 1 \quad (6.9)$$

Thus, there exists an integer S , smaller than L , so that:

$$\frac{S}{L} < \frac{b}{a} < \frac{S+1}{L} \quad (6.10)$$

In other words, any number between 0 and 1 can be limited by two fractional values with any common denominator. Let us take the above example: $Z_{T2} = 400$ km and $Z_{T3} = 997$ km. In this case $b/a = 0.4012$. Thus, for $L = 20$ we find $8/20 < b/a < 9/20$. In this case, S is equal to 8. Thus, we can choose either

$$\frac{1}{r} = \frac{b'}{a'} = \frac{S}{L} \quad (6.11)$$

or

$$\frac{1}{r} = \frac{b'}{a'} = \frac{S+1}{L} \quad (6.12)$$

For both cases, the following equation is fulfilled:

$$\left| \frac{1}{r} - \frac{b}{a} \right| < \frac{1}{L} = tol \quad (6.13)$$

The fractional Talbot effect is also observable with respect to the approximated Z_T .

If we take $S = 8$, we obtain, according to equation (6.11), $a' = L/4 = 5$ and $b' = S/4 = 2$ (4 is the greatest common divider of 8 and 20). This means that:

$$5Z_{T2} \cong 2Z_{T3} \quad (6.14)$$

For the same example, $5Z_{T2} = 2000 \text{ km} \cong 2Z_{T3} = 1994 \text{ km}$.

Thus, the common Talbot distance Z_T may be chosen as $5Z_{T2}$ or $2Z_{T3}$ or an intermediate value between $5Z_{T2}$ and $2Z_{T3}$ such as the average value:

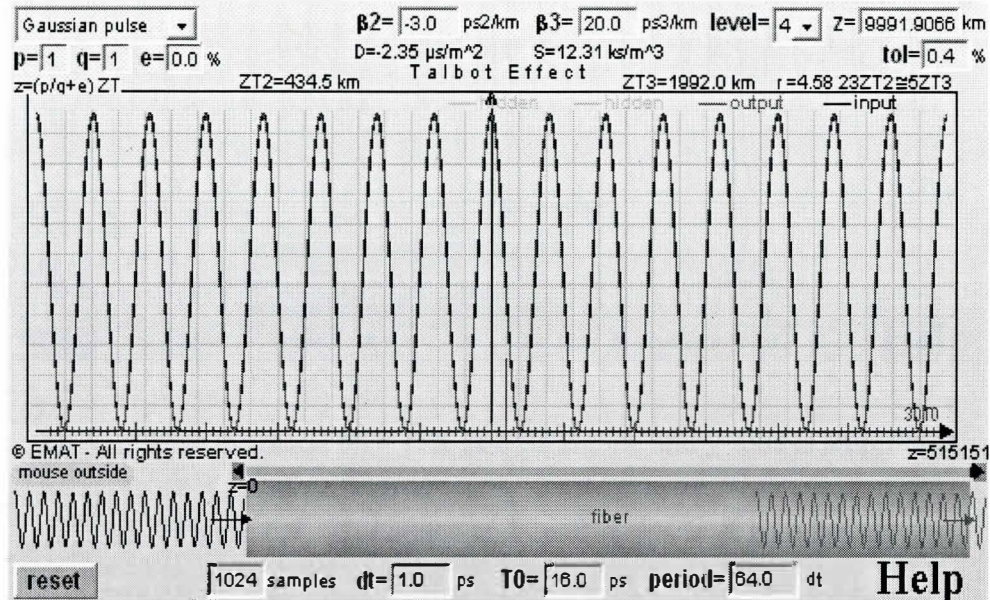
$$Z_T = a'Z_{T2} + \frac{b'Z_{T3} - a'Z_{T2}}{2} = \frac{a'Z_{T2} + b'Z_{T3}}{2} = \frac{5Z_{T2} + 2Z_{T3}}{2} \quad (6.15)$$

For our example, we can take $Z_T = (2000 \text{ km} + 1994 \text{ km}) / 2 = 1997 \text{ km}$. Because the second order Talbot distance Z_{T2} is more than twice as small as Z_{T3} , it is worth choosing an intermediate value closer to $5Z_{T2}$. By taking into account the ranges of the values of Z_{T2} and Z_{T3} , we suggest the following intermediate value:

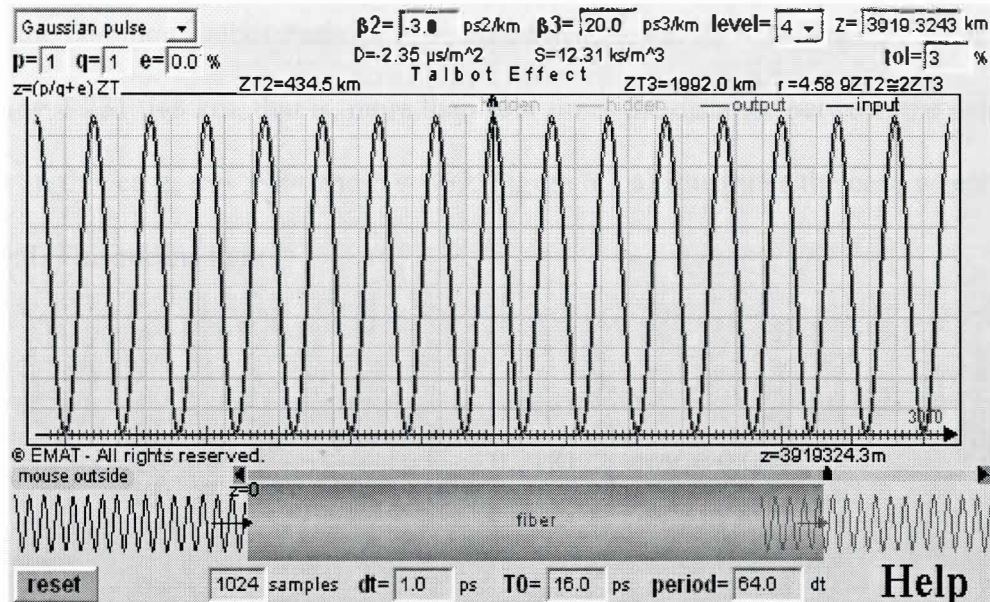
$$Z_T = a'Z_{T2} + r \frac{b'Z_{T3} - a'Z_{T2}}{2} = 5Z_{T2} + \frac{2}{5} \times \frac{2Z_{T3} - 5Z_{T2}}{2} \quad (6.16)$$

This intermediate value is closer to $5Z_{T2}$ than to $2Z_{T3}$, and it is even closer to $5Z_{T2}$ if Z_{T2} is smaller than Z_{T3} .

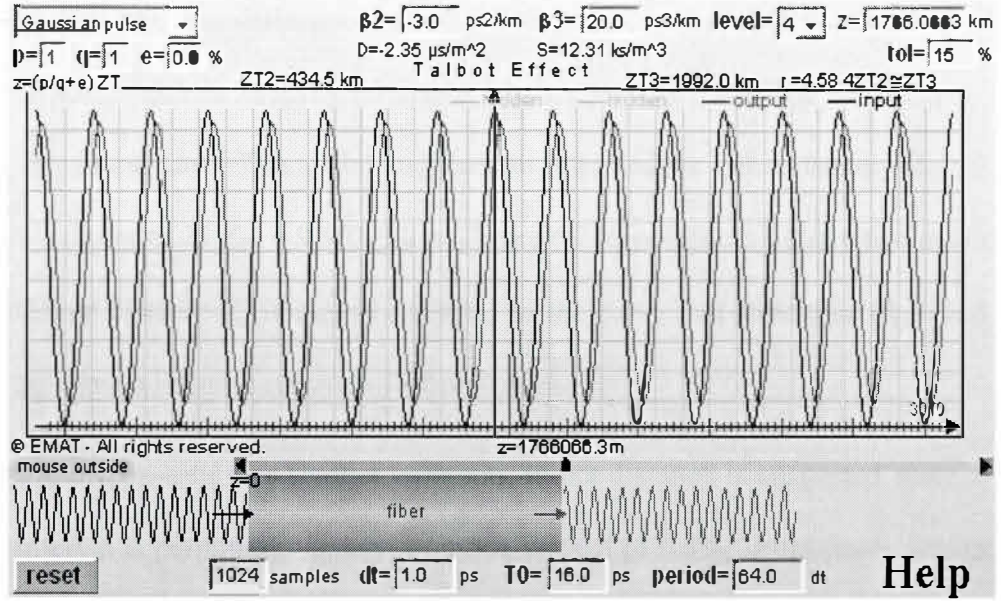
The matching values a' and b' found for the couple (Z_{T2}, Z_{T3}) can be also found for the couple $(Z_{T2}/2, Z_{T3}/6)$, since in these fractional distances the signal form is integrally reproduced except for a time shift.



a): Very small tolerance: $\text{tol} = 0.4\%$ (x-axis is time and y-axis is amplitude)



b): Larger tolerance: $\text{tol} = 3\%$ (x-axis is time and y-axis is amplitude)



c): Very large tolerance: tol = 15% (x-axis is time and y-axis is amplitude)

Figure 6.7 Tolerance and coefficients (a & b) relation

Let us consider Figure 6.7 a) where $Z_{T2} = 434.5$ km and $Z_{T3} = 1992$ km. Rigorously speaking, the common Talbot distance is obtained as follows: $Z_T = 3984 \times 434.5$ km = 869 x 1992 km = 1 731 048 km, that is, more than four times the distance between the earth and the moon. In this case, $a = 3984$ and $b = 869$. Figure 6.7 a) illustrates the case where 0.4% is permitted. This means that:

$$\left| \frac{b'}{a'} - \frac{b}{a} \right| = \left| \frac{b'}{a'} - \frac{869}{3984} \right| = \left| \frac{b'}{a'} - 0.218122 \right| < tol = 0.004 \quad (6.17)$$

is permitted. In this case, the applet suggests the following values for a' and b' : $a' = 23$ and $b' = 5$. This leads to a reasonable common Talbot distance since: $23 Z_{T2} = 9 993.5$ km

$\cong 5 Z_{T3} = 9\,960$ km. The difference between both multiple Talbot distances is $|23 Z_{T2} - 5 Z_{T3}| = 33.5$ km, which is roughly 13 times smaller than the smallest of the two Talbot distances, Z_{T2} in our case. The applet suggests an intermediate value, namely $Z_T = 9\,991.6$ km, which is closer to $23 Z_{T2} = 9\,993.5$ km. Figure 6.7 a) points out clearly that the curve at the intermediate distance Z_T is almost identical to the curve that should be observed at the rigorous, but almost infinite, common Talbot distance.

In Figure 6.7 b), a further smaller common Talbot distance is suggested since a larger tolerance interval is permitted, namely $tol = 3\%$ instead of 0.4% . In this case, we obtain: $9 Z_{T2} = 3\,910.5$ km $\cong 2 Z_{T3} = 3\,984$ km. The difference between both distances is $|9 Z_{T2} - 2 Z_{T3}| = 73.5$ km, which is more than twice as large as that of Figure 6.7 a). It is in fact roughly 6 times smaller than Z_{T2} . The applet suggests an intermediate value, namely $Z_T = 3\,919.32$ km, which is closer to $9 Z_{T2} = 3\,910.5$ km. This distance is almost three times smaller than that suggested by Figure 6.7 a). Of course, we can use $Z_T/2$ instead of Z_T since the effect at both distances is identical except for a lateral shift by half the period. In this case, the signal quality will be better because the difference between both half multiple Talbot distances is 36.75 km instead of 73.5 km.

One can go farther in enlarging the tolerance interval as pointed out in Figure 6.7 c). The signal is more deformed but remains acceptable. The advantage is that a shorter fiber is required since $4 Z_{T2} = 1\,738$ km $\cong Z_{T3} = 1\,992$ km. The difference between both distances is larger than those in Figures 6.7 a) and b). In the present case, we find $|4 Z_{T2} - Z_{T3}| = 254$ km, which is more than half of Z_{T2} . The applet suggests an intermediate value, namely $Z_T = 1\,766.0666$ km, which is closer to $4 Z_{T2} = 1\,738$ km. The difference between Z_T and $4 Z_{T2}$ is 28 km, yielding a noticeable deformation. If we take the average value $(4 Z_{T2} + Z_{T3}) / 2$

instead of the value suggested by the applet, we find $Z_T = (4 Z_{T2} + Z_{T3}) / 2 = 1865$ km and the difference between Z_T and $4 Z_{T2}$ will be 127 km, which is $0.29 Z_{T2}$ (between $Z_{T2}/4$ and $Z_{T2}/3$). This difference leads to the creation of a replica of the signal because both quarter Talbot and third Talbot effects result in signal duplication (the replica is shifted by a half and a third of the period respectively. For example, if we take the intermediate value $Z_T = 4 Z_{T2} + Z_{T2}/4$, we observe, as predicted, a signal duplication (with overlap) as illustrated in Figure 6.8 below.

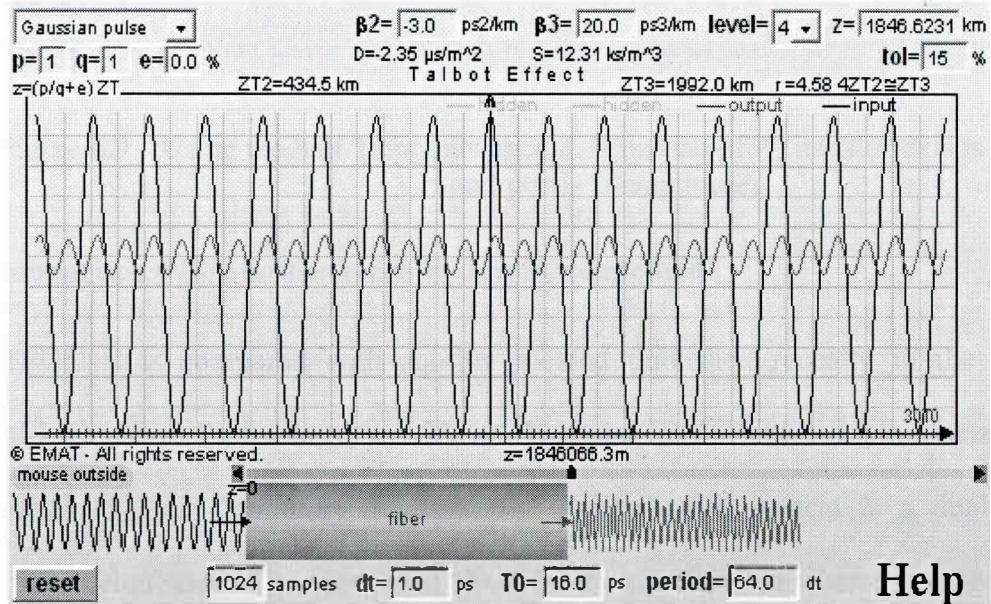


Figure 6.8 Duplication of the signal when we observe the replay field at $4 Z_{T2} + Z_{T2}/4$ (x-axis is time and y-axis is amplitude)

To obtain a better signal quality than that of Figure 6.7 c), we can use half of the common Talbot distance $Z_T/2$ instead of the Z_T itself (Figure 6.8). In this case the difference between both halves of the multiple Talbot distances $|4 Z_{T2} - Z_{T3}|/2$ will be 127 km instead of 254 km. We obtain a better signal except for a lateral shift by half the period.

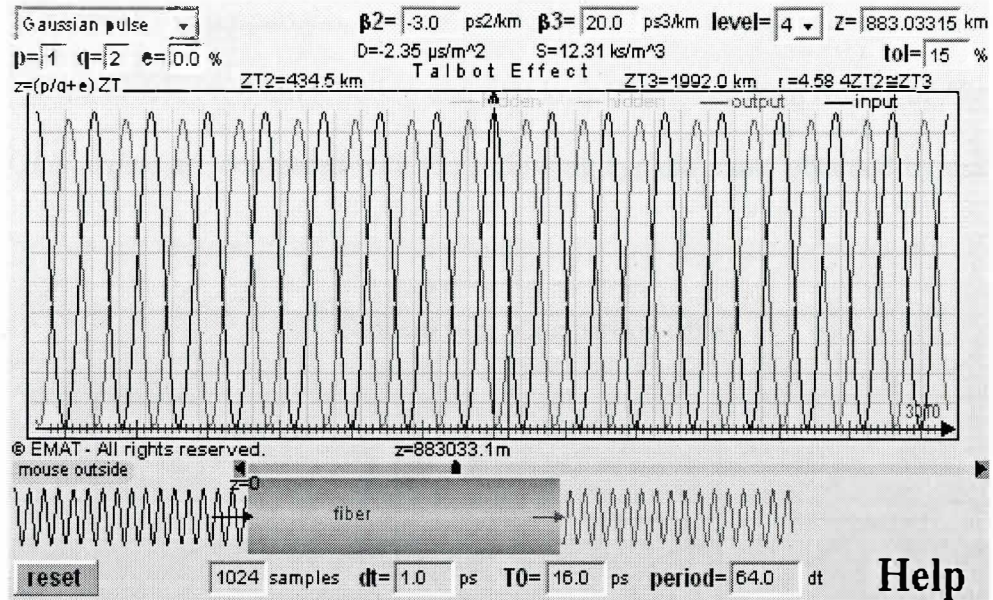


Figure 6.9 Using the half Talbot distance $Z_T/2$ instead of Z_T itself (x-axis is time and y-axis is amplitude)

6.7 Comparison with another recently developed method

The TEChDC is compared with another method published recently in the IEEE “Journal of Light-wave Technology, vol. 23, no. 1, January 2005” entitled “*An Electrically Pre-Equalized 10-Gb/s Duobinary Transmission System*” This system is a duobinary signaling that is combined with a proposed electrical pre-equalization scheme to extend the reach of 10-Gb/s signals that are transmitted over standard single-mode fiber. This scheme is based on predistorting the duobinary signal using two $T/2$ -spaced finite-impulse response (FIR) filters. The outputs of the FIR filters then modulate two optical carriers that are in phase quadrature. Their results show that distances in excess of 400 km at bit-error rates less than 10^{-15} are possible. Incorporating a forward-error correction scheme can extend the reach to distances in excess of 800 km. The reach limitation arises not from CD but from fiber nonlinearity, relative intensity noise due to phase-modulation-to-amplitude-modulation noise conversion, and optical amplifier noise accumulation.

For the purpose of comparison, we transmitted a 10 Gb/s through similar distances as proposed by the article (400 km, 500 km and 600 km). The simulation results of *Figures 9 and 10 of this article* are compared with the following eye diagrams obtained by using our method.

Tableau 6-2: Comparison table

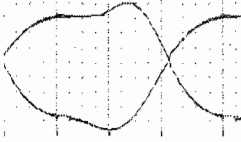
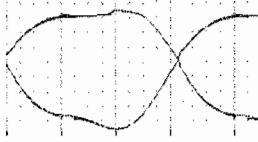
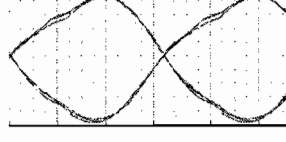



	400km	500 km	600 km
Our Method			
Method in article			

Table 2 clearly shows that the eye diagram of the TEChDC method depicts wider horizontal and vertical openings, leading to better signal sampling.

6.8 Conclusion

Chapter 6 deals with simulation. A setup description of the system is provided for different fibers (Z_1 and Z_2). Simulations of eyes diagrams for different fiber lengths are presented. Bit error rates are calculated and demonstrate an insignificant amount of error present when the proposed solution is employed. A major investigation is spent verifying robustness using the applet.

Both second and third order dispersion were handled by the TEChDC technique either separately or simultaneously. In this case, both Talbot distances Z_{T2} and Z_{T3} are calculated, leading to a common Talbot distance Z_T that may be infinite if calculated rigorously. We demonstrated, however, that reasonable quasi-common Talbot distances can be found. For this purpose, an algorithm was developed to easily calculate parameters a and b in the following equation: $Z_T = aZ_{T2} = bZ_{T3}$.

Both the a and b parameters are not taken literally as calculated so as to avoid obtaining larger numbers leading to an enormous fiber length, as previously explained. In terms of acceptable tolerance, two alternatives a' and b' are calculated using a proposed algorithm to obtain a reasonable fiber length.

A tolerance of the fiber length was proved acceptable up to 5%, which is quite large. The robustness of the method was proved flexible when choosing the length of the additional fiber. A comparison was made with a recently published technique and showed a major improvement in the eye diagram.

Chapter 7 - Conclusion

7.1 Summary

Although equalization is very well known in lower rate communication systems, its potential in Gb/s optical communication has not yet been fully exploited. The main obstacle lies in the very high speed implementation requirements that limit the available options for implementation. The effectiveness of linear equalizers, which are the simplest and most amenable to high speed implementation, is limited because direct detection receivers convert the distortion that results from chromatic dispersion (CD), which is linear in the optical domain, into a nonlinear distortion that is difficult to cancel.

As the demand for high bandwidth (more than 10 Giga bytes order) increases, so does the need for signal compensation at the receiver side. The TEChDC equalization scheme (pre or post) can substantially compensate for dispersion inherent in the reach of 40 Gb/s signals running over SSMF for up to 6,000 km as shown.

The TEChDC method is based on the Talbot Effect (TE). The latter occurs when a periodic sequence of pulses, produced by a laser for example, propagates in a dispersive medium. In such a medium the various harmonics making up the pulse propagate with different speeds, thus causing a large stretching of the pulse during propagation so that each pulse overlaps with the neighboring as well as additional pulses. After propagation through the dispersive medium with a length Z_1 , the received signal is unfortunately affected by fiber impairments, mainly CD, as shown in section 6.2 of Chapter 6. Indeed, the signal may

be significantly corrupted and totally deformed, making its reconstruction very difficult if not impossible. Our alternative consists of introducing a periodizer and propagating the periodized signal through another standard fiber with length Z_2 in such a way that $Z_1 + Z_2 = nZ_T$, where n is a positive integer. The propagated signal along the distance Z_2 is an exact replica of the originally transmitted signal. Next, a truncation process is performed at the very end to restore the desired signal.

Both second and third order dispersion can be handled by the TEChDC technique either separately or simultaneously. In this case, both Talbot distances Z_{T2} and Z_{T3} are calculated, leading to a common Talbot distance Z_T , which may be infinite if calculated rigorously. We showed that reasonable quasi-common Talbot distances can be found, however. For this purpose, an algorithm was developed to easily calculate parameters a and b in the following equation: $Z_T = aZ_{T2} = bZ_{T3}$. Both parameters a and b are not taken literally as calculated so as to avoid obtaining larger numbers leading to an enormous fiber length as previously explained. In terms of acceptable tolerance, two alternatives a' and b' are calculated by means of a proposed algorithm to obtain a reasonable fiber length.

The new method developed has many advantages including:

1. Total restoration of the transmitted signal after being altered by CD.
2. Offering a total freedom to choose the period, the high order Talbot distances.
3. No need to increase the number of repeaters, which results in major cost savings.
4. It is independent of the bit rate sent originally, which means it can handle higher data rates
5. No special fiber is required

6. Standard single mode fibers can be used.

Extensive results are obtained through simulating various cases, as shown above. 40 Gbit/s was carried out through different fiber lengths, and the eye diagram illustrated is a clear indication of the possibilities open for better signal sampling once the method is used. To quantify the observed signal degradation, BER simulations are performed on the measured outputs. Different fiber lengths are considered. For example, Fig. 4 demonstrates a significant reduction in laser power used to achieve a BER in the range of 10^{-16} . The achievable BER was about 10^{-20} , which is low enough to be of no significant practical concern.

A tolerance of the fiber length is proved acceptable up to 5%, which is quite large. The robustness of the method is proved flexible for choosing the length of the additional fiber. As shown in Figure 6, the received signal starts to diverge from the input signal when the error reaches 5%. The error tolerance in the fiber length is acceptable if it is less than 5% of the total fiber length. Furthermore, our method turns out to be efficient when both second and third order dispersions are involved.

Although this work focuses entirely on CD compensation and does not compensate for polarization mode dispersion (PMD) and non-linear effects phenomenon, it can be easily combined with other compensation methods to serve the purpose. This will be the subject of future work.

7.2 Future Work

In this section, we give some ideas for future extension of this work:

1. Throughout this research work, we have focused on the CD compensation and does not compensate for polarization mode dispersion (PMD) and non-linear effects phenomenon, it can be easily combined with other compensation methods to serve the purpose.
2. Study the effect of power consumption on TEChDC.
3. Study the impact of robustness of the TEChDC system using different parameters.
4. In this work, only bursty data is considered as an input level of the simulation set-up is Chapter 6. It would be interesting to investigate the results of the simulation when continuous data is considered.

References

- [1] «From loss test to fiber certification fiber characterization today part I: Chromatic dispersion», White Paper, Agilent Technologies, Apr. 2003.
- [2] J. Ryan, «Fiber considerations for metropolitan networks», *Alcatel Telecommunication Review*, 1st Quarter, pp. 52–55, 2002.
- [3] N. Takachio and K. Iwashita, «Compensation of fiber chromatic dispersion in optical heterodyne detection», *Electron. Lett.*, vol. 24, no. 2, pp. 108–109, Jan. 1988.
- [4] J. Winters, «Equalization in coherent lightwave systems using microwave waveguides», *J. Lightwave Technol.*, vol. 7, no. 5, pp. 813–815, May 1989.
- [5] M. S. Chaudhry and J. J. O'Reilly, «Post-detection chromatic dispersion equalization using GaAs MMICs in heterodyne detection systems», *IEE Colloquium on Optical Detectors and Receivers*, pp. 11/1–11/4, Oct. 1993.
- [6] K. Iwashita and N. Takachio, «Chromatic dispersion compensation in coherent optical communications», *J. Lightwave Technol.*, vol. 8, no. 3, pp. 367–375, Mar. 1990.
- [7] «Equalization in coherent lightwave systems using a fractionally spaced equalizer», *J. Lightwave Technol.*, vol. 8, no. 10, pp. 1487–1491, Oct. 1990.
- [8] H. Bulow, F. Buchali, W. Baumert, R. Ballentin, and T. Wehren, «PMD mitigation at 10 Gbit/s using linear and nonlinear integrated electronic equalizer circuits» *Electron. Lett.*, vol. 36, no. 2, pp. 163–164, Jan. 2000.
- [9] M. Fregolent, S. Herbst, H. Soehnle, and B. Wedding, «Adaptive optical receiver for performance monitoring and electronic mitigation of transmission impairments», in *Proc. 26th European Conference on Optical Communication (ECOC'00)*, 2000, pp. 63–64.
- [10] G. L. Frazer, M. W. Goodwin, K. E. Leonard, J. P. Moffatt, and F. Zhang, «Static and dynamic performance of an adaptive receiver for 10 Gbit/s optical transmission», in *Proc. 26th European Conference on Optical Communication (ECOC'00)*, 2000, pp. 113–114.

- [11] H. Bulow, W. Baumert, H. Schmuck, F. Mohr, T. Schulz, F. Kuppers, and W. Weiershausen, «Measurement of the maximum speed of PMD fluctuation in installed field fiber», in *Optical Fiber Communication Conference and the International Conference on Integrated Optics and Optical Fiber Communication (OFC/IOOC '99)*, Dig. Tech. Papers, vol. 2, 1999, pp. 83–85.
- [12] B. Wedding, A. Chiarotto, W. Kuebart, and H. Bulow, «Fast adaptive control for electronic equalization of PMD», in *Proc. Optical Fiber Communication Conference and Exhibit (OFC'01)*, vol. 2, 2001, pp. TuP4-1 – TuP4-3.
- [13] B. Widrow and J. McCool, «A comparison of adaptive algorithms based on the methods of steepest descent and random search», *IEEE Trans. Antennas Propagation.*, vol. 24, no. 5, pp. 615–637, Sept. 1976.
- [14] M. Fregolent, S. Herbst, H. Soehnle, and B. Wedding, «Adaptive optical receiver for performance monitoring and electronic mitigation of transmission impairments», in *Proc. 26th European Conference on Optical Communication (ECOC'00)*, 2000, pp. 63–64.
- [15] T. Ellermeyer, U. Langmann, B. Wedding, and W. Pohlmann, «A 10-Gb/s eye opening monitor IC for decision-guided adaptation of the frequency response of an optical receiver», *IEEE J. Solid-State Circuits*, vol. 35, no. 12, pp. 1958–1963, Dec. 2000.
- [16] H. F. Haunstein, K. Sticht, and R. Schlenk, «Control of 3-tap electrical feed-forward equalizer by conditional error counts from FEC in the presence of PMD», in *Proc. Optical Fiber Communication Conference and Exhibit (OFC'02)*, 2002, pp. 307–308.
- [17] K. Sticht, H. F. Haunstein, M. Lorang, W. Sauer-Greff, and R. Urbansky, «Adaptation of electronic PMD equalizer based on BER estimation derived from FEC decoder», in *Proc. 27th European Conference on Optical Communication (ECOC'01)*, vol. 3, 2001, pp. 454–455.
- [18] J. Winters and R. Gitlin, «Electrical signal processing techniques in long-haul fiber optic systems», *IEEE Trans. Communication*, vol. 38, no. 9, pp. 1439–1453, Sept. 1990.
- [19] H. Haunstein, K. Sticht, A. Dittrich, M. Lorang, W. Sauer-Greff, and R. Urbansky, «Implementation of near optimum electrical equalization at 10 Gbit/s», in *Proc. 26th European Conference on Optical Communication (ECOC'00)*, vol. 3, 2000, pp. 223–224.
- [20] H. Bulow and G. Thielecke, «Electronic PMD mitigation from linear equalization to maximum-likelihood detection», in *Proc. Optical Fiber Communication Conference and Exhibit (OFC'01)*, vol. 3, 2001, pp. WAA3-1 – WAA3-3.

- [21] M. Cavallari, C. Fludger, and P. Anslow, «Electronic signal processing for differential phase modulation formats», in *Proc. Optical Fiber Communication Conference and Exhibit (OFC'04)*, 2004, p. TuG2.
- [22] C. Fludger, J. Whiteaway, and P. Anslow, «Electronic equalization for low cost 10Gbit/s directly modulated systems», in *Proc. Optical Fiber Communication Conference and Exhibit (OFC'04)*, 2004, p. WM7.
- [23] H. Bäulow and G. Thielecke, «Electronic PMD mitigation from linear equalization to maximum likelihood detection», in *Optical Fiber Communication Conference and Exhibit, 2001. OFC 2001*, vol. 3, 2001, pp. WAA3-1 - WAA3-3.
- [24] M. Nakamura, H. Nosaka, M. Ida, K. Kurishima, and M. Tokumitsu, «Electrical PMD equalizer ICs for a 40-Gbit/s transmission», in *Optical Fiber Communication Conference and Exhibit, 2004. OFC 2004*, vol. TuG4, 2004.
- [25] A. Hazneci and S. P. Voinigescu, «A 49-Gb/s, 7-tap transversal filter in 0.18 μ m SiGe BiCMOS for backplane equalization», in *IEEE Compound Semiconductor Integrated Circuits Symposium*, Monterey, CA, Oct. 2004.
- [26] L. Mäoller, S. Thiede, S. Chandrasekhar, W. Benz, M. Lang, T. Jakobus, and M. Schlechtweg, «ISI mitigation using decision feedback loop demonstrated with PMD distorted 10Gbit/s signals», *Electronic Letters*, vol. 35, no. 24, pp. 2092-2093, 1999.
- [27] K. Azadet, E. F. Haratsch, H. Kim, F. Saibi, J. H. Saunders, M. Shafer, L. Song, and M. L. Yu, «Equalization and FEC techniques for optical transceivers», *IEEE Journal of Solid-State Circuits*, vol. 37, no. 3, pp. 317-327, Mar. 2002.
- [28] G. Kanter, P. Capofreddi, S. Behtash, and A. Gandhi, «Electronic equalization for extending the reach of electro-absorption modulator based transponders», in *Optical Fiber Communication Conference and Exhibit, 2003. OFC 2003*, vol. 2, 2003, pp. 476-477.
- [29] H. Wu, J. A. Tierno, P. Pepeljugoski, J. Schaub, S. Gowda, J. A. Kash, and A. Hajimiri, «Integrated transversal equalizers in high-speed fiber-optic systems», *IEEE Journal of Solid-State Circuits*, vol. 38, no. 12, pp. 2131-2137, Dec. 2003.
- [30] Chongjin Xie, Lothar Möller, Roland Ryf, «Improvement of Optical NRZ- and RZ-Duo binary Transmission Systems With Narrow Bandwidth Optical Filters», *IEEE Photonics Technology Letters*, Vol. 16, No. 9, September 2004
- [31] Lothar Möller, Chongjin Xie, Wei, Xiang «A Novel 10-Gb/s Duo binary Receiver With Improved Back-to-Back Performance and Large Chromatic Dispersion Tolerance», *IEEE Photonics Technology Letters*, Vol. 16, No. 4, April 2004.
- [32] A. H. Gnauck, X. Liu, E. C. Burrows «Comparison of Modulation Formats for 42.7-Gb/s Single-Channel Transmission Through 1980 km of SSMF», *IEEE Photonics Technology Letters*, Vol. 16, No. 3, March 2004.

- [33] J. Winters and R. Gitlin, «Electrical signal processing techniques in long-haul fiber optic systems», *IEEE Trans. Communication.*, vol. 38, no. 9, pp. 1439–1453, Sept. 1990.
- [34] H. Bulow, «Electronic equalization of transmission impairments», in *Proc. Optical Fiber Communication Conference and Exhibit (OFC'02)*, 2002, pp. 24–25.
- [35] S. Guizani, H. Hamam «Optical Fiber Communications,” Encyclopedia 2006, Edited by Hussein Bidgoli, California State—Fullerton.
- [36] S. Guizani, H. Hamam «Chromatic dispersion compensation by means of optical fiber components», in *Optical Fiber Components: Design and Applications*, Edited by Habib Hamam, Research Signpost Edition, 2006.
- [37] Kao, K. C. , and G. A. Hockham . 1966. Dielectric-fiber surface waveguides for optical frequencies. *Proceedings of the IEE*, 133: 1151 – 8 .
- [38] Dutton, H. J. R. 1998 . *Understanding optical communications*. Upper Saddle River, NJ : Prentice Hall .
- [39] B. Zhu, L. Leng, L. Nelson, S. Knudsen, J. Bromage, D. Peckham, S. Stulz, K. Brar, C. Horn, K. Feder, H. Thiele, and T. Veng, «1.6 Tb/s (40 x 42.7 Gb/s) transmission over 2000 km of fiber with 100-km dispersion-managed spans», in *Proc. 27th European Conference on Optical Communication (ECOC'01)*, vol. 6, pp. 16–17, 2001.
- [40] Y. Frignac, G. Charlet, W. Idler, R. Dischler, P. Tran, S. Lanne, S. Borne, C. Artinel, G. Veith, A. Jourdan, J. Hamaide, and S. Bigo, «Transmission of 256 wavelength-division and polarization-division-multiplexed channels at 42.7 Gb/s (10.2 Tb/s capacity) over 3 x 100km of teralight fiber», in *Proc. Optical Fiber Communication Conference and Exhibit (OFC'02)*, 2002, pp. FC5–1 – FC5–3.
- [41] G. Keiser, «Optical Fiber Communication», Mc Graw Hill, 3rd Ed, 2000
- [42] B. Razavi, *Design of Integrated Circuits for Optical Communications*. New York: McGraw-Hill, 2002.
- [43] G. P. Agrawal, «Fiber-Optic Communication Systems», New York: John Wiley & Sons, Inc., 2002.
- [44] Bise , R. T. , R. S. Windeler , K. S. Kranz , C. Kerbage, B. J. Eggleton , and D. J. Trevor . 2002. « Tunable photonic band gap fiber In Optical Fiber Communication Conference, vol. 70 of OSA Trends in Optics and Photonics, pp. 466 – 8 . Washington DC Optical Society of America.
- [45] Cregan , R. F. , B. J. Mangan , J. C. Knight , T. A. Birks, P. S. J. Russell , P. J. Oberts, and D. C. Allan . 1999. Single-mode photonic band gap guidance of light in air. *Science*, 285 (3): 1537 – 9.

- [46] Birks, T. A., J. C. Knight, and P. S. Russell. 1997. Endlessly single-mode photonic crystal fiber. *Optics Letters*, 22:961–3.
- [47] Saitoh, K., M. Koshiba, T. Hasegawa, and E. Sasaoka. 2003. Chromatic dispersion control in photonic crystal fibers: Application to ultra-flattened dispersion. *Optics Express*, 11:843–52.
- [48] Ferrando, A., E. Silvestre, and P. Andrés. 2001. Designing the properties of dispersion flattened photonic crystal fibers. *Optics Express*, 9:687–97.
- [49] Hansen, K. P. 2003. Dispersion flattened hybrid-core nonlinear photonic crystal fiber. *Optics Express*, 11:503–9.
- [50] Crawford, G. P., D. W. Allender, and J. W. Doane. 1992. Surface elastic and molecular-anchoring properties of nematic liquid crystals confined to cylindrical cavities. *Physical Review*, A 45:8693–710.
- [51] Burylov, S. V. 1997. Equilibrium configuration of a nematic liquid crystal confined to a cylindrical cavity. *Journal of Experimental and Theoretical Physics*, 85:873–86.
- [52] Du, F., Y.-Q. Lu, and S.-T. Wu. 2004. Electrically tunable liquid-crystal photonic crystal fiber. *Applied Physics Letters*, 85:2181–3.
- [53] Larsen, T. T., A. Bjarklev, D. S. Hermann, and J. Broeng. 2003. Optical devices based on liquid crystal photonic band gap fibers. *Optics Express*, 11:2589–96.
- [54] Kosmidou, E. P., E. E. Kriezis, and T. D. Tsiboukis. 2005. Analysis of tunable photonic crystal devices comprising liquid crystal materials as defects. *IEEE Journal of Quantum Electronics*, 41:657–65.
- [55] Alkeskjold, T. T., J. Lægsgaard, A. Bjarklev, D. S. Hermann, J. Broeng, J. Li, and S.-T. Wu. 2004. All-optical modulation in dye-doped nematic liquid crystal photonic Band gap fibers. *Optics Express*, 12:5857–871.
- [56] S. Guizani, H. Hamam, Y. Bouslimani, and A. Chériti. 2005. High bit rate optical communications: Limitations and perspectives. *IEEE Canadian Review* 50:11–15.
- [57] C. D. Poole and R. E. Wagner, «Phenomenological approach to polarization dispersion in long single-mode fibers», *Electron. Lett.*, vol. 22, no. 19, pp. 1029–1030, Jan. 1986.
- [58] C. D. Poole, R. W. Tkach, A. R. Chraplyvy, and D. A. Fishman, «Fading in lightwave systems due to polarization-mode dispersion», *IEEE Photon. Technol. Lett.*, vol. 3, no. 1, pp. 68–70, Jan. 1991.

- [59] F. Heismann, D. Fishman, and D. Wilson, «Automatic compensation of first-order polarization mode dispersion in a 10 Gb/s transmission system», in Proc. 24th European Conference on Optical Communication (ECOC'98), vol. 1, 1998, pp. 529–530.
- [60] F. Heismann, «Tutorial: Polarization mode dispersion: Fundamentals and impact on optical communication systems», in Proc. 24th European Conference on Optical Communication (ECOC'98), vol. 2, 1998, pp. 51–79.
- [61] G.P. Agrawal, Nonlinear Fiber Optics, 3rd edition (Academic Press, New York, 2001);
- [62] T. Jannson and J. Jannson, «Temporal self-imaging effect in single-mode fibers», Journal. Opt. Soc. Am. 71, 1373- (1981).
- [63] R. Driben, B.A. Malomed and P.L. Chu, «Transmission of pulses in a dispersion-managed fiber link with extra nonlinear segments», Opt. Commun. 22-227 (2004).
- [64] M. Razzak, H. Hamam and H. Hettak, «Chromatic Dispersion up to the Third Order: Application to Post equalization and Pulse Rate Multiplication», IEEE WirelessCom2005 (2005).
- [65] H. Hamam, S. Guizani, Chromatic dispersion. Available online at: <http://www.umoncton.ca/genie/electrique/Cours/Hamam/Telecom/Disper/Disper.htm>.

Appendix: Publications

Some of the articles that have been submitted and accepted are as follows:

Journals

- S. Guizani, M. Razzak, H. Hamam, Y. Bouslimani and A. Chérity (2006) “Fiber over wireless chromatic dispersion compensation for a better Quality of Service” Journal of Wireless Communications and Networking, EURASIP Journal on Wireless Communications and Networking, Volume 2006 (2006), Article ID 85980, pp. 1-6.
- S. Guizani, M. Razzak, H. Hamam, Y. Bouslimani and A. Chérity (2005) “Optical post- equalization Based on Self-Imaging”, Journal of Modern Optics, Volume 53, Number 12, 15 August 2006, pp. 1675-1684(10).
- S. Guizani, H. Hamam, Y. Bouslimani and A. Chérity (2005) “High bit rate optical communications: Limitations and perspectives” IEEE Canadian Review Summer 2005, pp. 11-15.

Conferences

- S. Guizani, M. Razzak, H. Hamam, Y. Bouslimani, A. Chérity (2006) “Effect of Chromatic dispersion on fiber over wireless systems” IEEE ICC 2006, Istanbul, Turkey, June 11-15, 2006, 6 pages.
- S. Guizani, M. Razzak, H. Hamam, Y. Bouslimani A. Chérity (2005) “A new Optical post- equalization based on self-Imaging”, Photonics North (SPIE) Conference, September 12-14, 2005, Toronto, Canada, 7 pages.
- S. Guizani, M. Razzak, Y. Bouslimani, H. Hamam and A. Chérity (2005), “A new optical post compensation technique for chromatic dispersion: Application to fiber-fed wireless”, IEEE Communication Society, International Conference on Wireless Networks, Communications, and Mobile Computing, June 2005, pp. 641-648.